PREDICTION OF HOT-SPOT AND TOP-OIL TEMPERATURES OF POWER TRANSFORMERS ACCORDING TO IEEE STANDARDS C57.110-1998 AND C57.91-1995

A THESIS SUBMITTED TO
THE GRADUATE SCHOOL OF NATURAL AND APPLIED SCIENCES
OF
MIDDLE EAST TECHNICAL UNIVERSITY

BY

HALDUN KARACA

IN PARTIAL FULLFILLMENT OF THE REQUIREMENTS
FOR
THE DEGREE OF MASTER OF SCIENCE
IN
ELECTRICAL AND ELECTRONICS ENGINEERING

DECEMBER 2007

Approval of the thesis:

PREDICTION OF HOT-SPOT AND TOP-OIL TEMPERATURES OF POWER TRANSFORMERS ACCORDING TO IEEE STANDARDS C57.110-1998 AND C57.91-1995

submitted by **HALDUN KARACA** in partial fulfillment of the requirements for the degree **of Master of Science in Electrical and Electronics Engineering Department, Middle East Technical University** by,

Prof. Dr. Canan Özgen
Dean, Graduate School of Natural and Applied Sciences _____

Prof. Dr. İsmet Erkmen
Head of Department, Electrical and Electronics Dept., METU _____

Prof. Dr. Muammer Ermiş
Supervisor, Electrical and Electronics Dept., METU _____

Examining Committee Members:

Prof. Dr. Nevzat ÖZAY
Electrical and Electronics Dept., METU _____

Prof. Dr. Muammer ERMİŞ
Electrical and Electronics Dept., METU _____

Prof. Dr. H. Bülent ERTAN
Electrical and Electronics Dept., METU _____

Prof. Dr. Işık ÇADIRCI
Electrical and Electronics Dept., HÜ _____

Assist. Prof. Dr. İres İSKENDER
Electrical and Electronics Dept., Gazi Ün. _____

Date: 14.12.2007

I hereby declare that all information in this document has been obtained and presented in accordance with academic rules and ethical conduct. I also declare that, as required by these rules and conduct, I have fully cited and referenced all material and results that are not original to this work.

Name, Last name : Haldun KARACA

Signature :

ABSTRACT

PREDICTION OF HOT-SPOT AND TOP-OIL TEMPERATURES OF POWER TRANSFORMERS ACCORDING TO IEEE STANDARDS C57.110-1998 AND C57.91-1995

Karaca, Haldun
M.Sc., Department of Electrical and Electronics Engineering
Supervisor: Prof. Dr. Muammer Ermiş

December 2007, 193 Pages

In this thesis, the effects of Harmonics on the Top Oil and Hot Spot Temperatures of Power Transformers used in Turkish Electricity Transmission System have been investigated. Due to the solid state equipment, the harmonic levels increase. This effect raises the losses and temperatures in the transformer windings. None of the power transformers currently used in Turkey has measuring equipment suitable for measuring the Hot-Spot temperatures. In this study, a computer program is written in LABVIEW which measures the harmonics and calculates the temperatures in accordance with the methods recommended in IEEE Standards C57.110-1998 and C57.91-1995. Also for sample transformers the work has been verified by measuring the Top-Oil temperatures of the transformers and then comparing with the calculated results.

Keywords: Harmonics, Power Transformer, Hot Spot, Top Oil, Labview

ÖZ

IEEE C57.110-1998 VE C57.91-1995 STANDARTLARINA GÖRE GÜÇ TRAFOLARININ EN SICAK NOKTA VE ÜST YAĞ SICAKLIKLARININ HESAPLANMASI

Karaca, Haldun

Yüksek Lisans, Elektrik ve Elektronik Mühendisliği Bölümü

Tez Yöneticisi: Prof. Dr. Muammer Ermiş

Aralık 2007, 193 Sayfa

Bu tezde, Harmoniklerin Türk Elektrik İletim Sistemindeki Güç Trafolarının En Sıcak Nokta ve Üst Yağ sıcaklıklarına etkileri incelenmiştir. Yarı iletken cihazların kullanımıyla harmoniklerin seviyesi yükselmektedir. Bu etki trafo sargılarındaki kayıpları ve sıcaklıkları arttırmaktadır. Türkiye'de kullanılan trafolarda en sıcak nokta sıcaklılarını ölçebilecek ekipmanlar yoktur. Yapılan çalışmada Labview'de yazılmış olan bir bilgisayar programı ile harmonikler ölçülmekte ve IEEE Standartları C57.110-1998 ve C57.91-1995'de tavsiye edilen metotlar ile bu sıcaklıklar hesaplamaktadır. Bunun yanında seçilen trafolardan direkt olarak ölçülen üst yağ sıcaklıkları ile programın hesapladığı değerler karşılaştırılarak sonuçların doğrulaması da yapılmıştır.

Anahtar Kelimeler: Harmonikler, Güç Trafosu, En sıcak Nokta, Üst Yağ, Labview

To my dear family

and to

My beloved wife Dilek

ACKNOWLEDGMENTS

I would like to thank to my supervisor Prof. Dr. Muammer Ermiş for his excellent ability to direct, support, encouragement, guidance, criticism, insight and farsightedness.

This research work is fully supported by Public Research Grant Committee (KAMAG) of TÜBİTAK within the scope of National Power Quality Project (105G129).

I want to thank, in particular to Prof. Dr. Işık Çadırcı for her comments and contributions, Serkan Buhan in Labview program integration and Erinç Altıntaş for his brilliant and logistic support; and all the other personnel of TÜBİTAK who are working within the National Power Quality Project.

I also would like to thank to Çiğdem Topçu, Yener Akkaya and all the other personnel of TEİAŞ, for helping and assisting me in the data gathering process.

I want to thank to my family for their support during my studies and untiring care. Without them I could not find the courage to complete this thesis.

Finally, my thanks are due to my dear wife Dilek, for her patience and her ability to give me support in times of need.

TABLE OF CONTENTS

ABSTRACT iv
ÖZ v
ACKNOWLEDGMENTS vii
TABLE OF CONTENTS viii
LIST OF FIGURES xii
LIST OF TABLES xix
LIST OF SYMBOLS AND ABBREVIATIONS xx
CHAPTERS
1.INTRODUCTION 1
1.1 Background 1
1.2 Existing Temperature Measurement Facilities 2
1.3 Temperature Calculation Methods 2
1.4 IEEE Guides for Temperature Estimation 2
1.5 Scope of the Thesis 4
2.DETECTION OF TOP-OIL AND HOT-SPOT TEMPERATURES OF AN OIL-IMMERSED POWER TRANSFORMER 6
2.1 INTRODUCTION 6
2.2 IEEE Std. C57.110-1998 (IEEE Recommended Practice for Establishing Transformer Capability When Supplying Nonsinusoidal Load Currents) 7
2.2.1 Transformer per-unit losses 8
2.2.2 Transformer losses at measured currents 9
2.2.3 Harmonic Loss Factor for winding eddy currents 10
2.2.4 Harmonic Loss Factor for other stray losses 12

2.2.5 Transformer capability equivalent calculation using data available from certified test report 13
2.2.6 Transformer capability equivalent calculation when certified test report is unavailable 16
2.3 IEEE Std C57.91 (IEEE Guide for Loading Mineral-Oil- Immersed Transformers) 17
2.3.1 Top-Oil rise over ambient 18
2.3.2 Oil time constant 18
2.3.3 Winding Hot-Spot rise 19
2.4 Further Research Studies on Top-Oil and Hot Spot Temperatures 20
2.4.1 Improvement on the calculation of temperatures 21
2.4.2 Improvement on Dynamic Thermal Behavior 22
2.5 Final Method 23
3. TEMPEST (Temperature Estimation) PROGRAM 25
3.1 Introduction 25
3.2 Hardware 26
3.3 Software 33
3.4 Discussions 39
4. APPLICATION EXAMPLES 42
4.1 80/100 MVA ONAN/ONAF Intermittent Load (Verification) 43
4.1.1 Loading and Harmonic Content 47
4.1.2 Temperature Verification 61
4.1.2.1 Hot Spot Temperature Spikes 66
4.1.2.2 Effect of the Loading Condition 67
4.1.2.3 Ambient Temperature Changes 69
4.1.3 IEEE Loading Guide's Original Time Constant vs. Corrigendum Time Constant 70
4.1.4 Unbalanced Loading between phases 72
4.1.5 Sample Temperature Calculation 83
4.2 25/32.5 MVA ONAN/ONAF Conventional Load 87

4.21 Loading and Harmonic Content 89
4.2.2 Temperature Prediction 90
4.2.3 Sample Temperature Calculation 95
5. CONCLUSIONS 99
REFERENCES 102
APPENDICES
Appendix A: Transformer Losses and Temperature Rise 107
Appendix B: Installation of Resistive Thermometer 190

LIST OF FIGURES

Figure 1 Flowchart of the performed method 24

Figure 2 Block diagram of PQ monitoring set-up upgraded for Hot-Spot and Top-Oil temperature prediction 29

Figure 3 RT 3 wire configuration..... 30

Figure 4 Installation of RT for Top-Oil Temperature measurement in the field .. 31

Figure 5 Resistive Thermometer of Ambient Temperature installed in the field . 32

Figure 6 On-line PQ analysis software upgraded for HST and TOT prediction .. 36

Figure 7 TEMPEST integrated into Mobile Monitoring System..... 38

Figure 8 TEMPEST integrated into Mobile Monitoring System (Background) .. 38

Figure 9 Erroneous Alçuk-B, 5th Harmonic Comp. of the Sec Current..... 40

Figure 10 Corrected Alçuk-B, 5th Harmonic Comp. of the Secondary Current.... 40

Figure 11 Transformer Alçuk-B..... 43

Figure 12 Alçuk-B test setup..... 46

Figure 13 Alçuk-B, TDD 47

Figure 14 Alçuk-B, Fundamental Component of the Secondary Current..... 48

Figure 15 Alçuk-B, 2nd Harmonic Component of the Secondary Current..... 48

Figure 16 Alçuk-B, 3rd Harmonic Component of the Secondary Current..... 49

Figure 17 Alçuk-B, 4th Harmonic Component of the Secondary Current 49

Figure 18 Alçuk-B, 5th Harmonic Component of the Secondary Current..... 50

Figure 19 Alçuk-B, 6th Harmonic Component of the Secondary Current..... 50

Figure 20 Alçuk-B, 7th Harmonic Component of the Secondary Current..... 51

Figure 21 Alçuk-B, 8th Harmonic Component of the Secondary Current..... 51

Figure 22 Alçuk-B, 9th Harmonic Component of the Secondary Current..... 52

Figure 23 Alçuk-B, 10th Harmonic Component of the Secondary Current 52

Figure 24 Alçuk-B, 11th Harmonic Component of the Secondary Current..... 53

Figure 25 Alçuk-B, 12th Harmonic Component of the Secondary Current..... 53

Figure 26 Alçuk-B, 13th Harmonic Component of the Secondary Current..... 54

Figure 27 Alçuk-B, 14th Harmonic Component of the Secondary Current..... 54

Figure 28 Alçuk-B, 15th Harmonic Component of the Secondary Current..... 55

Figure 29 Alçuk-B, 16th Harmonic Component of the Secondary Current..... 55

Figure 30 Alçuk-B, 17th Harmonic Component of the Secondary Current..... 56

Figure 31 Alçuk-B, 18th Harmonic Component of the Secondary Current..... 56

Figure 32 Alçuk-B, 19th Harmonic Component of the Secondary Current..... 57

Figure 33 Alçuk-B, 20th Harmonic Component of the Secondary Current..... 57

Figure 34 Alçuk-B, 21st Harmonic Component of the Secondary Current 58

Figure 35 Alçuk-B, FHL vs. Load 59

Figure 36 Alçuk-B, FHL-STR vs. Load 59

Figure 37 Alçuk-B, Calculated vs. Measured TOT with respect to Loading 61

Figure 38 Alçuk-B, Calculated vs. Measured TOT excluding Loading and HST 62

Figure 39 Alçuk-B, TOT deviations between Calculated and Measured Temperatures with respect to loading 63

Figure 40 Alçuk-B, TOT deviations between Calculated and Measured Temperatures with respect to Ambient Temperature..... 64

Figure 41 Alçuk-B, Detail showing HST Spikes 66

Figure 42 Alçuk-B, Detail showing HST Spikes excluding Loading 67

Figure 43 Alçuk-B, Detail showing the Shut-Down Response-1 68

Figure 44 Alçuk-B, Detail showing the Shut Down Response-2 69

Figure 45 Alçuk-B, Deviations Related to the Changes in Ambient Temperature 70

Figure 46 Alçuk-B, Corrigendum Time Constant vs. Original Time Constant 71

Figure 47 Alçuk-B, Fundamental currents of Phases A, B and C for the whole measurement duration 74

Figure 48 Alçuk-B, TOT calculated from the currents of Phases A, B and C 75

Figure 49 Alçuk-B, HST calculated from the currents of Phases A, B, C 75

Figure 50 Alçuk-B, TOT Deviation between the Phases B and A 77

Figure 51 Alçuk-B, TOT Deviation between the Phases C and A 78

Figure 52 Alçuk-B, HST Deviation between the Phases B and A 79

Figure 53 Alçuk-B, HST Deviation between the Phases C and A 80

Figure 54 Alçuk-B, Top Oil rise over Ambient Temperature 81

Figure 55 Alçuk-B, Hot Spot Conductor rise over Top Oil Temperature 82

Figure 56 Maltepe-2 Transformer 87

Figure 57 Maltepe-2 Harmonic Spectrum 89

Figure 58 Maltepe-2 TOT vs. HST 91

Figure 59 Maltepe-2, Top Oil rise over Ambient Temperature 92

Figure 60 Maltepe-2, TOT deviations between Calculated and Measured Temperatures with respect to loading 93

Figure 61 Maltepe-2, TOT deviations between Calculated and Measured Temperatures with respect to Ambient Temperature 93

Figure 62 Types of Transformer Losses 108

Figure 63 View of a transformer leakage flux region modeling..... 112

Figure 64 Problem definition in COMSOL software and the obtained electric field and potential distributions (Draw Mode and Mesh Solution)..... 113

Figure 65 Problem definition in COMSOL software and the obtained electric field and potential distributions (Counter and Color Solutions) 113

Figure 66 Draw mode view of a FEM analysis using MATLAB PDA Toolbox 115

Figure 67 Counter and Color mode solutions of a FEM analysis using MATLAB PDA Toolbox 115

Figure 68 Steady-state temperature relationships 117

Figure 69 Transformer Insulation Life..... 119

Figure 70 Aging acceleration factor (relative to 110 ^{o}C)..... 119

Figure 71 Allowable load currents at different ambient temperatures..... 120

Figure 72 Oil and Winding Thermometers 123

Figure 73 Winding thermometer principal diagram..... 124

Figure 74 Fiber optic sensor directly in contact with CTC cable 127

Figure 75 Transformer Almak-A 128

Figure 76 Almak-A, TDD..... 130

Figure 77 Almak-A, Fundamental Component of the Secondary Current 131

Figure 78 Almak-A, 2nd Harmonic Component of the Secondary Current..... 131

Figure 79 Almak-A, 3rd Harmonic Component of the Secondary Current..... 132

Figure 80 Almak-A, 4th Harmonic Component of the Secondary Current..... 132

Figure 81 Almak-A, 5th Harmonic Component of the Secondary Current..... 133

Figure 82 Almak-A, 6th Harmonic Component of the Secondary Current..... 133

Figure 83 Almak-A, 7th Harmonic Component of the Secondary Current 134

Figure 84 Almak-A, 8th Harmonic Component of the Secondary Current 134

Figure 85 Almak-A, 9th Harmonic Component of the Secondary Current 135

Figure 86 Almak-A, 10th Harmonic Component of the Secondary Current 135

Figure 87 Almak-A, 11th Harmonic Component of the Secondary Current 136

Figure 88 Almak-A, 12th Harmonic Component of the Secondary Current 136

Figure 89 Almak-A, 13th Harmonic Component of the Secondary Current 137

Figure 90 Almak-A, 14th Harmonic Component of the Secondary Current 137

Figure 91 Almak-A, 15th Harmonic Component of the Secondary Current 138

Figure 92 Almak-A, 16th Harmonic Component of the Secondary Current 138

Figure 93 Almak-A, 17th Harmonic Component of the Secondary Current 139

Figure 94 Almak-A, 18th Harmonic Component of the Secondary Current 139

Figure 95 Almak-A, 19th Harmonic Component of the Secondary Current 140

Figure 96 Almak-A, 20th Harmonic Component of the Secondary Current 140

Figure 97 Almak-A, 21st Harmonic Component of the Secondary Current 141

Figure 98 Almak-A, FHL vs. Load 141

Figure 99 Almak-A, FHL-STR vs. Load 142

Figure 100 Almak-A, Calculated vs. Measured TOT with respect to Loading .. 144

Figure 101 Almak-A, Calculated vs. Measured TOT excluding Loading 144

Figure 102 Almak-A, TOT deviations between Calculated and Measured Temperatures with respect to Loading 145

Figure 103 Almak-A, TOT deviations between Calculated and Measured Temperatures with respect to Ambient Temperature 146

Figure 104 Almak-A, TOT calculated from the currents of Phases A, B and C 147

Figure 105 Almak-A, HST calculated from the currents of Phases A, B and C. 148

Figure 106 Almak-A, TOT Deviation between the Phases B and A 149

Figure 107 Almak-A, TOT Deviation between the Phases C and A 150

Figure 108 Almak-A, HST Deviation between the Phases B and A 151

Figure 109 Almak-A, HST Deviation between the Phases C and A 152

Figure 110 Almak-A, Hot Spot Conductor rise over Top Oil Temperature 153

Figure 111 Transformer Habaş-C 154

Figure 112 Habaş-C, TDD 156

Figure 113 Habaş-C, Fundamental Component of the Secondary Current 157

Figure 114 Habaş-C, 2nd Harmonic Component of the Secondary Current..... 157

Figure 115 Habaş-C, 3rd Harmonic Component of the Secondary Current 158

Figure 116 Habaş-C, 4th Harmonic Component of the Secondary Current 158

Figure 117 Habaş-C, 5th Harmonic Component of the Secondary Current 159

Figure 118 Habaş-C, 6th Harmonic Component of the Secondary Current 159

Figure 119 Habaş-C, 7th Harmonic Component of the Secondary Current 160

Figure 120 Habaş-C, 8th Harmonic Component of the Secondary Current 160

Figure 121 Habaş-C, 9th Harmonic Component of the Secondary Current 161

Figure 122 Habaş-C, 10th Harmonic Component of the Secondary Current 161

Figure 123 Habaş-C, 11th Harmonic Component of the Secondary Current 162

Figure 124 Habaş-C, 12th Harmonic Component of the Secondary Current 162

Figure 125 Habaş-C, 13th Harmonic Component of the Secondary Current 163

Figure 126 Habaş-C, 14th Harmonic Component of the Secondary Current 163

Figure 127 Habaş-C, 15th Harmonic Component of the Secondary Current 164

Figure 128 Habaş-C, 16th Harmonic Component of the Secondary Current 164

Figure 129 Habaş-C, 17th Harmonic Component of the Secondary Current 165

Figure 130 Habaş-C, 18th Harmonic Component of the Secondary Current 165

Figure 131 Habaş-C, 19th Harmonic Component of the Secondary Current 166

Figure 132 Habaş-C, 20th Harmonic Component of the Secondary Current 166

Figure 133 Habaş-C, 21st Harmonic Component of the Secondary Current..... 167

Figure 134 Habaş-C, FHL vs. Load 167

Figure 135 Habaş-C, FHL-STR vs. Load 168

Figure 136 Habaş-C, Calculated vs. Measured TOT with respect to Loading ... 170

Figure 137 Habaş-C, Calculated vs. Measured TOT excluding Loading 171

Figure 138 Habaş-C, TOT deviations between Calculated and Measured Temperatures with respect to Loading..... 172

Figure 139 Habaş-C, TOT deviations between Calculated and Measured Temperatures with respect to Ambient Temperature..... 173

Figure 140 Habaş-C, TOT calculated from the currents of Phases A, B and C.. 174

Figure 141 Habaş-C, HST calculated from the currents of Phases A, B and C.. 175

Figure 142 Habaş-C, TOT Deviation between the Phases B and A 176

Figure 143 Habaş-C, TOT Deviation between the Phases C and A 177

Figure 144 Habaş-C, HST Deviation between the Phases B and A..... 178

Figure 145 Habaş-C, HST Deviation between the Phases C and A..... 179

Figure 146 Habaş-C, Hot Spot Conductor rise over Top Oil Temperature 180

Figure 147 Transformer Ümitköy-A 181

Figure 148 Ümitköy-A Harmonic Spectrum 183
Figure 149 Ümitköy-A TOT vs. HST 184
Figure 150 Ümitköy-B Transformer 185
Figure 151 Ümitköy-B Harmonic Spectrum 187
Figure 152 Ümitköy-B TOT vs. HST 188
Figure 153 Safety Precaution-Glove 190
Figure 154 Safety Precaution-Helmet 191
Figure 155 Safety Precaution-Grounding 191
Figure 156 Removal of oil tap 192
Figure 157 Oil tap Removed 192
Figure 158 Oil Thermometer adaptor installation 193
Figure 159 Oil Thermometer installed 193

LIST OF TABLES

Table 1 Assumptions for Power Transformers Losses 17

Table 2 TEMPEST Input data for Alçuk-B 45

Table 3 Harmonic distribution and parameter calculation for Alçuk-B 83

Table 4 Load distribution for Alçuk-B..... 85

Table 5 TEMPEST Input data for Maltepe-2..... 88

Table 6 Harmonic distribution and parameter calculation for Maltepe-2..... 95

Table 7 Load distribution for Maltepe-2..... 97

Table 8 Input data for PDA Toolbox 114

Table 9 TEMPEST Input data for Almak-A..... 129

Table 10 TEMPEST Input data for Habaş-C..... 155

Table 11 TEMPEST Input data for Ümitköy-A..... 182

Table 12 TEMPEST Input data for Ümitköy-B..... 186

LIST OF SYMBOLS AND ABBREVIATIONS

B	Magnetic Flux Density
C	Thermal capacity of the transformer
d	Conductor diameter in the direction of B
FEM	Finite Element Method
F_{HL}	Harmonic loss factor for winding eddy currents
F_{HL-STR}	Harmonic loss factor for other stray losses
GIS	Gaseous Isolated System
h	Harmonic order
h_{max}	Highest significant harmonic number
HST	Hot Spot Temperature
HV	High Voltage
I	RMS load current (amperes)
I_1	RMS fundamental load current (amperes)
I_h	RMS current at harmonic "*h*" (amperes)
I_{1-R}	High voltage (HV) rms fundamental line current under rated frequency and rated load conditions (amperes)
I_{2-R}	Low voltage (LV) rms fundamental line current under rated frequency and rated load conditions (amperes)
IEC	The International Electrotechnical Commission
IEEE	The Institute of Electrical and Electronics Engineers
LV	Low Voltage
N1	Number of Windings
ODAF	Oil Directed and Air Forced
OFAF	Oil Forced and Air Forced
ONAF	Oil Natural and Air Forced
ONAN	Oil Natural and Air Natural

P_{NL}	No load loss (watts)
P_{LL}	Load loss (watts)
P_{LL-R}	Load loss under rated conditions (watts)
P_{I^2R}	Total calculated I^2R losses at ambient temperature (watts)
P_{TSL}	Total stray loss (watts)
P_{TSL-R}	Total stray loss under rated conditions (watts)
P_{EC}	Winding eddy-current loss (watts)
P_{EC-R}	Winding eddy-current loss under rated conditions (watts)
P_{EC-O}	Winding eddy-current losses at the measured current and the power frequency (watts)
P_{OSL}	Other stray loss (watts)
P_{OSL-R}	Other stray loss under rated conditions (watts)
R	DC resistance (ohms)
R_1	DC resistance measured between two HV terminals (ohms)
R_2	DC resistance measured between two LV terminals (ohms)
T	Conductor thickness (height or width) in the direction of B
TDD	Total Demand Distortion
TEİAŞ	Turkish Electricity Transmission Corporation
TOT	Top Oil Temperature
w	Angular frequency ($2\pi f$)
U_h	Harmonic Voltage
ρ	Conductor Resistivity
σ	Electrical conductivity
μ	Permeability
μ_r	Relative Permeability
Θ_A	Ambient Temperature (^oC)
Θ_g	Hot-Spot conductor temperature (^oC)
$\Delta\Theta_g$	Hot-Spot conductor rise over Top-Oil temperature (^oC)

$\Delta\Theta_{g\text{-}R}$	Hot-Spot conductor rise over Top-Oil temperature under rated conditions (^{o}C)
Θ_{TO}	Top-Oil temperature (^{o}C)
$\Theta_{TO\text{-}R}$	Top-Oil-rise temperature under rated conditions (^{o}C)
$\Theta_{TO,i}$	Initial Top-Oil-rise temperature (^{o}C)
$\Theta_{TO,U}$	Ultimate Top-Oil-rise temperature (^{o}C)
$\Delta\Theta_{TO}$	Top-Oil-rise over ambient temperature (^{o}C)
$\Delta\Theta_{TO\text{-}R}$	Top-Oil-rise over ambient temperature under rated conditions (^{o}C)
$\Delta\Theta_{TO,i}$	Initial Top-Oil-rise over ambient temperature (^{o}C)
$\Delta\Theta_{TO,U}$	Ultimate Top-Oil-rise over ambient temperature (^{o}C)
τ_{TO}	oil time constant of transformer
$\tau_{TO,R}$	oil time constant of transformer under rated conditions
τ_{W}	winding time constant at Hot-Spot location
(pu)	This symbol modifier may be added to the listed symbols to represent a per-unit value of that quantity. Current quantities are referred to the rated rms load current I_R , and loss quantities are referred to the rated load I^2R loss density. e.g.: I_h(pu) and $P_{EC\text{-}R}$(pu)

CHAPTER 1

INTRODUCTION

1.1 Background

Power transformers can operate under pre-specified operating conditions (i.e. maximum power rating, maximum permissible voltage or current harmonic content, environmental operating temperature range) determined by the degree of isolation for long time durations.

The most critical thermal parameters are Top-Oil and Hot-Spot temperatures. As defined in IEEE Std. C57.12.80-2002[1]; the Top-Oil temperature is the temperature of the top layer of the insulating liquid in a transformer. The Hot-Spot temperature is defined as the hottest temperature of the current carrying components of a transformer in contact with insulation or insulating fluid [1].

The operating conditions of the power transformers can be different than the pre-specified operating conditions. Whether or not the power transformer can operate under these conditions and how much overloading can be applied regarding maximum MVA power or harmonic content, solely depends on the Hot-Spot and Top-Oil temperatures defined by the manufacturer.

Because of all these reasons, by measuring these temperatures, the power transformers can be operated or overloaded under these new circumstances.

Ideally, these temperatures shall be measured and monitored. The Hot-Spot location can be accurately predicted by the transformer manufacturer. Generally, the Hot-Spot location occurs near the top level of the windings.

1.2 Existing Temperature Measurement Facilities

The existing power transformers use Top-Oil thermometers with mechanical indicators, as shown in Appendix A. The winding temperature is measured indirectly by thermometers with mechanical indicators. However in new, modern power transformers, the Hot-Spot temperature is measured with fiber optic sensors (Appendix A).

1.3 Temperature Calculation Methods

In the temperature calculation process, the Power Transformer's 3-Dimensional structure, thermal model and parameters for Finite Element Method (FEM) shall be made available by the transformer manufacturer. The FEM can be applied as 3-Dimensional or 2-Dimensional [2].

1.4 IEEE Guides for Temperature Estimation

Top-Oil and Hot-Spot temperatures for both oil-immersed and dry-type transformers can be determined by using IEEE Std. C57.110-1998 [3]. The purpose of this standard is to establish uniform methods for determining the capability of transformers to supply nonsinusoidal load currents of known characteristics.

This standard recommends methods to calculate temperatures for constant load and fixed harmonic content. The manufacturer's certified test report is used for empirically determined data.

The IEEE Loading Guide (IEEE Std. C57.91-1995) [4] is only used for mineral oil-immersed transformers. A number of temperature estimation methods are recommended to take into account the variations in the load. Applications of loads in excess of nameplate rating involve some degree of risk. It is the purpose of this guide to identify these risks and to establish limitations and guidelines, the application of which will minimize the risks to an acceptable level.

Within the original document, an oil time constant to evaluate the variations in the Top-Oil temperature has been defined. This oil time constant was erroneous and later on has been corrected with a corrigendum [5].

There are various studies performed to further improve the standards.

A corrected Harmonic Loss Factor has been suggested which claims to provide more accurate calculations [6]. Another method [2] has been reported to perform further improvements to the Harmonic Loss Factor. In this method the penetration depth which has a significant effect on the Harmonic Loss Factor has been taken into account.

A theoretical model [7] has been developed based on boundary value problem of heat conduction in transformer winding using finite integral transform techniques.

In the original Loading Guide, the ambient temperature changes have not been taken into account in the thermal model. In order to take the continuous variation of the ambient temperature into account, the model in Clause 7 is modified by [8] and [9].

In the original study of Susa [10], the models with the ability to perform on manufacturer's test report data had performed near or less accurate than the IEEE method. However a very recent research [11, 12] has made use of his method which reported to be more accurate than the IEEE method. Larger datasets are needed to validate the applicability or the superiority of the models.

There are also various methods which are based on the data and test results given by the manufacturer of the power transformer [8, 10, 11, 12, 13, 14, 15, 16]. The number of assumptions increases with the lack of the available test and manufacturer data.

1.5 Scope of the Thesis

Within the scope of National Power Quality Project, Mobile and Permanent Power Quality Monitoring Devices have been developed. These monitors utilize the current and voltage data (3200 samples per second per channel) of the secondary windings of the power transformers. It collects the raw data in accordance with IEC 61000-4-30/Class B [17], and carries out on-line data processing according to IEC 61000-4-7/Class B [18], IEC 61000-4-15/Class B [19] and IEEE Std. 519 [20] to determine the Power Quality indices.

In this thesis, the estimation of Hot-Spot and Top-Oil temperatures by adding hardware and software to these systems and also using the related power transformer's manufacturer's certified test report or its nameplate data has been aimed.

To achieve this goal, only the sampling of the measured ambient temperature and then transferring to the system is adequate.

Within the scope of this thesis, the TEMPEST (TEMPerature ESTimation) program has been developed. TEMPEST program estimates the Top-Oil and Hot-Spot temperatures according to IEEE Standards C57.110-1998 and C57.91-1995. This program predicts the temperatures not only for constant load and fixed harmonic content, but also can track the changes for the dynamic load variations.

By including pre-specified maximum permissible temperature limits to this program, warning functions can be implemented using remote internet channels. The verification of the temperature thermometers already installed on the transformers can be achieved. The Top-Oil and Hot-Spot temperature data stack on the Monitoring Devices can be transferred to the headquarters and then transferred into more meaningful graphical representations.

Chapter 1 provides an introduction. Chapter 2 describes the present Top-Oil and Hot-Spot temperature detection methods. Chapter 3 describes the prepared computer program and performed work. Chapter 4 presents the application examples on selected transformers. Chapter 5 underlines the conclusions. Appendix A provides detailed information about losses, temperatures and measurements. Appendix B describes the Resistive Thermometer installation.

CHAPTER 2

DETECTION OF TOP-OIL AND HOT-SPOT TEMPERATURES OF AN OIL-IMMERSED POWER TRANSFORMER

2.1 INTRODUCTION

Since the prediction of the Top-Oil and Hot-Spot temperatures are vital in determination of the acceptable limit in the operation of power transformers with loads including some degree of harmonic content, various methods have been developed. Among these methods, the methods defined in IEEE Std. C57.110-1998 [3] have been accepted as a baseline.

One of the main disadvantages of the IEEE Std. C57.110-1998 [3] is that, its methods are conservative. A second disadvantage of the IEEE Std. C57.110-1998 is that, it only provides methods to determine temperatures instantaneously so the dynamic thermal modeling of temperatures is only possible with the addition of more complex formulation even if these formulas are somewhat based on the methods defined in the standard.

To overcome this handicap, the IEEE Std. C57.91-1995 [4] is used in this thesis. There are two different methods described in this standard to determine the dynamic behavior of the temperature variation, in Clause 7 and in the Annex G. The method defined in the Clause 7 is the baseline method and the method in the Annex G is an alternate method to be used if more data can be acquired.

2.2 IEEE Std. C57.110-1998 (IEEE Recommended Practice for Establishing Transformer Capability When Supplying Nonsinusoidal Load Currents)

IEEE Std. C57.110-1998 [3] has provided guidance in conservative loading practices so that overloading could be avoided for transformers carrying nonsinusoidal load currents. Precise determination of the extra eddy-current loss produced by harmonic currents is a complex subject that is highly dependent on the design and construction of the transformer and may involve sophisticated computer analysis.

More specifically, it is expected that IEEE Std C57.110-1998 [3] would be used for the following situations:

a) For a new transformer which will be required to carry some nonsinusoidal load currents, but ***will not*** be entirely devoted to a rectifier load.

b) For an existing transformer which was not originally specified for supplying nonsinusoidal load currents, but is now required to supply a load, a ***Portion*** of which is nonsinusoidal.

It should be recognized that liquid-filled transformers may have different load limitations than dry-type transformers and that the harmonic loading practices should treat the two transformer types differently when necessary.

Since the only main power transformers in the use of Turkish Electricity Transmission System are liquid-filled transformers, the Dry-Type transformers have not been implemented in this study.

In order to perform the calculations in this recommended practice, the characteristics of the nonsinusoidal load current must be defined either in terms of the magnitude of the fundamental frequency component or the magnitude of the total rms current. Each harmonic frequency component must also be defined from power system measurements.

2.2.1 Transformer per-unit losses

Since the greatest concern about a transformer operating under harmonic load conditions will be for overheating of the windings, it is convenient to consider loss density in the windings on a per-unit basis (base current is rated current and base loss density is the I^2R loss density at rated current) [3].

$$P_{LL\text{-}R}(\text{pu}) = 1 + P_{EC\text{-}R}(\text{pu}) + P_{OSL\text{-}R}(\text{pu}) \text{ pu} \tag{2.1}$$

Given the eddy-current loss under rated conditions for a transformer winding or portion of a winding, ($P_{EC\text{-}R}$), the eddy-current loss due to any defined nonsinusoidal load current can be expressed as:

$$P_{EC} = P_{EC\text{-}R} \sum_{h=1}^{h=h_{max}} \left(\frac{I_h}{I_R} \right)^2 h^2 \text{ watts} \tag{2.2}$$

For nonsinusoidal load currents, the equation for the rms current in per-unit form will be:

$$\text{I(pu)} = \sqrt{\sum_{h=1}^{h=h_{max}} I_h(pu)^2} \quad \text{pu} \tag{2.3}$$

Equation (2.2) can also be written in per-unit form (base current is rated current and base loss density is the I^2R loss density at rated current).

$$P_{EC}(\text{pu}) = P_{EC\text{-}R}(\text{pu}) \sqrt{\sum_{h=1}^{h=h_{max}} I_h(pu)^2 h^2} \quad \text{pu} \tag{2.4}$$

2.2.2 Transformer losses at measured currents

Equations (2.1) through (2.4) assume that the measured application currents are taken at the rated currents of the transformer. Since this is seldom encountered in the field, a new term is needed to describe the winding eddy losses at the measured current and the power frequency, $P_{EC\text{-}O}$.

Equations (2.2) and (2.4) may now be written more generally in the following equation:

$$P_{EC} = P_{EC\text{-}O} \sum_{h=1}^{h=h_{max}} \left(\frac{I_h}{I} \right)^2 h^2 \text{ watts} \tag{2.5}$$

By removing the rms current term, I from the summation, the equation becomes:

$$P_{EC} = P_{EC-O} \frac{\sum_{h=1}^{h=h_{max}} (I_h)^2 h^2}{I^2} \text{ Watts} \tag{2.6}$$

The rms value of the nonsinusoidal load current is then given by:

$$I = \sqrt{\sum_{h=1}^{h=h_{max}} (I_h)^2} \text{ Amperes} \tag{2.7}$$

The rms current term, I, may be expressed in terms of the component frequencies.

$$P_{EC} = P_{EC-O} \frac{\sum_{h=1}^{h=h_{max}} (I_h)^2 h^2}{\sum_{h=1}^{h=h_{max}} (I_h)^2} \text{ Watts} \tag{2.8}$$

2.2.3 Harmonic Loss Factor for winding eddy currents

It is convenient to define a single number which may be used to determine the capabilities of a transformer in supplying power to a load. FHL is a proportionality factor applied to the winding eddy losses, which represents the effective rms heating as a result of the harmonic load current.

FHL is the ratio of the total eddy current losses due to the harmonics, (P_{EC}), to the eddy-current losses at the power frequency, as if no harmonic currents existed, (P_{EC-O}).

The Harmonic Loss Factor is similar but not identical to the K-factor referenced in other standards.

$$FHL = \frac{P_{EC}}{P_{EC-O}} \frac{\sum_{h=1}^{h=h_{max}} (I_h)^2 h^2}{\sum_{h=1}^{h=h_{max}} (I_h)^2} \tag{2.9}$$

Equation (2.9) permits FHL to be calculated in terms of the actual rms values of the harmonic currents. Various measuring devices permit calculations to be made in terms of the harmonics normalized to the total rms current or to the first or fundamental harmonic. Equation (2.9) may be adapted to these situations by dividing the numerator and denominator by either I_1, the fundamental harmonic current, or by I, the total rms current.

Note that the quantity $\frac{I_h}{I_1}$ may be directly read on a meter, by passing the computation procedure. In either case, FHL remains the same value, since it is a function of the harmonic current distribution and is independent of the relative magnitude.

$$FHL = \frac{\sum_{h=1}^{h=h_{\max}} \left(\frac{I_h}{I_1}\right)^2 h^2}{\sum_{h=1}^{h=h_{\max}} \left(\frac{I_h}{I_1}\right)^2} \tag{2.10}$$

$$FHL = \frac{\sum_{h=1}^{h=h_{\max}} \left(\frac{I_h}{I}\right)^2 h^2}{\sum_{h=1}^{h=h_{\max}} \left(\frac{I_h}{I}\right)^2} \tag{2.11}$$

2.2.4 Harmonic Loss Factor for other stray losses

Although the heating due to other stray losses is generally not a consideration for dry-type transformers, it can have a substantial effect on liquid-filled transformers. A relationship similar to the Harmonic Loss Factor for winding eddy losses exists for these other stray losses in a transformer, and may be developed in a similar manner. However, the losses due to bus bar connections, structural parts, tank, etc. are proportional to the square of the load current and the harmonic frequency to the 0.8 power.

$$P_{OSL} = P_{OSL-R} \sum_{h=1}^{h=h_{\max}} \left(\frac{I_h}{I_R}\right)^2 h^{0.8} \text{ watts} \tag{2.12}$$

The equations corresponding to the Harmonic Loss Factor, normalized to the fundamental current and normalized to the rms current respectively are:

$$FHL-STR=\frac{\sum_{h=1}^{h=h_{\max}}\left(\frac{I_h}{I_1}\right)^2 h^{0.8}}{\sum_{h=1}^{h=h_{\max}}\left(\frac{I_h}{I_1}\right)^2} \tag{2.13}$$

$$FHL-STR=\frac{\sum_{h=1}^{h=h_{\max}}\left(\frac{I_h}{I}\right)^2 h^{0.8}}{\sum_{h=1}^{h=h_{\max}}\left(\frac{I_h}{I}\right)^2} \tag{2.14}$$

2.2.5 Transformer capability equivalent calculation using data available from certified test report

For the determination of Top-Oil and Hot-Spot temperatures in existing transformers for which the manufacturer did not perform a test to measure the winding eddy current losses, the recommended practice proposes to use the limited data in the certified test report. In order to make the calculation with limited data, certain assumptions have been made that are considered to be conservative. These assumptions may be modified based on guidance from the manufacturer for a particular transformer.

A high percentage of the leakage flux flowing axially in and between the windings is attracted radially inward at the ends of the windings because there is a

lower reluctance return path through the core leg than through the unit permeability space outside the windings. As a result, the highest magnitude of the radial component of leakage flux density (and highest eddy loss) occurs in the end regions of the inner winding. In the absence of other information, the inner winding may be assumed to be the low-voltage winding.

The stray loss component of the load loss is calculated by subtracting the I^2R loss of the transformer from the measured load loss. Therefore:

$$P_{TSL\text{-}R} = P_{LL\_R} - \underbrace{K \times [(I_{1\text{-}R})^2 \times R_1 + (I_{2\text{-}R})^2 \times R_2]}_{P_{I^2R}} \text{ watts} \qquad (2.15)$$

where:

K = 1.0 for single-phase transformers

= 1.5 for three-phase transformers

Many test reports for three-phase transformers show the resistance of three phases in series. In these cases values for R_1 and R_2 may be calculated as follows:

Delta Winding: R_1 or R_2 = 2/9 of three-phase resistance
Wye Winding : R_1 or R_2 = 2/3 of three-phase resistance

For oil-filled transformers, the winding eddy loss is assumed to be:

$$P_{EC-R} = P_{TSL-R} \times 0.33 \text{ watts} \qquad (2.16)$$

The other stray losses are then calculated as follows:

$$P_{OSL-R} = P_{TSL-R} - P_{EC-R} \text{ watts} \quad (2.17)$$

In order to determine the Top-Oil rise, the total losses must be corrected to reflect the rms current and also the effects of the harmonic content.

$$P_{LL}(pu) = I(pu)^2 \times \frac{I_1}{I_R} \text{ (pu)} \quad (2.18)$$

$P_{LL}(pu)$ is used to correct the losses and the newly calculated losses are used in the temperature calculations.

The Top-Oil temperature rise can be calculated using the following formulation, where n is 0.8 for ONAN, 0.9 for ONAF or OFAF and 1 for ODAF typed cooling.

$$\Delta\Theta_{TO} = \Delta\Theta_{TO-R} \times \left(\frac{P_{LL} + P_{NL}}{P_{LL-R} + P_{NL}} \right)^n \ ^oC \quad (2.19)$$

The winding Hot-Spot conductor rise is also proportional to the load losses to the 0.8 exponent and may be calculated as follows:

$$\Delta\theta_g = \Delta\theta_{g-R} \times \left(\frac{1 + 2.4 \times F_{HL} \times P_{EC-R}(pu)}{1 + 2.4 \times P_{EC-R}(pu)} \right)^{0.8} \ ^oC \quad (2.20)$$

or

$$\Delta\theta_g = \Delta\theta_{g-R} \times \left(\frac{1 + 2.8 \times F_{HL} \times P_{EC-R}(pu)}{1 + 2.8 \times P_{EC-R}(pu)} \right)^{0.8} \quad ^oC \tag{2.21}$$

2.2.6 Transformer capability equivalent calculation when certified test report is unavailable

It is desired that TEMPEST can be applied to all transformers in Turkish Electricity Transmission System. These include the transformers which do not possess the manufacturer's certified test reports. Although few in number, these transformers can be covered, too. The calculation inputs can be acquired from only the nameplate of the transformer and a number of assumptions. The accuracy of the results will be highly decreased when compared to the measurements with more available data and it is highly recommended to acquire a certified test report for TEMPEST to operate effectively.

The main lacking inputs are the Load and the No-Load Losses under rated conditions. There are assumptions to apply for the loss calculations [21, 22]. Considering the most suitable percentage rate, the following assumptions for TEMPEST to operate successfully were performed as seen on Table 1.

Also the HV and LV winding resistances were predicted by comparing the initial calculated Top-Oil temperature value to the oil temperature thermometer located on the transformer.

Table 1 Assumptions for Power Transformers Losses (as percentage of Total Power) [21, 22]

Load Loss	0.7%
No-Load Loss	0.1%

2.3 IEEE Std C57.91 (IEEE Guide for Loading Mineral-Oil- Immersed Transformers)

Since IEEE Std. C57.110-1998 only gives instantaneous results, a method is needed to analyze the dynamic thermal characteristics of the transformer so that the previous temperatures values are taken into account.

The "IEEE Loading Guide", IEEE Std. C57.91-1995, which has been used by electricity companies [23], provides a baseline (Clause 7) and an alternate method (Annex G) to predict the dynamic thermal behavior of Top-Oil and Hot-Spot temperatures. The alternate method (Annex G) requires one more critical input data from the manufacturer's report; the bottom-oil temperature.

The bottom-oil temperature is not provided by manufacturers worldwide [9]. Also the technical specifications of TEİAŞ do not require the bottom-oil temperature under rated load values to be declared in the manufacturer's test report. So the Annex G method cannot be implemented for monitoring the dynamic thermal behavior of the system.

The Clause 7 model described below is used in this thesis which has shown comparable good results when compared to the works performed by other research projects [2, 10].

2.3.1 Top-Oil rise over ambient

The Top-Oil temperature rise at a time after a step load change is given by the following exponential expression containing an oil time constant:

$$\Delta\Theta_{TO} = \left(\Delta\Theta_{TO,U} - \Delta\Theta_{TO,I}\right)\left(1 - \exp^{-\frac{t}{\tau_{TO}}}\right) + \Delta\Theta_{TO,I} \tag{2.22}$$

2.3.2 Oil time constant

As a very practical approach, the former IEC 354 loading guide for oil immersed power transformers [24] suggests oil time constant as 150 min for the oil natural-air natural (ONAN) and oil natural-air forced cooling modes (ONAF). In the case of the oil forced-air forced cooling mode (OFAF) it is suggested to use the oil temperature of the oil leaving the winding. This has not been practiced in industry due to difficulties in recording the temperature of the oil leaving the winding. Therefore it suggests using an oil-time constant of 90 min for OFAF cooled units.

However in the IEEE Loading Guide, a method which defines the time constant according to the weight of the components of the transformers has been suggested. The time constant varies according to the cooling types of the transformer such as the ONAN, ONAF and OFAF.

For ONAN and ONAF type transformers;

C=0.1323 (weight of core and coil assembly in kilograms) (2.23)

+ 0.0882 (weight of tank and fittings in kilograms)

+ 0.3513 (liters of oil)

For OFAF type transformers; (2.24)

C=0.1323 (weight of core and coil assembly in kilograms)

+ 0.1323 (weight of tank and fittings in kilograms)

+ 0.5099 (liters of oil)

The Top-Oil time constant at rated kVA is given by the following:

$$\tau_{TO,R} = \frac{C\Delta\Theta_{TO,R}}{P_{T,R}} \tag{2.25}$$

2.3.3 Winding Hot-Spot rise

Transient Winding Hot-Spot temperature rise over Top-Oil temperature is given by:

$$\Delta\Theta_H = \left(\Delta\Theta_{H,U} - \Delta\Theta_{H,I}\right)\left(1 - \exp^{-\frac{t}{\tau_W}}\right) + \Delta\Theta_{H,I} \tag{2.26}$$

The winding time constant (τ_w) is the time it takes the winding temperature rise over oil temperature rise to reach 63.2% of the difference between final rise and initial rise during a load change. The winding time constant may be estimated from the resistance cooling curve during thermal tests or calculated by the manufacturer using the mass of the conductor materials.

For use in TEMPEST program, the winding time constant is estimated from the resistance curve during thermal tests since the manufacturer does not provide the winding time constant separately.

2.4 Further Research Studies on Top-Oil and Hot Spot Temperatures

Although the IEEE Standards have been accepted as the baseline for the studies performed later on, there are also considerable works to improve the accuracy and the precision of the temperature prediction.

Even if these methods are reported to provide improved calculations, they require more input data (such as winding eddy-current loss data, bottom-oil temperature under rated load) which is not provided by the manufacturers' of the transformers operating worldwide [9] and also in Turkey. Another important factor is that this work has been performed to provide practical temperature calculations. Most of the input data can be acquired from the transformer's nameplate. The rest can be acquired from the manufacturer's test report or by estimating the values of the required data. In any case, no special data will be needed for the method defined.

2.4.1 Improvement on the calculation of temperatures

As described also in IEEE Std. C57.110-1998, the assumption that eddy losses are proportional to the square of the frequency will cause accurate results for the small conductors and low harmonics, with errors on the high side, for a combination of larger conductors and higher harmonics.

A corrected Harmonic Loss Factor has been suggested which provides more accurate calculations [6]. However, this method is not practical because it requires complicated data such as the type, thickness of the conductor and the winding-eddy current loss data.

Another method [2] has been reported to perform further improvements to the Harmonic Loss Factor. This method is based on the work of [6], however the penetration depth has been taken into account. Penetration depth has a significant effect on the Harmonic Loss Factor, especially as the conductor get larger in diameter and the harmonic frequency increases. This effect is called skin effect. This corrected eddy current loss factor considers the field penetration in the conductor due to skin effect. This method requires the axial and radial winding eddy current losses which shall be calculated using Finite Element Method in addition to the data mentioned for the method of [6].

A theoretical model has been developed based on boundary value problem of heat conduction in transformer winding using finite integral transform techniques [7]. However the model requires, in addition to electrical parameters of the transformer, information on the actual design data. Also in addition to these, the

authors admit that their findings are not compared to experimental data. The results are compared only theoretically.

2.4.2 Improvement on Dynamic Thermal Behavior

The IEEE Std. C57.91-1995 provides two methods to predict the dynamic behavior of the temperatures and more research has been applied to further improve the method in Annex G. In the case that the bottom-oil temperature under rated load data is received from the manufacturer's test report, there are many suggestions to be performed which are reported to improve the Annex G method [2, 10].

There are also researches on the method in Clause 7 [8, 9, 10, 13]. In the original Loading Guide, the ambient temperature changes have not been taken into account in the thermal model. [8, 9] modified to Clause 7 model to take the continuous variation of the ambient temperature into account.

The ambient temperature varies on a daily and seasonal basis [8]. The thermal time constant of a large transformer can be on the order of hours; thus, the transformer temperature will naturally lag behind the daily cycle of ambient temperature changes. Even if the loading were constant, the Top-Oil temperature rise over ambient temperature would not be. This effect is not captured by the IEEE/ANSI model but is significant for a transformer placed in an environment subject to daily variations in ambient temperature that are of the same order of magnitude as the Top-Oil temperature rises due to load loss. For monitoring and diagnostic purposes it is essential to capture this phenomenon.

The Top-Oil temperature calculation Equation (2.27) is the modified version of the equation (2.22) which takes into account the variations in the ambient temperature [8]. This Top-Oil temperature model has been used to simulate the dynamic thermal modeling of the transformer in this thesis.

$$\Theta_{TO} = \left(\Theta_{TO,U} - \Theta_{TO,I} + \Theta_A\right)\left(1 - \exp^{-\frac{t}{\tau_{TO}}}\right) + \Theta_{TO,I} \tag{2.27}$$

In the original study of Susa [10], the TM1 and TM2 models; the models with the ability to perform on manufactures test report data rather than requiring the additional bottom oil temperature, had performed somewhat less accurate than the IEEE method. However a very recent research [11, 12] has made use of Susa's method which reported to be more accurate than the IEEE method. Larger datasets are needed to validate the applicability or the superiority of the models.

2.5 Final Method

The final method imports the Top-Oil and Hot-Spot temperature calculations from IEEE Std. C57.110-1998. The dynamic thermal modeling is adopted from Clause 7 of IEEE Std. C57.91-1995 with a slight difference; the method proposed by [8]. The simplified diagram has been shown in Figure 1.

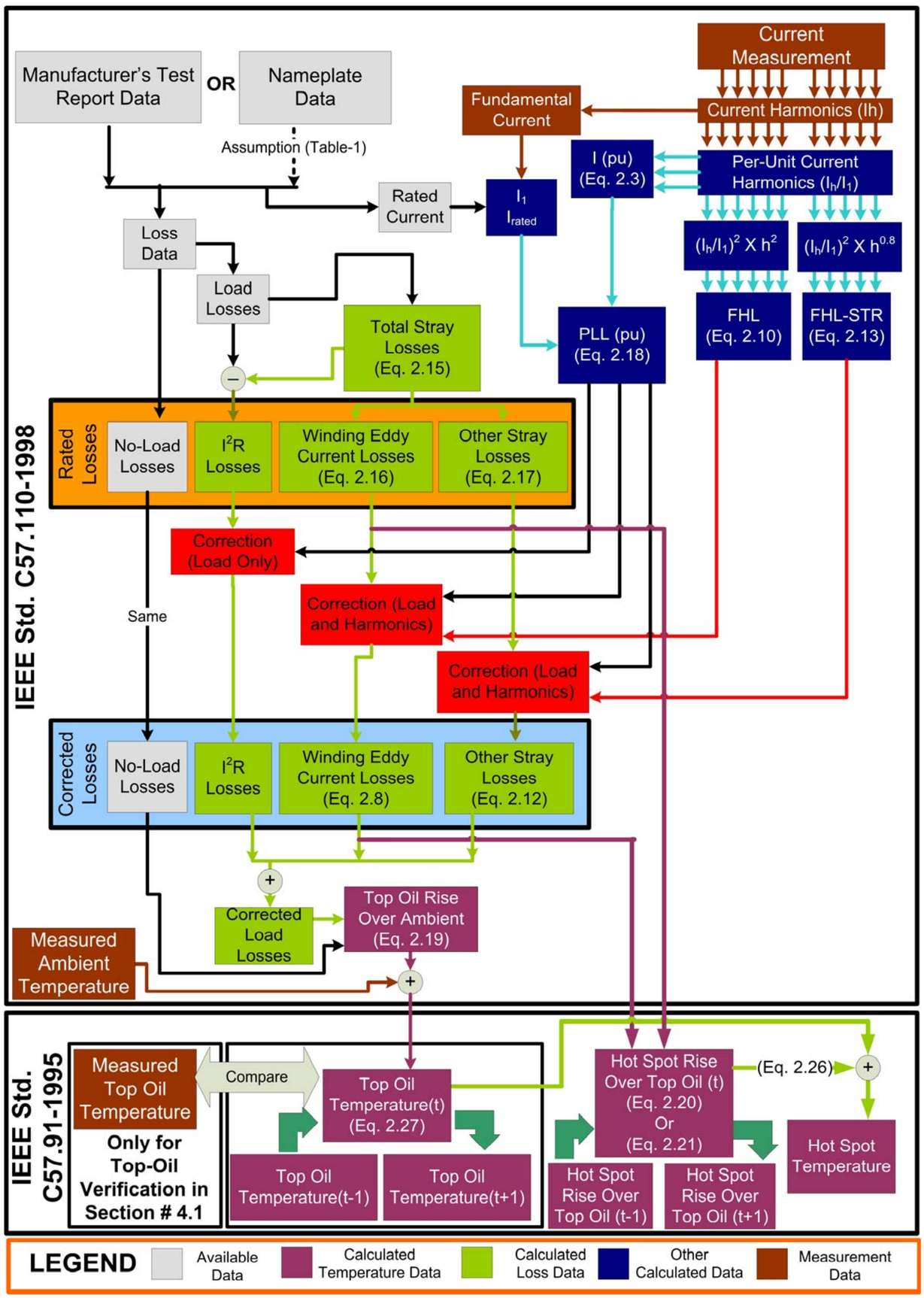

Figure 1 Flowchart of the performed method

CHAPTER 3

TEMPEST (Temperature Estimation) PROGRAM

3.1 Introduction

To estimate the temperatures correctly, the load current and its harmonics should be accurately measured. Failure to measure these data will result in miscalculation and the invalidity of the measurement. So the measurements shall be performed on a measurement device which has already validated its usefulness, accuracy and precision.

Mobile Power Quality Monitoring Devices provided successful measurements during the National Power Quality Project of TÜBİTAK. Their capability to measure currents, sensitivity to harmonic content, ability to notice transients effectively etc., have been proven by continuously performed measurements throughout Turkey.

In this thesis, a computer program called TEMPEST (TEMPerature ESTimation) has been developed as an upgrade to the already available program of the Mobile Power Quality Monitoring Devices. TEMPEST utilizes the existing program and devices to measure the required data (such as the phase currents, corresponding current harmonics etc.). Most of the input data to the TEMPEST are already available from Mobile Monitoring System. TEMPEST then calculates the Top-Oil and Hot-Spot temperatures using the received data. The additional input data for

the TEMPEST (i.e. measured Top-Oil temperature for verification purposes and the ambient temperature) has been acquired by modifying the original program. All these measurements have been performed online using Labview as the software and Mobile Power Quality Monitoring Devices as the hardware.

To test the validity of the results, fiber optic sensors shall be placed to the possible Hot-Spot locations during the manufacturing process. Since there was no such power transformer being produced for TEİAŞ, the Top-Oil temperature has been selected as the verification parameter.

3.2 Hardware

Each Mobile Power Quality Monitor System [25] consists of: National Instruments SC-2040 Sample&Hold Card [26], National Instruments DAQ Card 6036E [27], 3 Current Probes (1mV/10 mA), Voltage Divider (100/3.8 V), Laptop Computer, NI Labview Software [28], uninterruptible power supply for current probes, and isolation transformer, as shown in Figure 2a.

The TEMPEST system modified for general use is as shown in Figure 2b. An additional input of measured ambient temperature is required for the TEMPEST to operate properly.

The TEMPEST system developed only for the comparison of measured and calculated Top-Oil temperature has been shown in Figure 2c. Also as a further research study, the measured and calculated Hot-Spot temperatures can be compared which has also been shown in the figure.

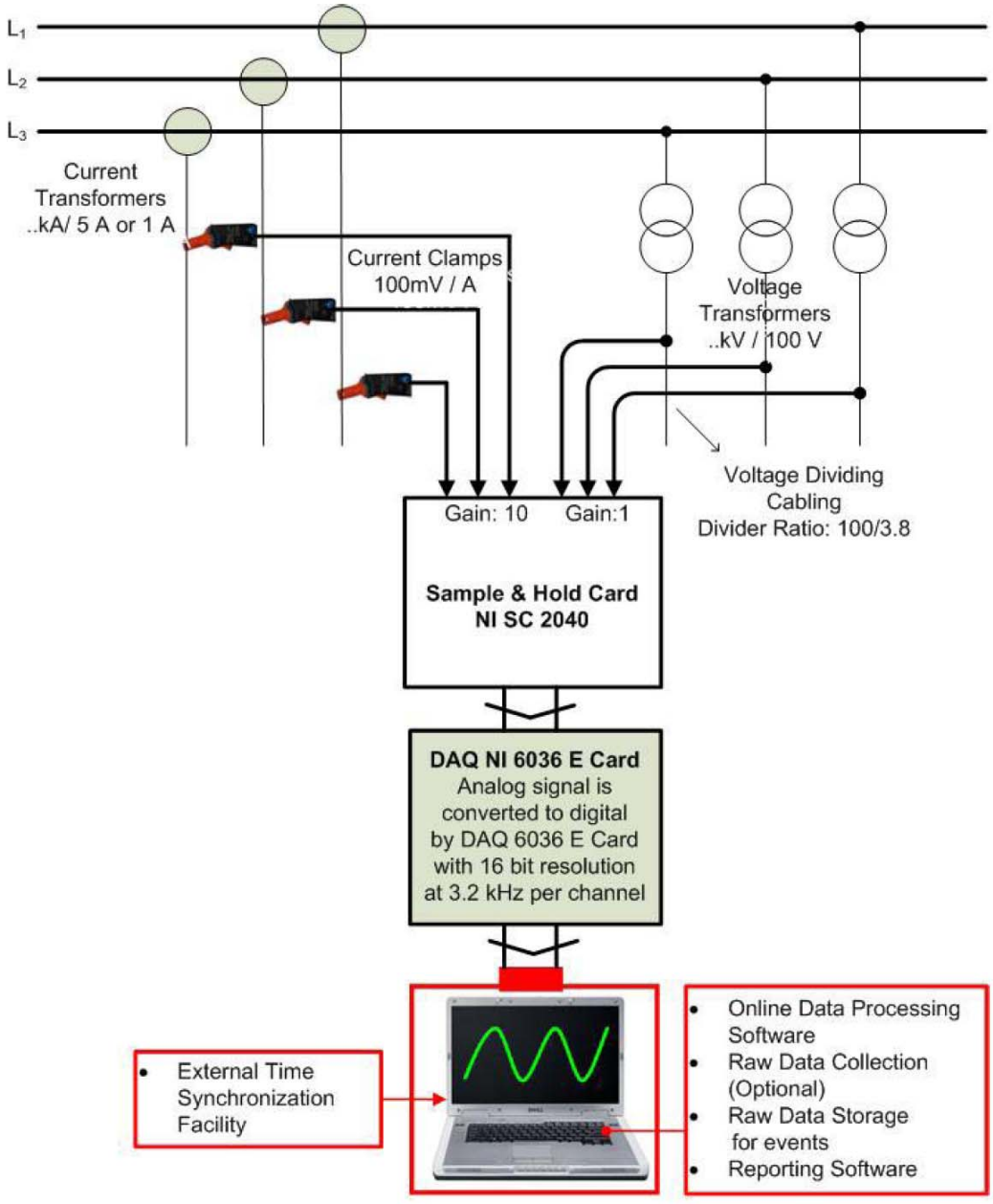

a. Hardware setup used in Mobile Power Quality Devices

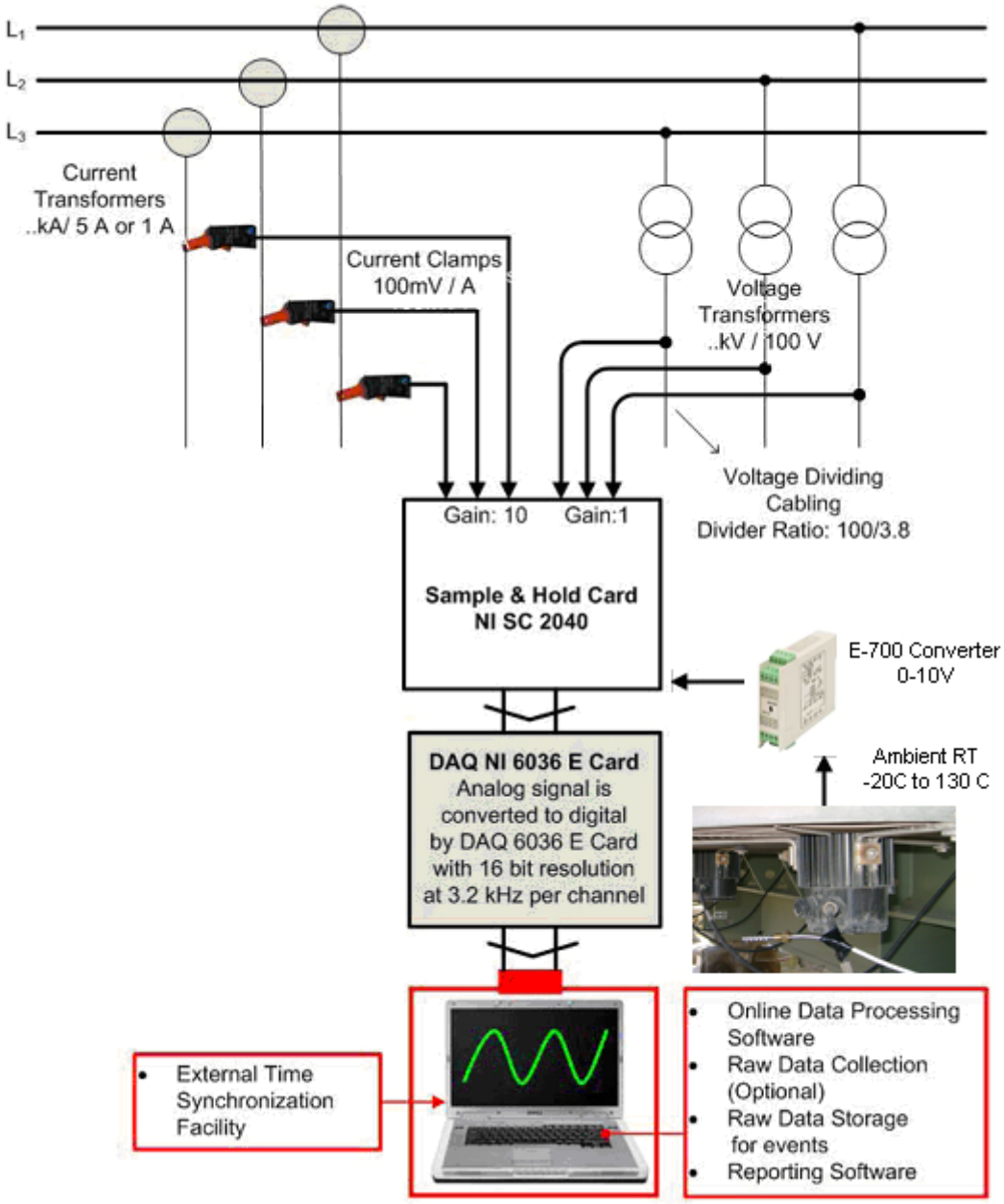

b. TEMPEST for generalized use

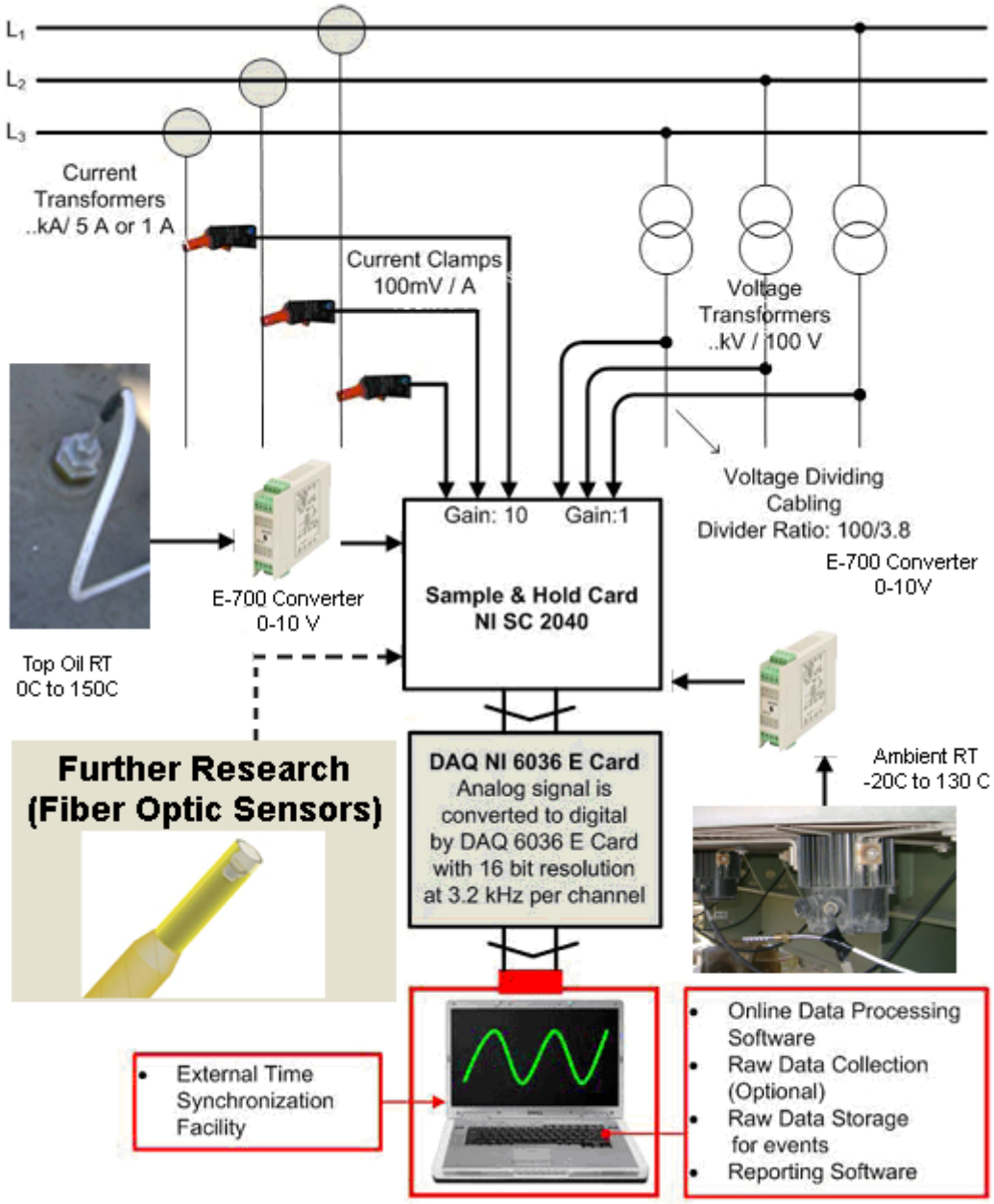

c. TEMPEST for experimental validation of temperature prediction

Figure 2 Block diagram of PQ monitoring set-up upgraded for Hot-Spot and Top-Oil temperature prediction

The thermometers used in this thesis are Resistive Thermometers (RT). The resistive thermometers are a more recent technology than the thermocouples which had been used for transformer temperature calculations in the previous studies. The RTs provide better performance in lower temperature values (such as the temperature range of -20 ^{o}C to 150 ^{o}C used in this thesis) compared to thermocouples.

The RT output is specially made from 3 wires, since the distance between the installation area and the DAQ Cards sometimes reach 40m. Between 10-150 m, it is best to use 3 wire configurations as seen in Figure 3 instead of 2 wire configuration.

The output of the RT is a resistance while the input of the sample&hold card needs a voltage level between ±10V. To perform this conversion, E-700 type converter has been used. The thermometers and E-700 type converters are PT-100 compatible. PT-100 is an accepted and widely used standard in temperature measurement equipment. The response of platinum to temperature changes is nearly linear. Combined with the performance increase in RTs, a PT-100 type RT is chosen as the ideal thermometer for this thesis.

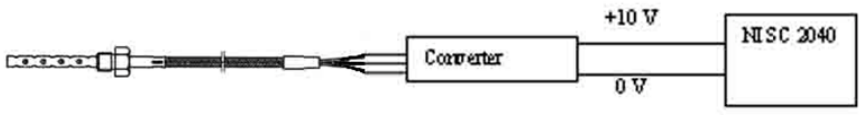

Figure 3 RT 3 wire configuration

Figure 4 Installation of RT for Top-Oil Temperature measurement in the field

Both the ambient temperature (which is directly used in TEMPEST with a temperature range from -20 to 130 ^{o}C) and the Top-Oil temperature (which is used in the stage when comparing the calculated Top-Oil and the measured Top-Oil temperature with a temperature range of 0 to 150 ^{o}C) thermometers use resistive thermometers (RT). The Top Oil Temperature RT is shown in Figure 4. The Ambient Temperature RT is shown in Figure 5.

Figure 5 Resistive Thermometer of Ambient Temperature installed in the field

Also a special model of the Top-Oil measurement RT is chosen so that the sinking length of the RT can be arranged by fastening the equipment when the tip of the RT is 50 mm below the top liquid surface. The 50 mm sinking depth is the recommended depth in [3]. Since the level of the oil may vary between each transformer, this kind of flexibility provides a practical solution.

3.3 Software

The software for the TEMPEST has been developed from the equations defined in the IEEE standards [3, 4] and the study performed in [8]. The computer language has been developed based on LABVIEW.

LabVIEW (Laboratory Virtual Instrument Engineering Workbench) is a graphical programming language that uses icons instead of lines of text to create applications. In contrast to text-based programming languages, where instructions determine the order of program execution, LabVIEW uses dataflow programming, where the flow of data through the nodes on the block diagram determines the execution order of the VIs and functions. VIs, or virtual instruments, are LabVIEW programs that imitate physical instruments [28].

TEMPEST has been designed to fully benefit from the Mobile Power Quality Monitoring Devices used in the National Power Quality Project. However some modifications had been performed to add the temperature prediction algorithm. The existing software defined in Figure 6a has been updated to include these changes. Figure 6b shows the system utilized in generalized use. Figure 6c shows the system utilized in Top-Oil temperature verification.

TEMPEST receives the required data from the original program, calculates the temperature and loss factors and then saves these data to a MS Excel worksheet.

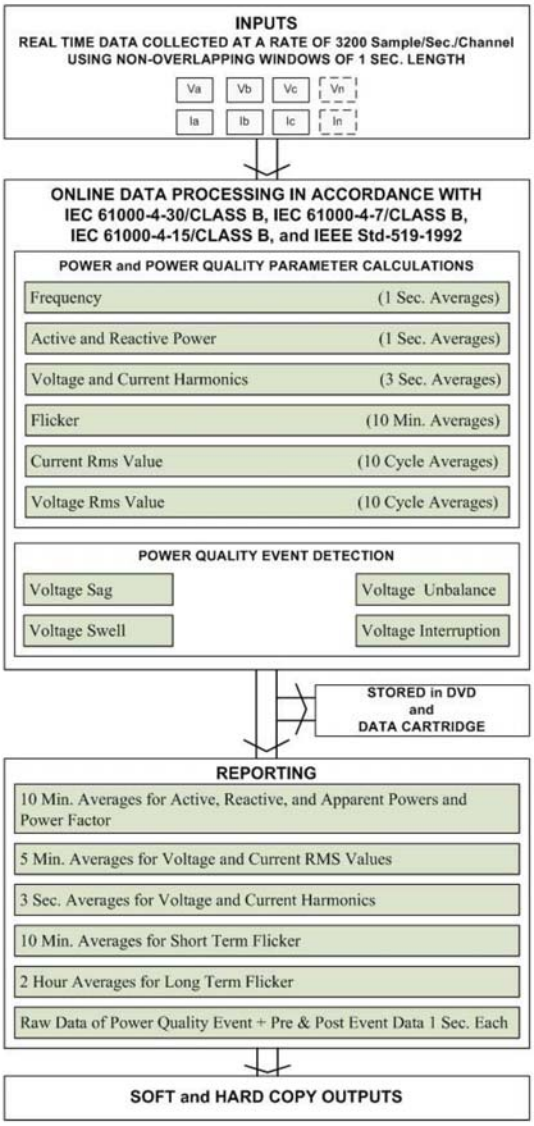

a. Algorithm of Power Quality Monitoring Device

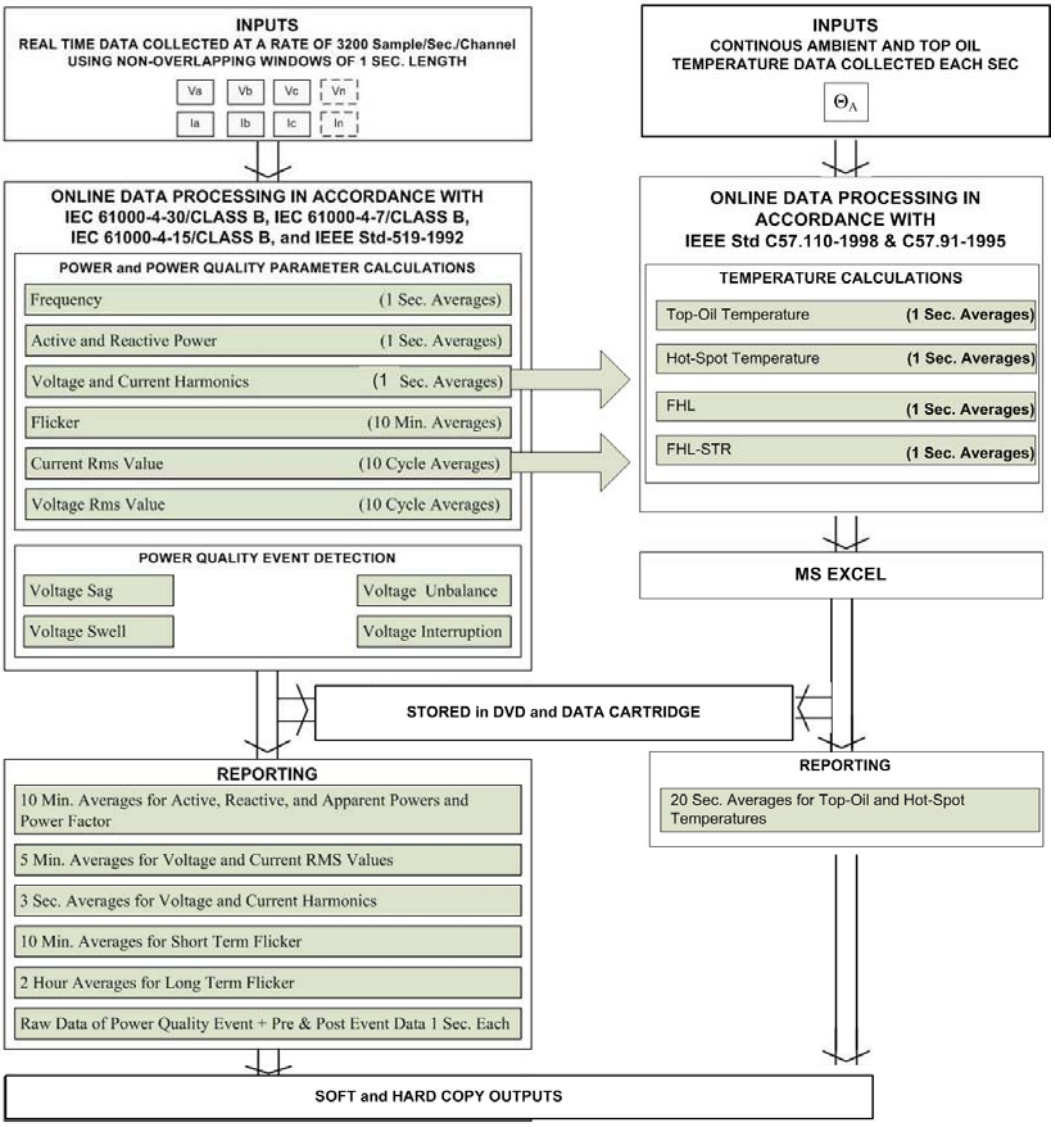

b. For generalized use

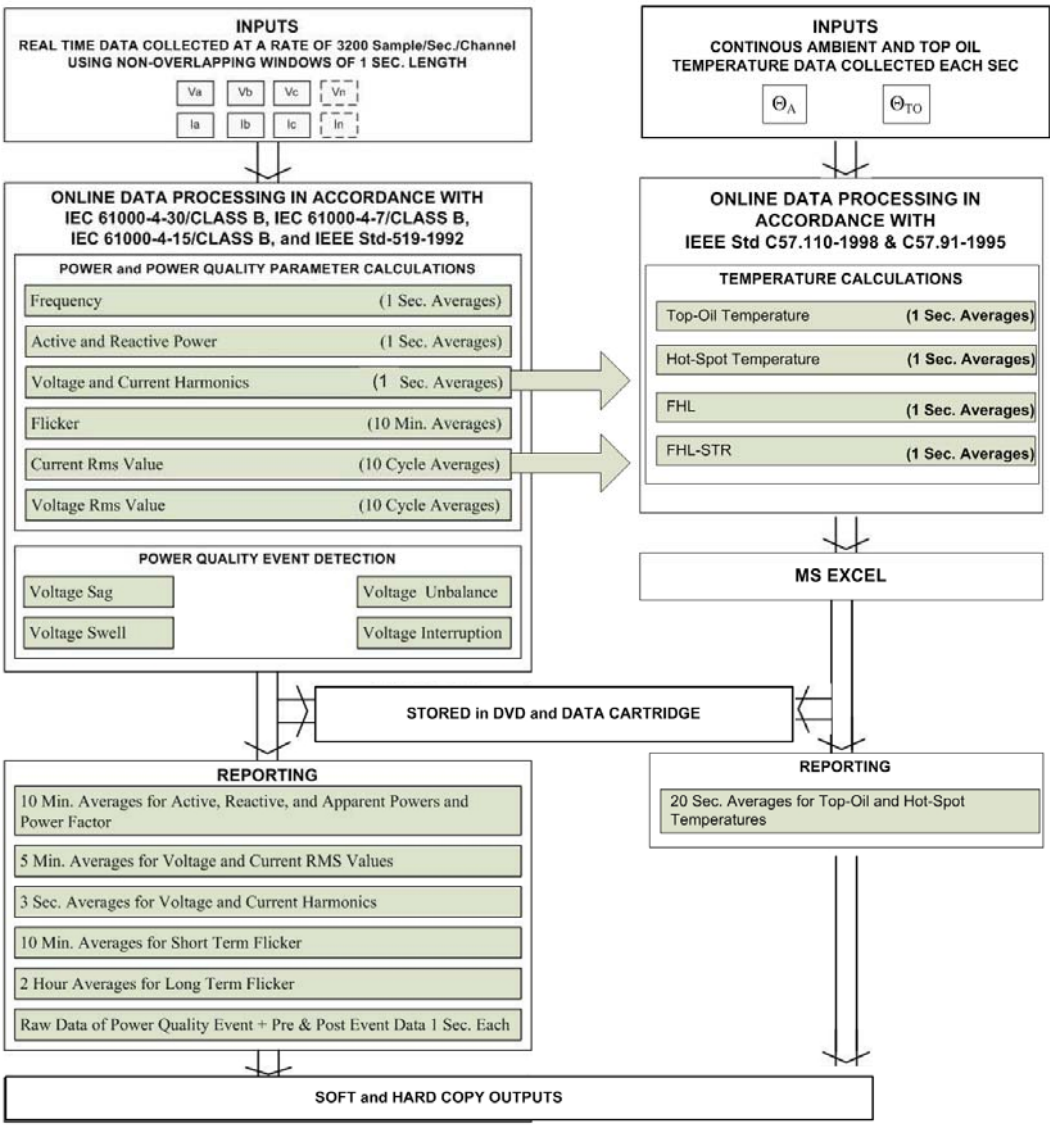

c. For experimental validation of Top-Oil temperature prediction

Figure 6 On-line PQ analysis software upgraded for HST and TOT prediction

TEMPEST calculates the Top-Oil and Hot-Spot temperatures using the rms current and its harmonics. In the original program, the current harmonics were calculated by taking the averages of measured harmonics in 3 second averages. A modification was performed which quickened the harmonic measurement to 1 second averages to provide increased sensitivity to the TEMPEST.

Each second, the harmonics and rms value of the current is transferred from the original program to TEMPEST. Here the temperatures and the harmonics loss factors (FHL and FHL-STR) are calculated.

The ambient and Top-Oil temperature thermometers continuously transfer the measured temperature data to the Labview software. These too are logged to the MS Excel.

For reporting processes, the graphs are generated by using MS Excel. 20 second averages of the measured temperature data are presented in the graphs.

The current harmonics and TDD graphs are generated by the log files of the original program which shows these data as 3 second averages.

It has been arranged that the TEMPEST module is another branch of measurement (As seen in Figure 7 as the Temperature Tab) so the user utilizes TEMPEST inside the main VI of the Mobile Monitoring system. Figure 8 shows a sample detailed view of the background coding of the main program. The TEMPEST program is marked with a red circle. The main program has been modified to transfer the required data to a SubVI which actually processes the temperature calculations.

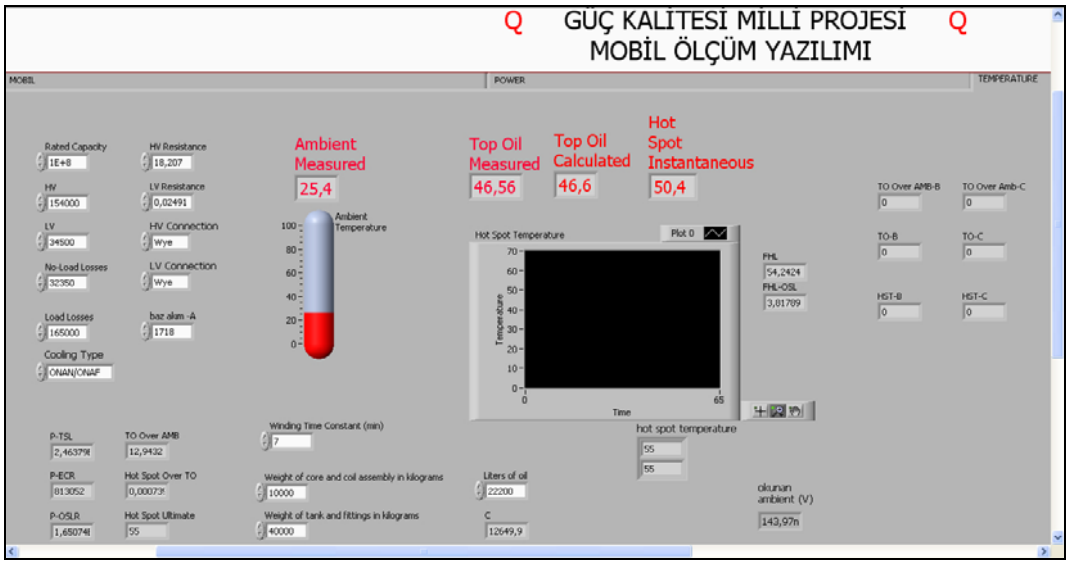

Figure 7 TEMPEST integrated into Mobile Monitoring System

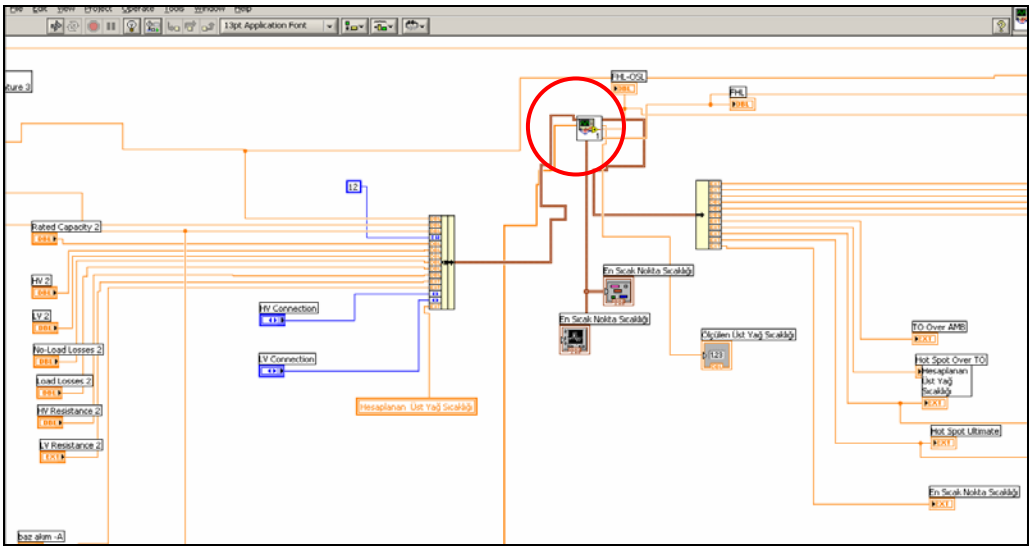

Figure 8 TEMPEST integrated into Mobile Monitoring System (Background)

3.4 Discussions

The temperature prediction is very practical considering the advantages it provides to the power transformer operators. This kind of temperature prediction systems are rapidly increasing throughout the world. Of all the methods defined on temperature estimations, the methods defined in IEEE standards are more popular because of the fact that they are practical and useful.

During the measurement process, a serious problem occurred when using Labview and MS Excel simultaneously. MS Excel was chosen for its capability to create figures which are compatible with other MS Office products such as Word or Power Point. The idea was the easy migration of data to provide compatibility. However, a typical MS Excel worksheet has 65536 rows. Since every second a new data is logged, total logging time lasts for approximately 18 hours. After the last row the program is halted and the program is aborted. The code had been updated to start another sheet after app. 8 hours to overcome this problem.

This solution led to another failure. At the end of each 8 hours, when the new MS Excel worksheet is being opened, the CPU processes the opening operation rather than the Labview's sampling operation. When the new worksheet is opened the CPU returns to process the buffered measurement samples. However, during the opening session, the buffered measurement samples exceed a certain acceptable number. This phenomena causes spikes to appear on the measurement as shown in Figure 9. This effect had been corrected and the related Figures have been produced without the erroneous measurements as shown in Figure 10.

It is concluded that this kind of measurement shall be performed on Labview's own logging files rather than using MS Excel and has been left as a further study.

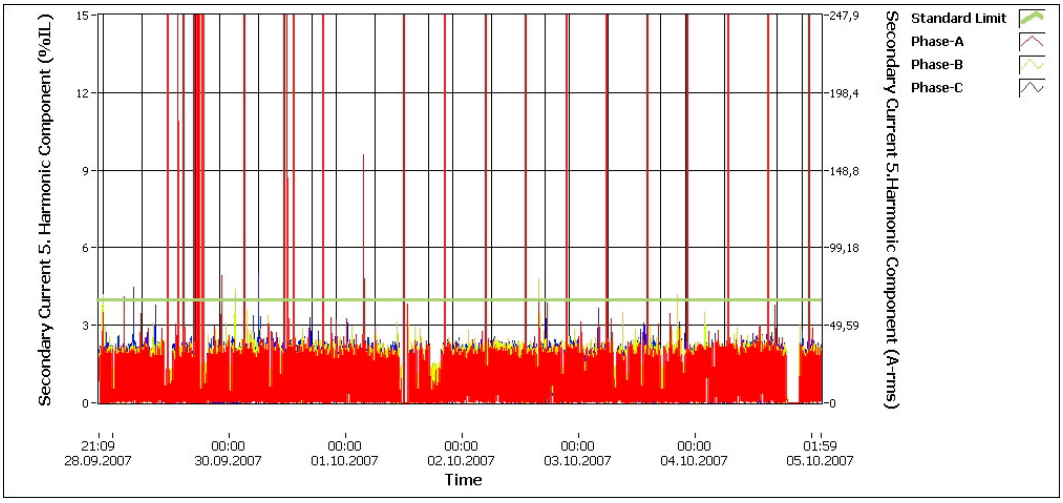

Figure 9 Erroneous Alçuk-B, 5th Harmonic Comp. of the Sec Current (Averaged in each 3 seconds)

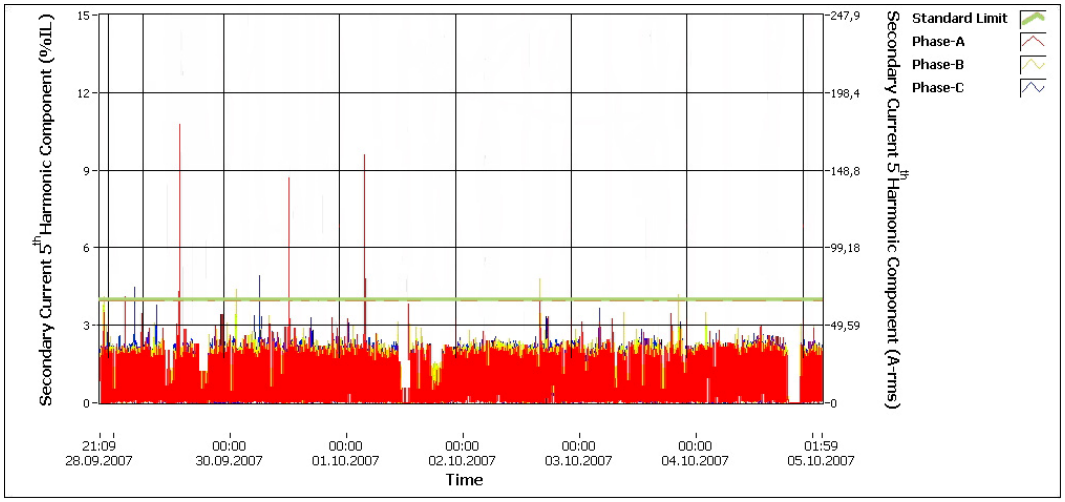

Figure 10 Corrected Alçuk-B, 5th Harmonic Comp. of the Secondary Current (Averaged in each 3 seconds)

Another problem encountered is the distance between the measurement location and the transformer. The main location for the Monitoring Devices is inside the Control Center. Here the current and voltage values are measured. However, the ambient temperature and the Top-Oil temperatures are measured on the transformer itself. This corresponds to a distance of 40m in some transformers. Aside from the long cabling activity this introduces another problem for thermocouples. The voltages generated by thermocouples are prone to noise for this increased length of cables. This had been overcome with the usage of a Resistive Thermometer (RT). RT does not generate a voltage but rather it shows a changing resistance versus temperature. Even if the resistance of the cable is added to the resistance of the RT, a 3 wired configuration is chosen which provided more reliable noise rejection. Also the converter used to convert resistance to voltage which would be an input to the TEMPEST has been placed as close as possible to the RT to further avoid temperature measurement errors.

A last encountered problem is the heating of the measurement equipment. When the temperature of equipment reaches high levels, the results of the measurements tend to become erroneous. The sample&hold and DAQ cards shall be left in relatively cool areas. The equipment shall be kept away from the direct sunlight.

CHAPTER 4

APPLICATION EXAMPLES

A total of 6 power transformer measurements have been performed. The first one to be examined is expected to provide information on the accuracy of TEMPEST. The second one to be presented in this section uses only the nameplate data to predict the temperatures. The remaining 4 measurements can be found in Appendix A.

For both of the transformer measurements presented in this section, the loss and temperature calculation examples are provided for loads with high and low harmonics respectively.

It shall be noted that the process of the installation of a thermometer to an active transformer is a process which shall be performed with haste. To perform this operation the factory has to be disconnected from the transformer and hence it receives no energy during the thermometer installation process. The installation takes approximately 45 minutes. Considering the removal of the thermometer, the factory is disconnected from power lines for a total time of approximately 1.5 hour. This results in a loss of income for the factory. In this thesis, the installation and removal processes have been performed as quickly as possible while giving the first priority to safety.

4.1 80/100 MVA ONAN/ONAF Intermittent Load (Verification)

Figure 11 Transformer Alçuk-B

The transformer B located in Alçuk Transformer Center has been chosen for the verification of TEMPEST. However, another important issue to be discussed is the Top-Oil time constant. Most of the past studies have been performed with the time constants defined in the original edition of the IEEE Loading Guide. There

are very few studies [10] referencing the corrigendum edition. However with the Corrigendum edition [5], the time constant has been corrected. The new time constant has been dramatically shortened. The study has been conducted to show the difference between the two time constants and the effect on the Top-Oil temperature variation.

In addition to the above mentioned situation, there is also another matter requiring attention; unbalanced phases. The methods defined in the standards require only one phase of the current to be used for the calculations even if the transformer is single or three phases. Although this property gives the user simplicity in measurement, the matter of unbalanced loads shall be considered. The verification has been conducted considering all the 3 phases of the transformer. The Top-Oil and the Hot-Spot temperatures have been calculated using the data received from each of the phases. The results have been recorded and the deviations have been compared.

Considering all of the above properties, the verification measurement has been performed in the Alçuk Transformer Center on Transformer B (Figure 11). It shall be noted that, the loading changes according to the stages of metal recycling. The stages in the factory determine the amount and the duration of the loading.

The installation of the Top-Oil temperature thermometer has been defined in Appendix B. The temperature measurements have been performed considering the directions recommended in Annex C of IEEE Std. C57.110-1998 [3]. The ambient temperature was measured by means of a Resistive Thermometer. The thermometer (Figure 12-top left) has been positioned such that the air entering the air inlet of the fans comes into contact with the thermometer.

Table 2 TEMPEST Input data for Alçuk-B

ALÇUK-B TRANSFORMER	
Rated Capacity	100 MVA
HV	154000 V
LV	34500 V
No-Load Losses	32350 W
Load Losses	165000 W
HV Connection	Wye
LV Connection	Wye
Base Current	1718.3 A
Top Oil Time Constant	3.53 hours
Winding Time Constant	7 minutes

Table 2 shows the TEMPEST input data for transformer Alçuk-B. These values have been acquired from manufacturer's certified test report. The temperature data is amplified by a converter and the data is then transferred to the sample&hold card. After the sample&hold card received the data, the information was transferred to the DAQ Card and the computer as shown in Figure 12.

The Top-Oil thermometers which have been already installed by the manufacturer have been periodically read in order to realize if there is an inconsistency between the measured and calculated Top-Oil values.

Figure 12 Alçuk-B test setup

During tests on different occasions, the Top-Oil and Winding temperatures of the thermometers were near equal values. This results from the fact that the harmonic effect to the Winding Hot-Spot temperatures are not taken into account for the winding temperature measurement thermometers. This showed that the winding temperature prediction algorithm used on the transformers is defective in impulsive loading.

4.1.1 Loading and Harmonic Content

Figure 13 shows the Total Demand Distortion graph for the full scale measurement. The overshoots in the graph are the results of erroneous measurements. On the general, the TDD's maximum value is around 15% and the average value is around 10%.

Figures 14-34 show the fundamental and harmonic components of the load current from 2nd to 21st, for all of the 3 phases. It can be seen that the required harmonic content for Hot-Spot temperature calculation is present for this transformer. The acceptable harmonic limits defined by the "Electricity Transmission Demand Safety and Quality Regulations" have been marked as "Standard Limit".

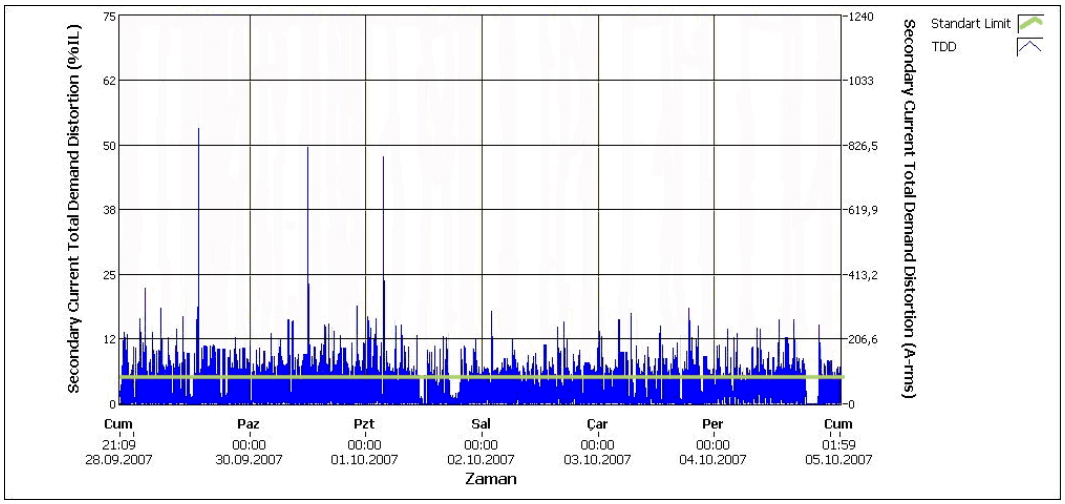

Figure 13 Alçuk-B, TDD

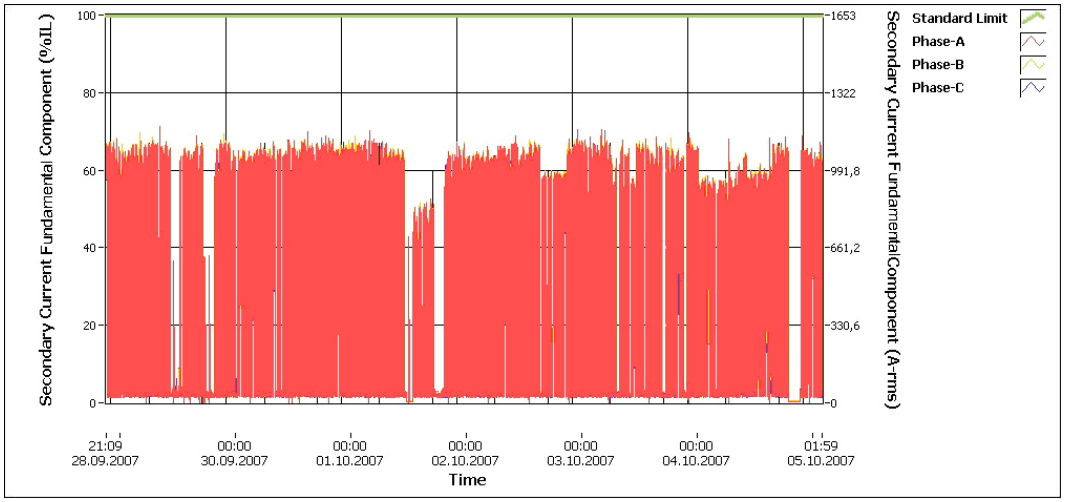

Figure 14 Alçuk-B, Fundamental Component of the Secondary Current (Averaged in each 3 seconds)

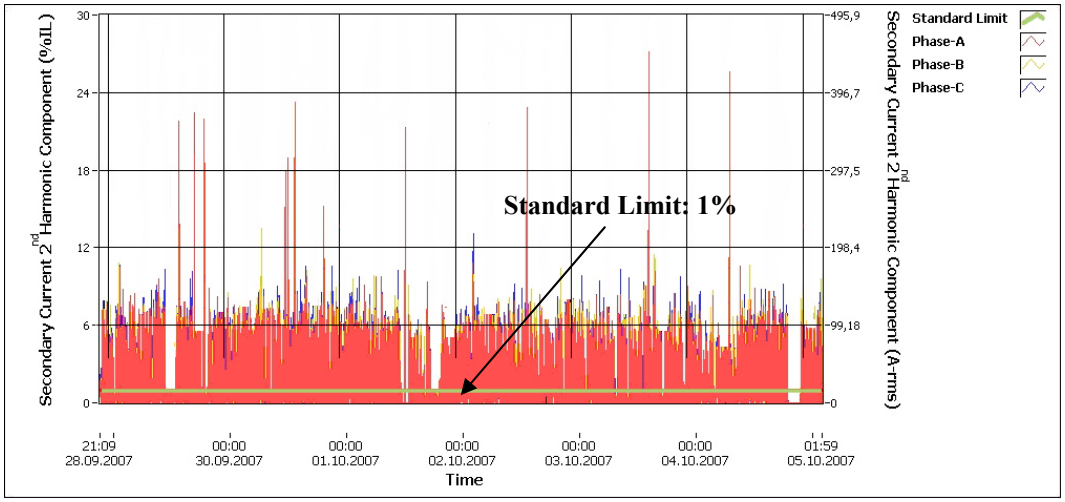

Figure 15 Alçuk-B, 2nd Harmonic Component of the Secondary Current (Averaged in each 3 seconds)

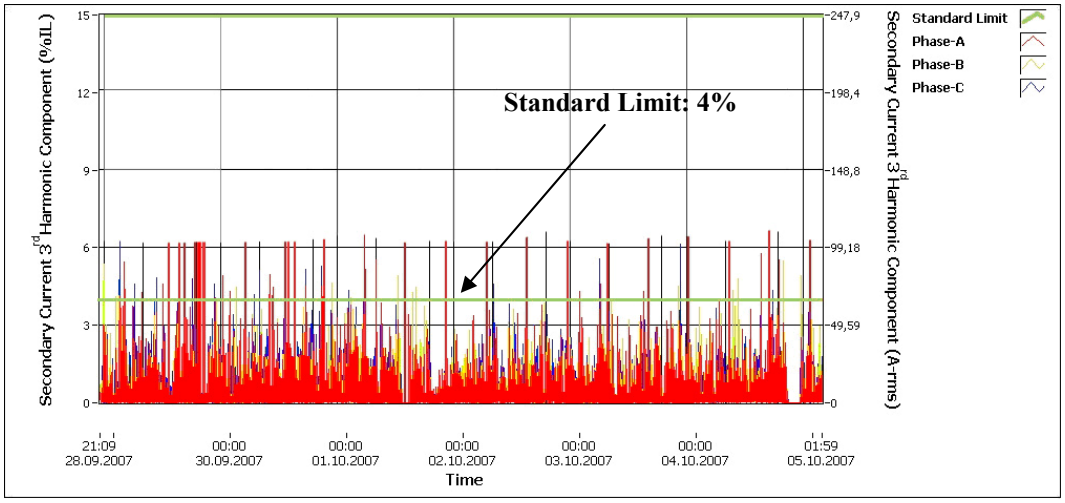

Figure 16 Alçuk-B, 3rd Harmonic Component of the Secondary Current (Averaged in each 3 seconds)

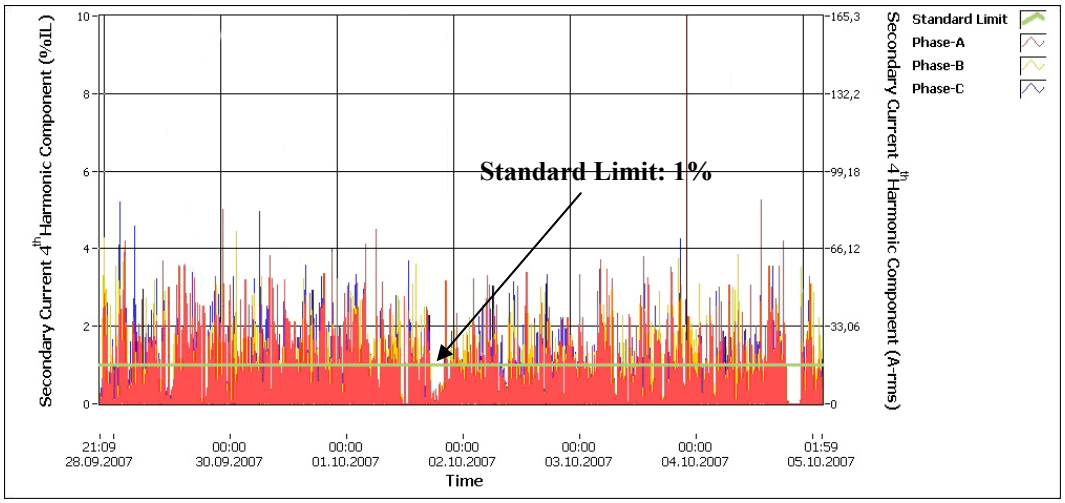

Figure 17 Alçuk-B, 4th Harmonic Component of the Secondary Current (Averaged in each 3 seconds)

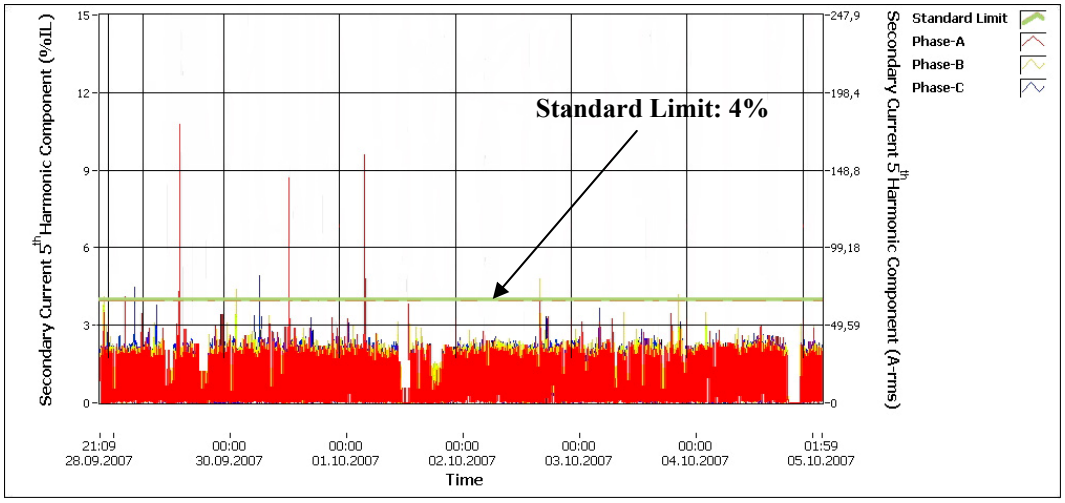

Figure 18 Alçuk-B, 5th Harmonic Component of the Secondary Current (Averaged in each 3 seconds)

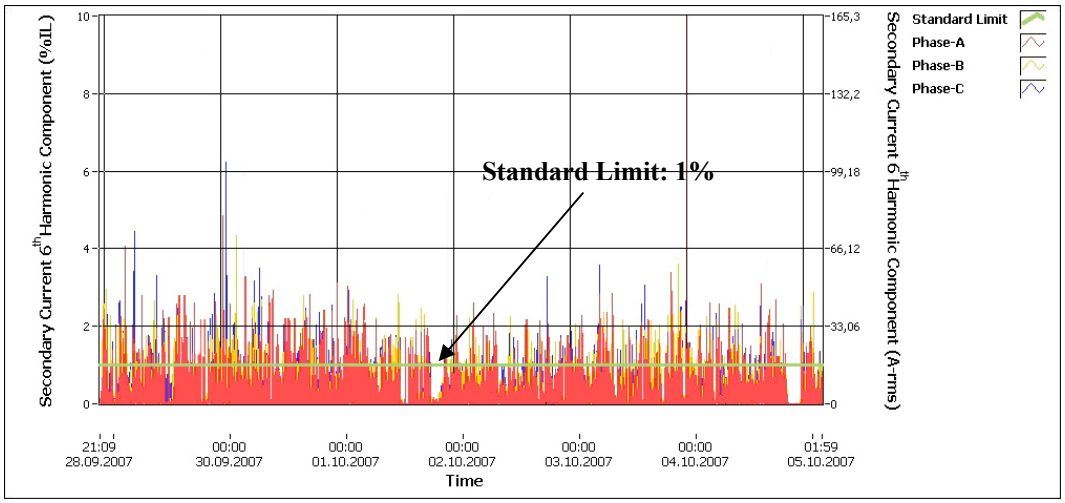

Figure 19 Alçuk-B, 6th Harmonic Component of the Secondary Current (Averaged in each 3 seconds)

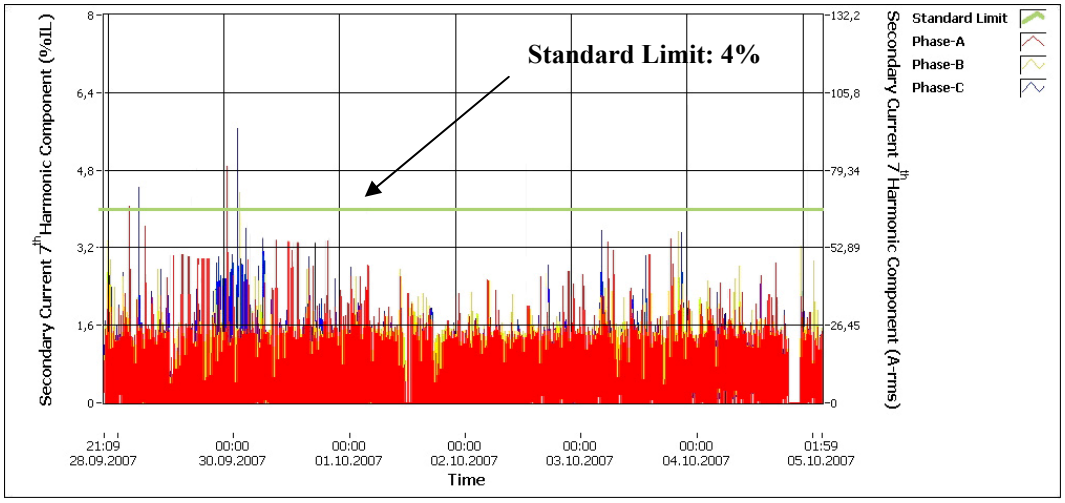

Figure 20 Alçuk-B, 7th Harmonic Component of the Secondary Current (Averaged in each 3 seconds)

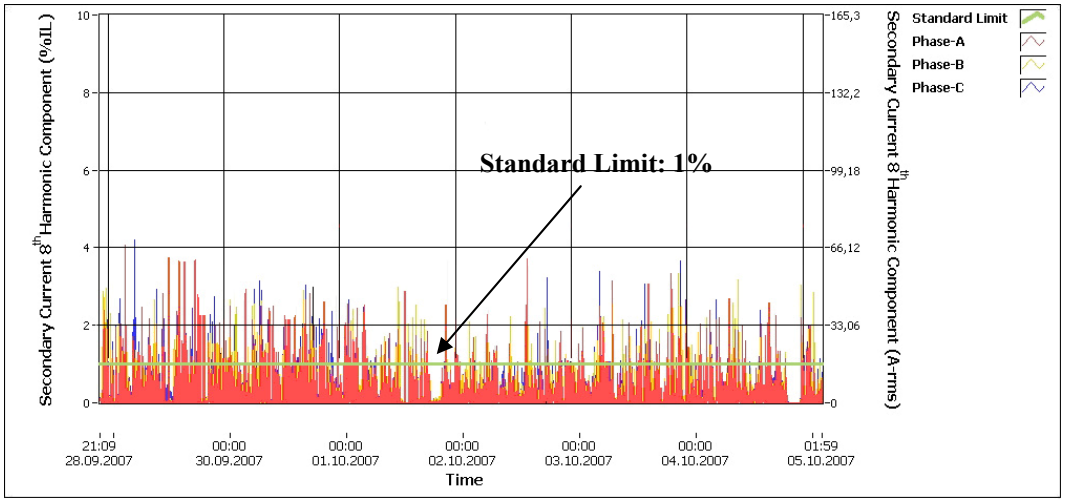

Figure 21 Alçuk-B, 8th Harmonic Component of the Secondary Current (Averaged in each 3 seconds)

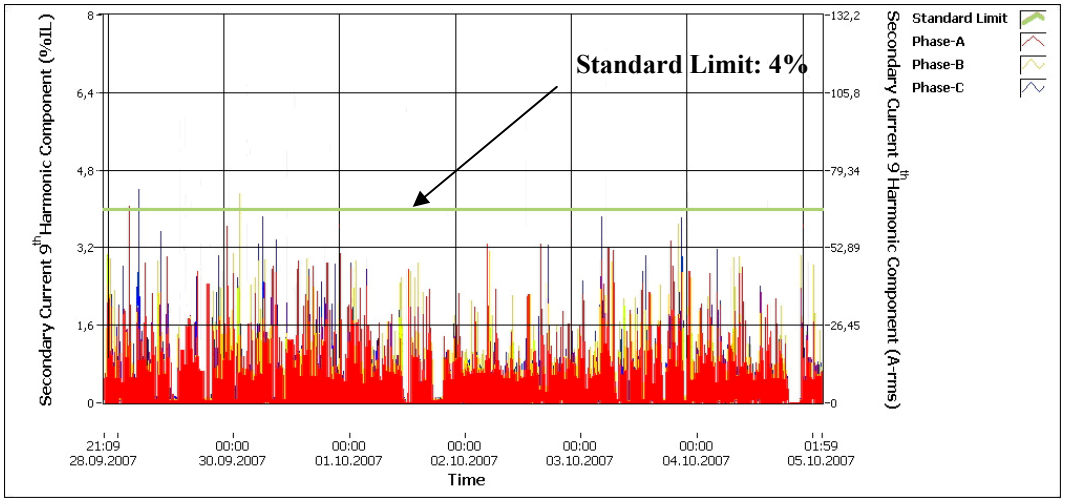

Figure 22 Alçuk-B, 9th Harmonic Component of the Secondary Current (Averaged in each 3 seconds)

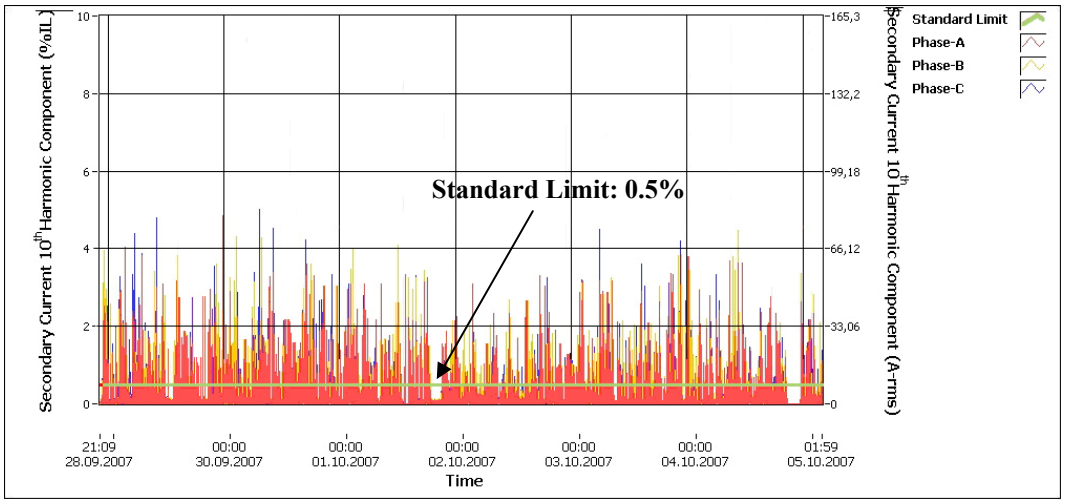

Figure 23 Alçuk-B, 10th Harmonic Component of the Secondary Current (Averaged in each 3 seconds)

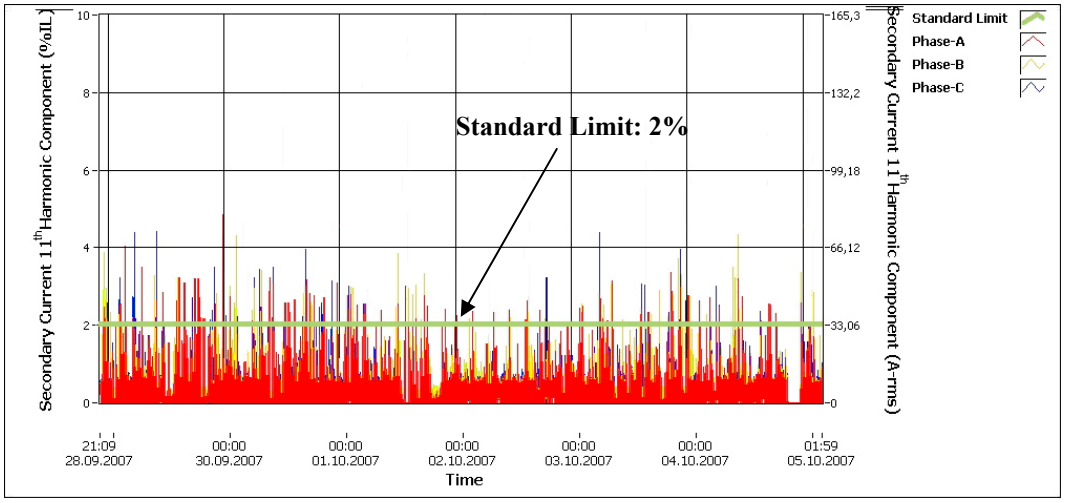

Figure 24 Alçuk-B, 11th Harmonic Component of the Secondary Current (Averaged in each 3 seconds)

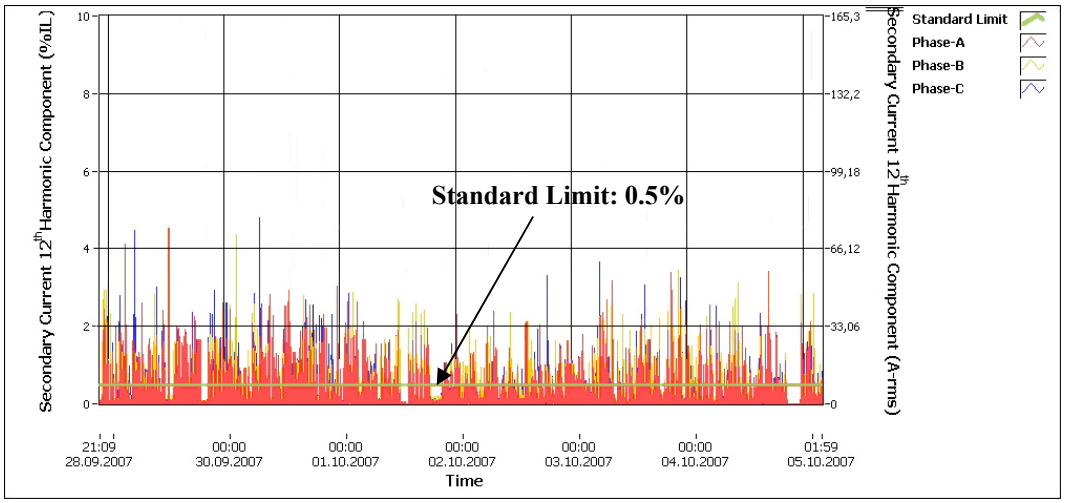

Figure 25 Alçuk-B, 12th Harmonic Component of the Secondary Current (Averaged in each 3 seconds)

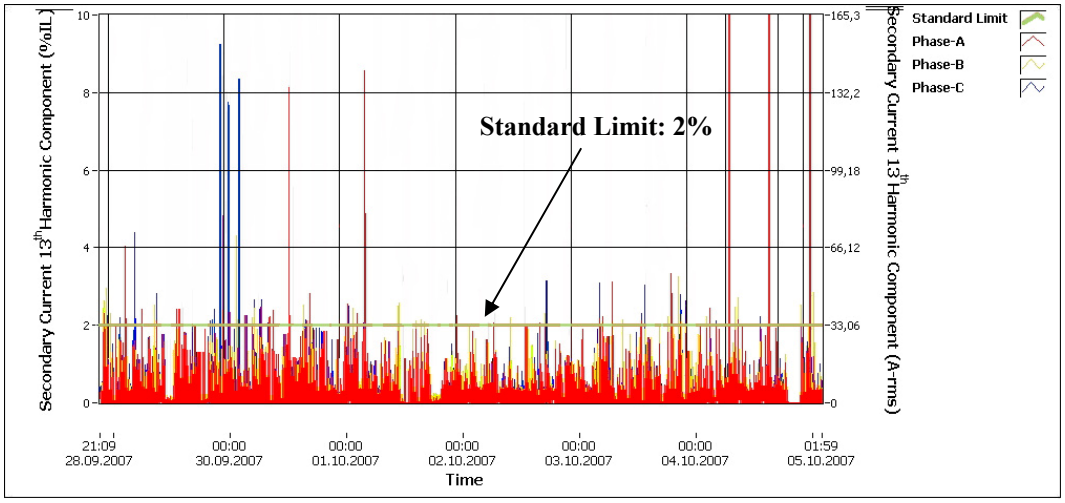

Figure 26 Alçuk-B, 13th Harmonic Component of the Secondary Current (Averaged in each 3 seconds)

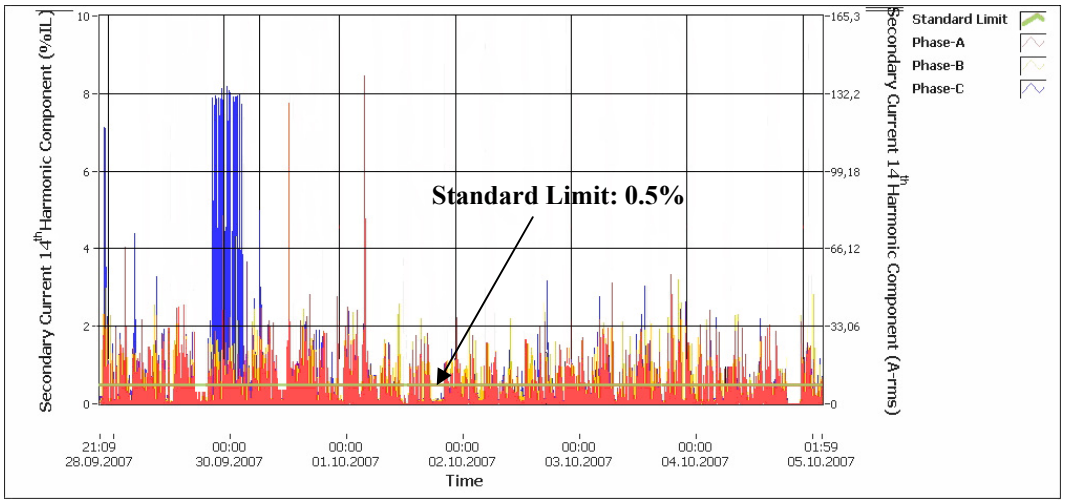

Figure 27 Alçuk-B, 14th Harmonic Component of the Secondary Current (Averaged in each 3 seconds)

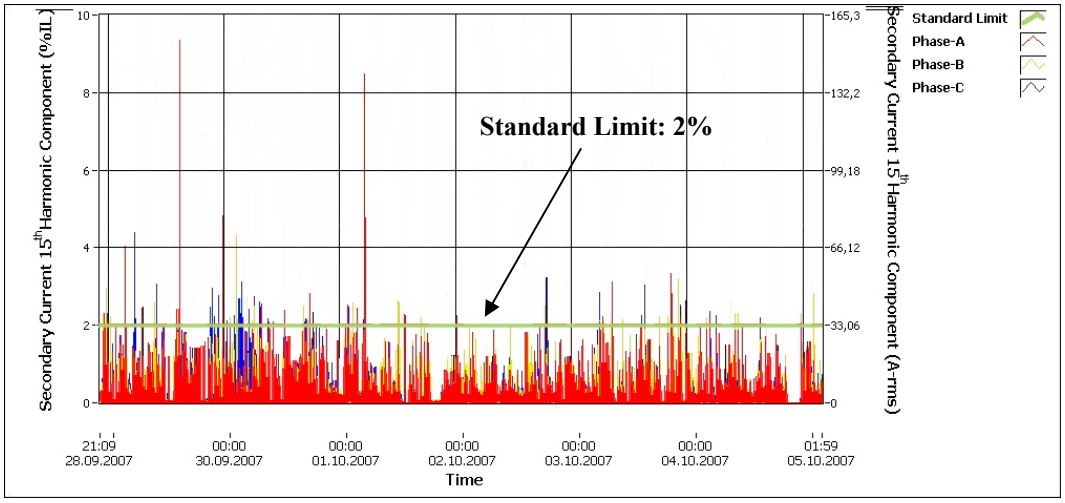

Figure 28 Alçuk-B, 15th Harmonic Component of the Secondary Current (Averaged in each 3 seconds)

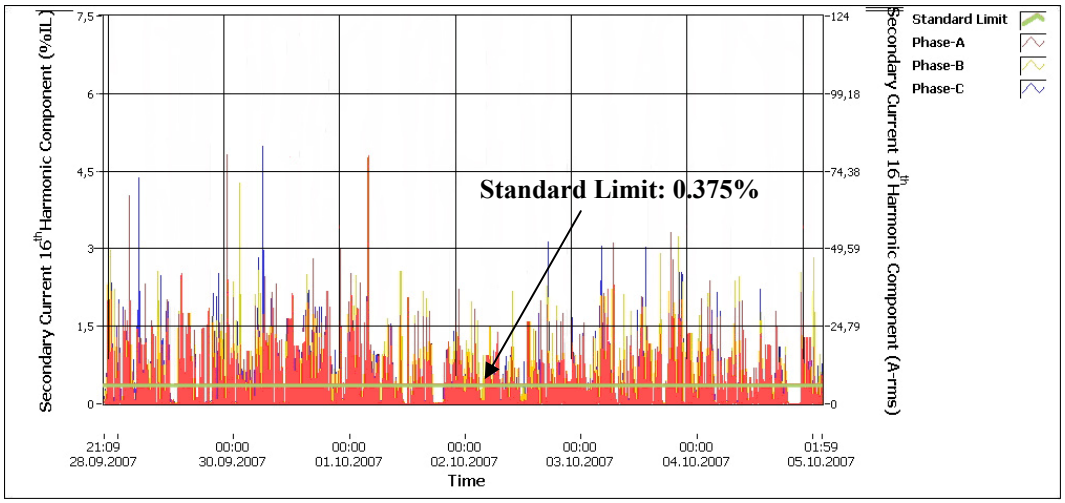

Figure 29 Alçuk-B, 16th Harmonic Component of the Secondary Current (Averaged in each 3 seconds)

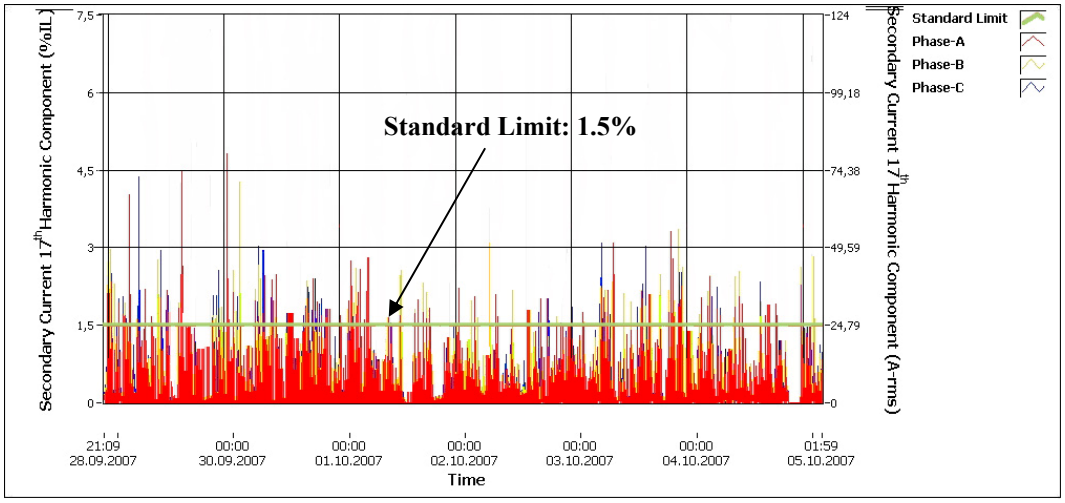

Figure 30 Alçuk-B, 17th Harmonic Component of the Secondary Current (Averaged in each 3 seconds)

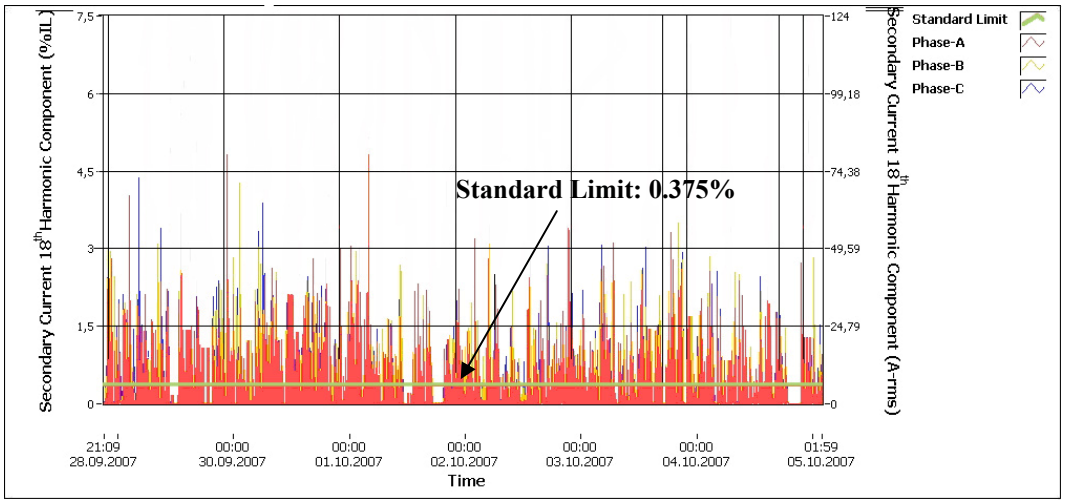

Figure 31 Alçuk-B, 18th Harmonic Component of the Secondary Current (Averaged in each 3 seconds)

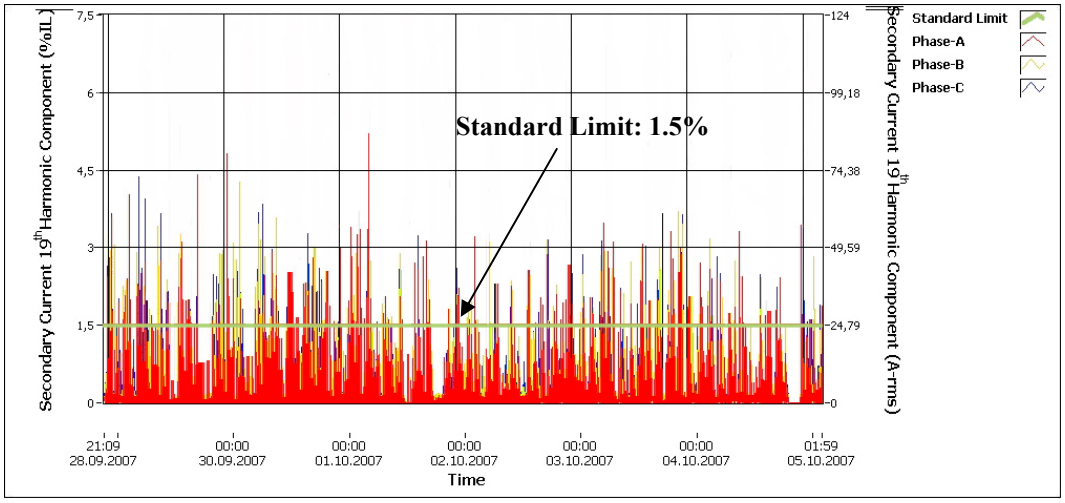

Figure 32 Alçuk-B, 19th Harmonic Component of the Secondary Current (Averaged in each 3 seconds)

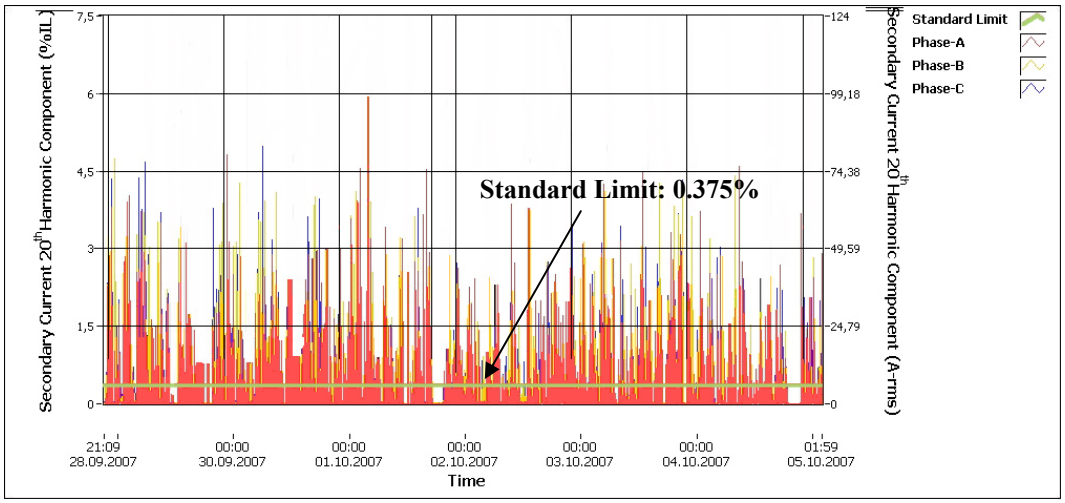

Figure 33 Alçuk-B, 20th Harmonic Component of the Secondary Current (Averaged in each 3 seconds)

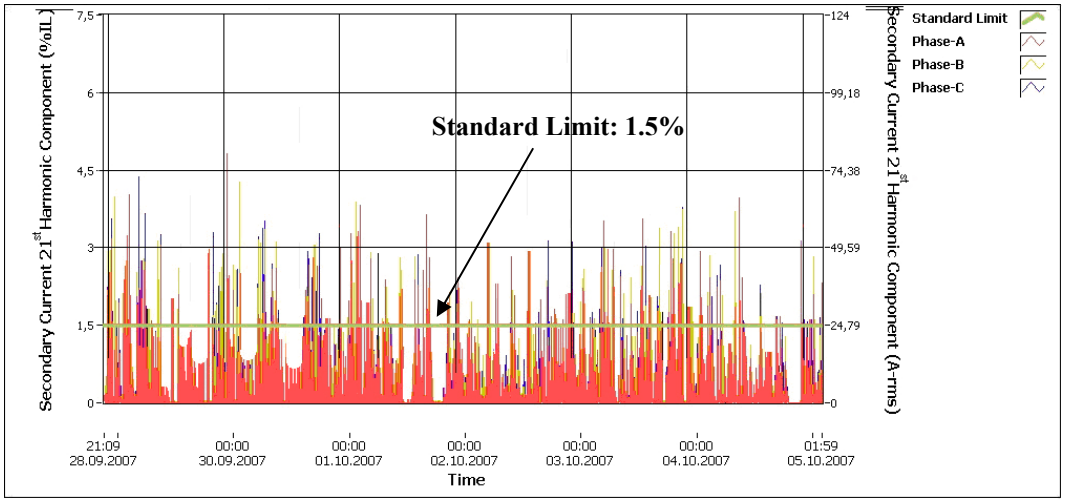

Figure 34 Alçuk-B, 21st Harmonic Component of the Secondary Current (Averaged in each 3 seconds)

Also to analyze the effect of harmonics to the temperatures more efficiently, the Harmonic Loss Factor for winding eddy current losses (FHL) and the Harmonic Loss Factor for other stray losses (FHL-STR) has been logged. Figures 35 and 36 show the FHL and FHL-STR in respect to the loading during the measurement period.

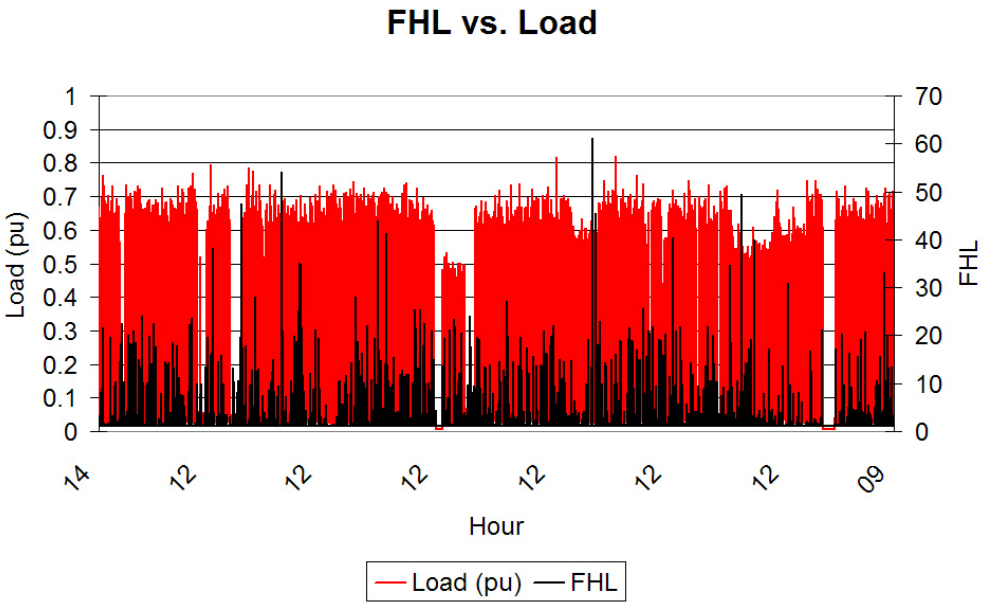

Figure 35 Alçuk-B, FHL vs. Load
(Averaged in each 20 seconds)

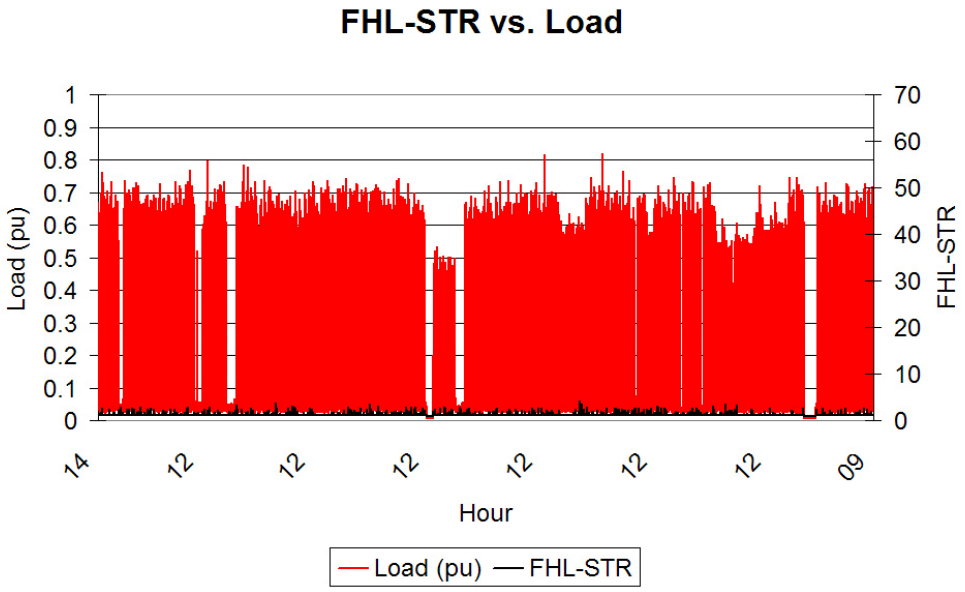

Figure 36 Alçuk-B, FHL-STR vs. Load
(Averaged in each 20 seconds)

Detailed analysis of Figure 35 shows the following properties;

- The average of the F_{HL} is 1,3.
- The maximum F_{HL} value during measurement is as high as 61.

Also, analysis of Figure 36 shows the following properties;

- The average of the $F_{HL\text{-}STR}$ is 1,02.
- The maximum $F_{HL\text{-}STR}$ value during measurement is as high as 4,5.

The difference between the maximum values of F_{HL} and $F_{HL\text{-}STR}$ indicates that the degree of harmonics is relatively high. This situation is because of the fact that F_{HL} is proportional to the harmonic level by a power of 2, whereas the $F_{HL\text{-}STR}$ is proportional to the harmonic level by a power of 0,8.

If, only the effect of the RMS value of the current has been taken into account, as in the case of the traditional measurement devices located on the present transformers, the effect of the harmonics would have been neglected. However for this particular transformer and its load, the effect of the harmonics is significant.

4.1.2 Temperature Verification

The verification of the TEMPEST's Top-Oil temperature calculation has been performed by inserting a Resistive Thermometer to the spare thermometer pocket as shown in Appendix B. Prior to the measurements, the EGEÇELİK factory has been warned accordingly and the load was disconnected from the transformer. Only after taking the required precautions had the thermometer been inserted. After the insertion, the factory has been energized and the measurement has been started.

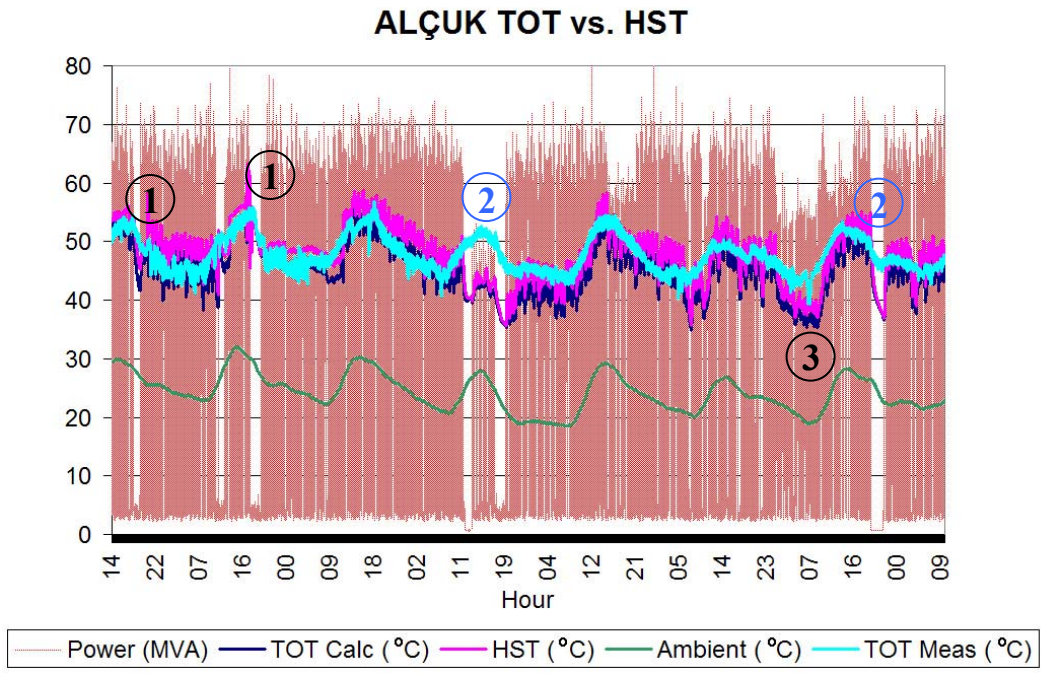

Figure 37 Alçuk-B, Calculated vs. Measured TOT with respect to Loading (Averaged in each 20 seconds)

The measured temperature value has been compared with the calculated temperature value on the computer. Both values are recorded and later on compared with each other. Figure 38 shows the results of the verification process. The Top-Oil and the Hot-Spot temperatures have been shown with respect to the changes in loading. Since the loading graphs show very unique impulsive characteristics, the results also show that the changes in the Top-Oil and Hot-Spot temperatures are rapid where they also follow the changes in the ambient temperatures.

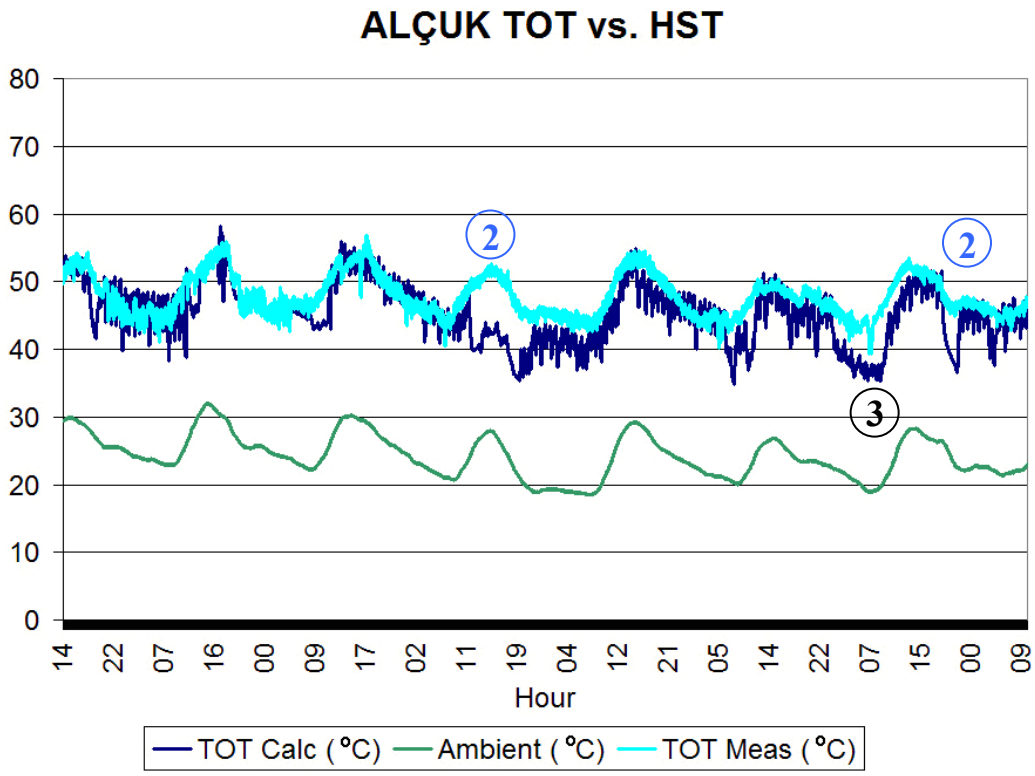

Figure 38 Alçuk-B, Calculated vs. Measured TOT excluding Loading and HST (Averaged in each 20 seconds)

To analyze the reaction of the temperatures more efficiently, some of the areas (1, 2 and 3) shall be closely examined. To better visualize the situation and to show the calculated and the measured Top-Oil temperatures clearly, the loading and also the Hot Spot temperature has been removed from Figure 38.

The effects of loading and ambient changes have significant value in temperature calculations. However they shall be separately discussed to visualize their response. Figures 39 and 40 show the deviations between calculated and measured Top-Oil temperatures with respect to the loading and the ambient temperature respectively.

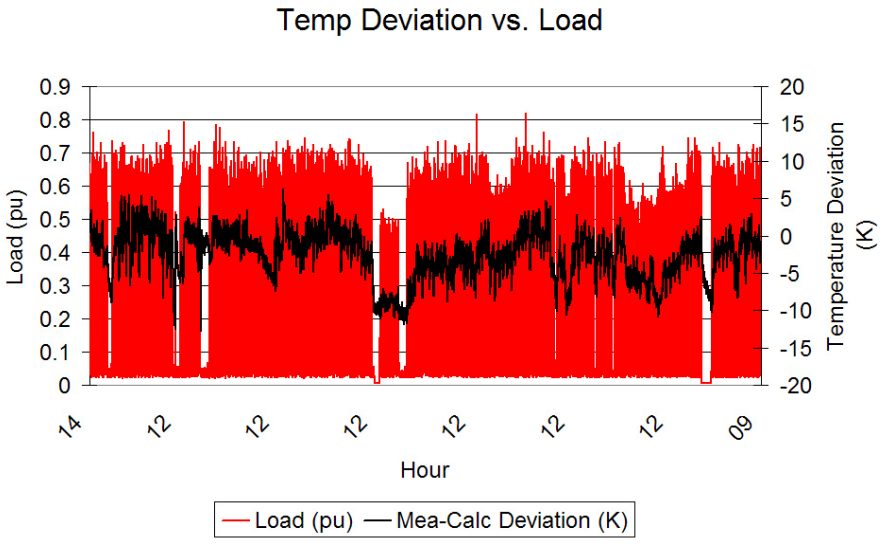

Figure 39 Alçuk-B, TOT deviations between Calculated and Measured Temperatures with respect to loading
(Averaged in each 20 seconds)

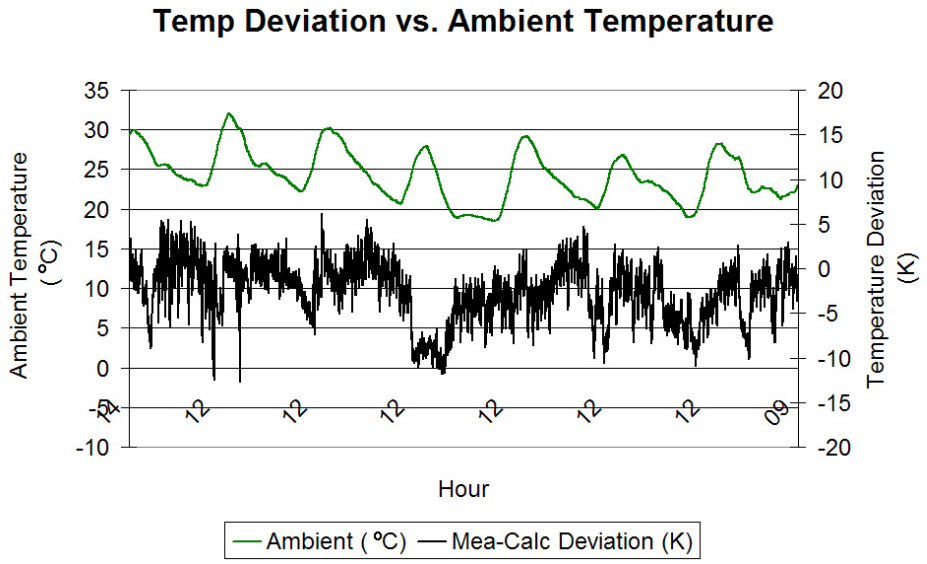

Figure 40 Alçuk-B, TOT deviations between Calculated and Measured Temperatures with respect to Ambient Temperature
(Averaged in each 20 seconds)

Figures 39 and 40 show the following properties;

- The maximum instantaneous deviation is -12 K.
- The maximum deviation with any duration longer than 1 hour is around -10 K.
- The average of all the deviations throughout the whole graph is -2.58 K.

The reason to have the main part of the deviations in the lower, minus part of the graphs is that the shut-down conditions (as described in section 4.1.2.2) of the transformer decreases the transformer Top-Oil temperature more than all the other

parameters and since no overloading effect has been detected in the measurement duration, no excessive increasing effect has effected the temperature.

There are some suggestions to apply to the results acquired to decrease the ripples on the calculated temperatures. [29] suggests applying a correction function such as equation (4-1);

$$\Delta_{CORR} = \Delta T_C . \exp^{\frac{-t}{\tau_C}} \tag{4-1}$$

However with the application of such a correction function to the data, the momentary peaks in the temperature variations will be smoothed. This will lead to the loss of valuable data. And for the intermittent operation of transformers, these data are vital in early excessive Hot-Spot temperature warnings.

[16] identifies the erroneous or miscalculated data and discards or corrects these data to acquire a better degree of quality throughout the measurement. The bad data which could have been corrected here are; erroneous measurements, ambient temperature out of range, rapid and large jumps in ambient temperature, spikes in TOT (Top Oil Temperature), large discrete load changes.

The load in this transformer changes every second so that the last item is out of focus. Spikes in TOT are more of a visual improvement than data correction. The ambient changes (such as due to raining) or erroneous measurements need to be standardized or more work needs to be performed on these items to apply them to the data.

4.1.2.1 Hot Spot Temperature Spikes

As the loading increased rapidly, the Hot-Spot temperature had also raised simultaneously since the Hot-Spot temperature time constant is lower than the Top-Oil temperature time constant. The advantage of visualizing this temperature spikes (as shown in Figures 41 and 42) is critical because the main transformer malfunctions related to the temperature changes occurs on the windings where Hot-Spot temperatures cause gas formations. As the changes in Hot-Spot temperatures have such significance, the early warning measures provided can help prevent harms to the transformer.

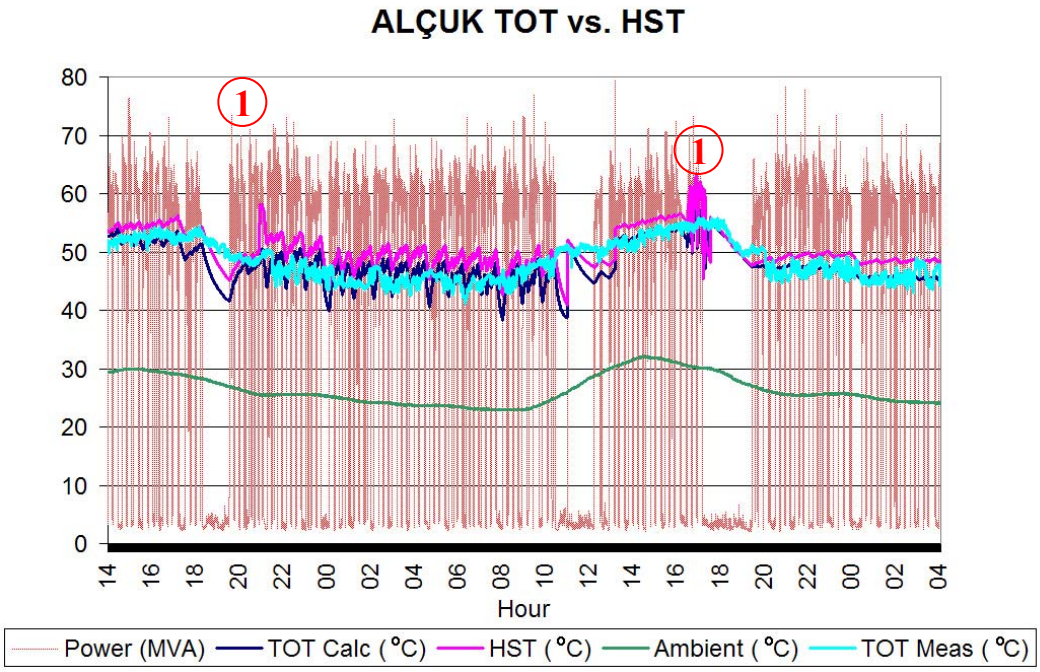

Figure 41 Alçuk-B, Detail showing HST Spikes
(Averaged in each 20 seconds)

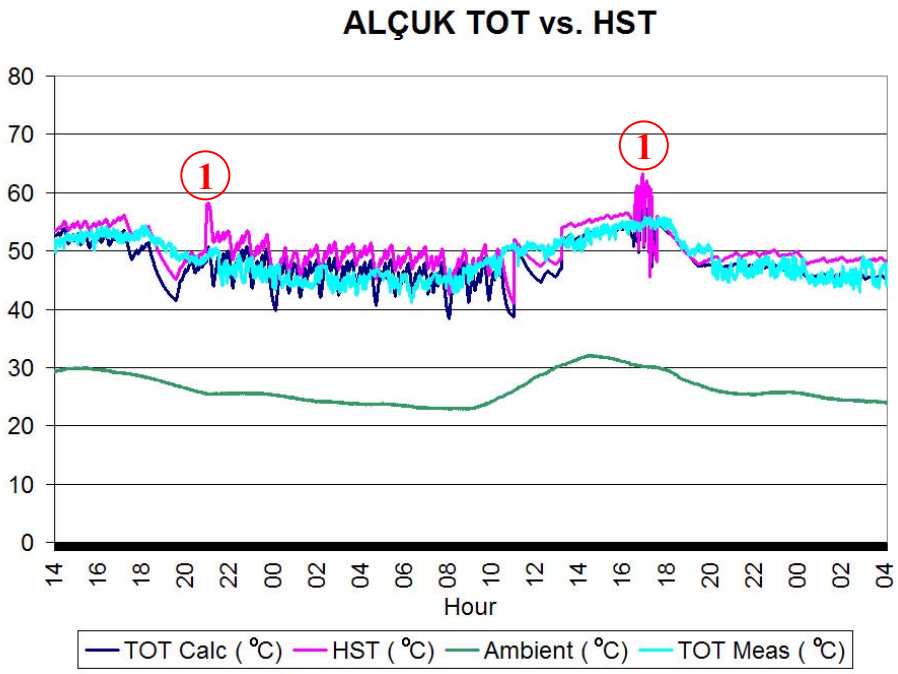

Figure 42 Alçuk-B, Detail showing HST Spikes excluding Loading (Averaged in each 20 seconds)

4.1.2.2 Effect of the Loading Condition

According to the results, the variation of Top-Oil temperature calculation under the intermittent loading changes is minor compared to the changes in the ambient temperature. However a special condition occurs when the loading falls dramatically until a shut-down condition occurs as shown in Figures 43 and 44.

The absence of the loading limits the contribution of transformer to the no-load losses where the load losses are not present in the system anymore. In this

particular transformer where nearly half of the Top-Oil temperature over ambient temperature value is the contributed by the load losses, the calculated Top-Oil temperature decreases rapidly. However the actual Top-Oil temperature is not affected as much as the calculated Top-Oil temperature and the deviation is significant. Such a special condition can be overcome with an algorithm to detect the event [14].

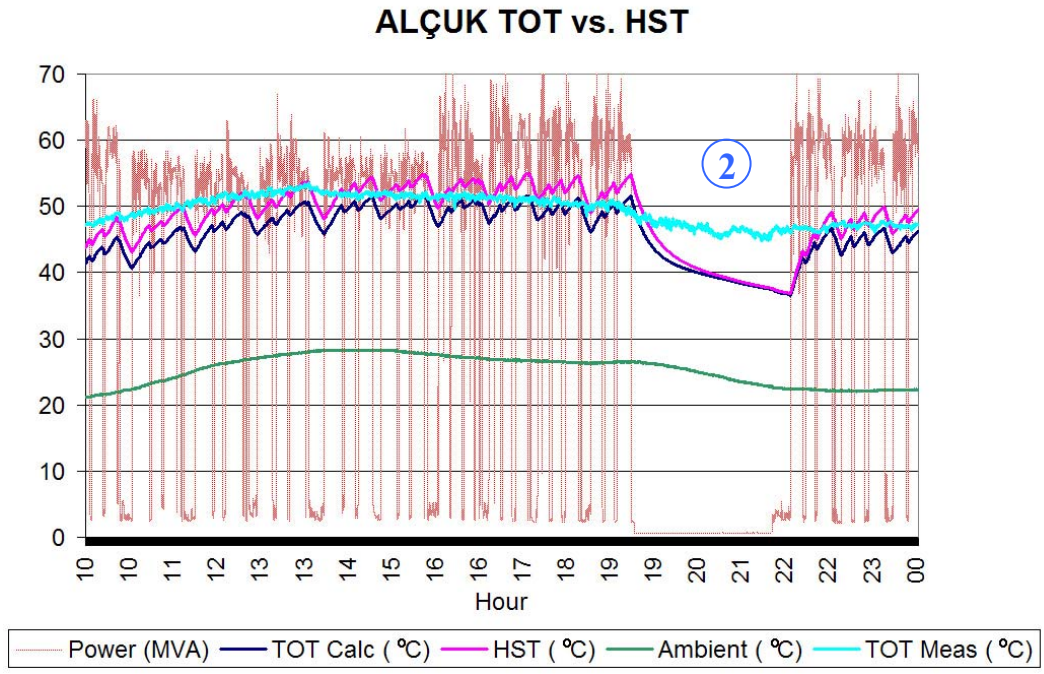

Figure 43 Alçuk-B, Detail showing the Shut-Down Response-1 (Averaged in each 20 seconds)

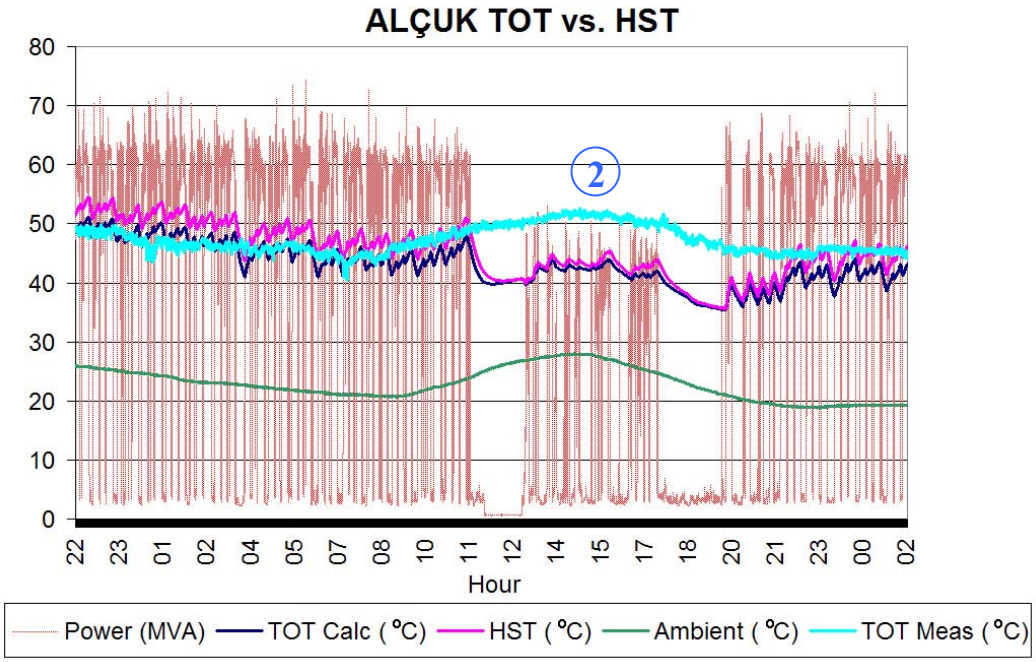

Figure 44 Alçuk-B, Detail showing the Shut Down Response-2 (Averaged in each 20 seconds)

4.1.2.3 Ambient Temperature Changes

The rapid change of ambient temperature has a dramatic effect to the Top-Oil and the related Hot-Spot temperature calculations [14]. The deviations related to these transient-states may exceed 10 K levels considering the gradient of the ambient temperature change. Figure 45 shows the sample of calculation deviations related to the rapid change in ambient temperature. There is a minor effect of change of loading which results in a greater deviation of calculated and measured values.

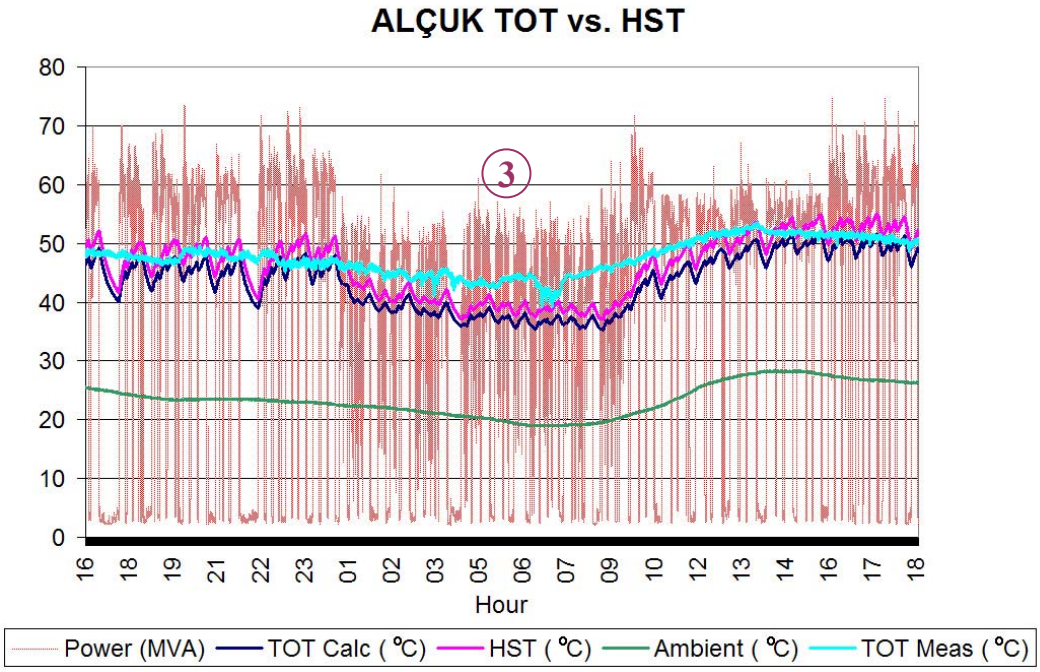

Figure 45 Alçuk-B, Deviations Related to the Changes in Ambient Temperature (Averaged in each 20 seconds)

4.1.3 IEEE Loading Guide's Original Time Constant vs. Corrigendum Time Constant

In the first edition of the IEEE Loading Guide, the Top-Oil temperature time constant formulation for SI units was resulting in time constants more than 10 hours. This was the result of an erroneous conversion from imperial units to SI units. Some of the previous studies which used the IEEE Loading Guide did not mention the resultant time constant. Therefore there is a possibility that previous studies have used a defective time constant. A study has been performed in this thesis which can be used to identify the differences between the time constant

values defined in the original Loading Guide and the Corrigendum. To compare the old and new time constant effectivity, both of the time constants were applied and the results have been compared as shown in Figure 46.

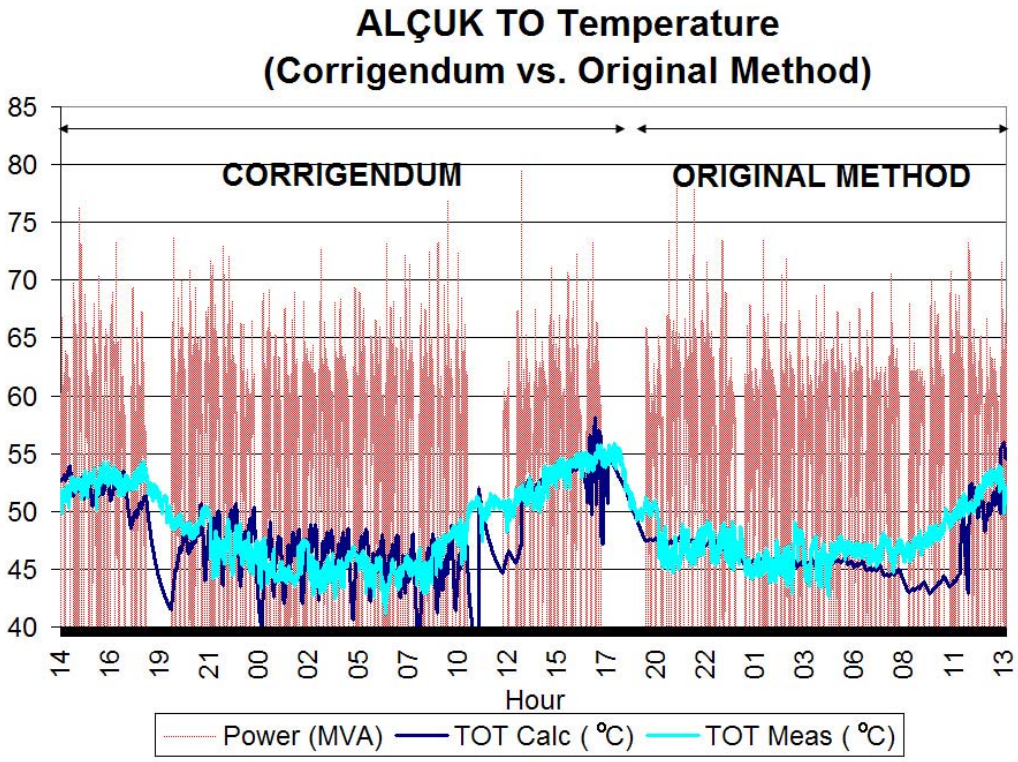

Figure 46 Alçuk-B, Corrigendum Time Constant vs. Original Time Constant (Averaged in each 20 seconds)

In the special loading characteristics of the intermittent loading of arc furnaces, the newer, corrected method has proven to be significantly better than the original, older method. The newer method follows the actual, measured temperature values with more accuracy where the older method with longer time constant has provided a straighter and less sensitive response to the loading.

The crucial point in avoiding the older, original version of time constants lies in surge reactions. With a longer time constant, the effect of excessive loading will be seen as less effective resulting in eliminating the early warning advantage of calculations.

Also the ageing effect can not be tracked accordingly with the original method where the Corrigendum method [5] is more accurate in tracking the temperature values.

4.1.4 Unbalanced Loading between phases

The methods to calculate Hot-Spot and Top-Oil temperatures defined in IEEE Loading Guide [4] and IEEE Std. C57.110 [3] utilizes only one phase's current values to calculate the temperatures. Both methods have an assumption that the loading will be divided equally between phases. This may not be possible in a transformer supplying power to arc furnaces since every phase contributes a different current value to the loading in any given time interval. Only the average loading on phases over long durations may be near equal. However, even if the True RMS components of the currents are equally loaded, the harmonics exerted on each phase differ momentarily.

The significance of the analysis is mostly related to the Hot-Spot temperature. This issue is a different concept than the thermal inhomogeneity of windings [30] however it is also equally critical. Although there may be a minor change in the Top-Oil temperature related to the unbalanced phases, the major effect of harmonics may increase the difference between the Hot-Spot temperatures of the phases.

Also since the Top-Oil temperature is common for all the phases, where the Hot-Spot temperatures are on each phase's own winding, one of the phases may have a Hot-Spot temperature higher than the other phases.

One last critical aspect of the situation is that the Hot-Spot temperature's time constant is lower than that of the Top-Oil where any unbalanced loading for even a short duration may result in significant changes in one phase's Hot-Spot temperature.

To verify the calculations, all of the phases have been used for the calculations and both of the temperatures have been calculated using each of the phase currents and related harmonics. Figure 47 shows the fundamental currents of all 3 phases over the total measurement duration averaged over 15 minute intervals.

It is seen that at some points there are differences between the current demanded from all phases. This situation can lead to a miscalculation if the differences are significant or the duration of the differences are long.

Also the time constant applied to the algorithm shall be sufficient so that these minor, instantaneous differences do not affect the overall performance of the system while still catching the variations of the original temperatures.

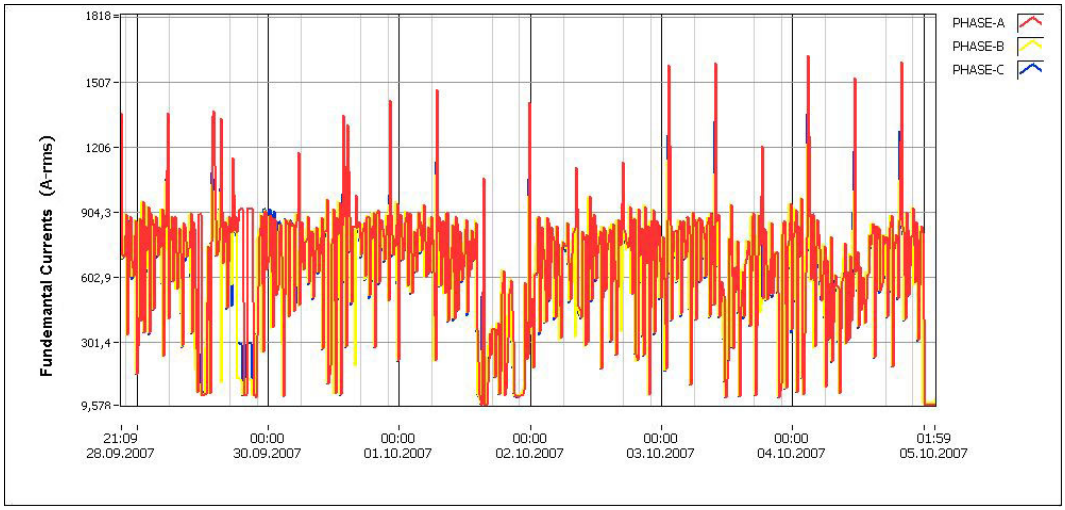

Figure 47 Alçuk-B, Fundamental currents of Phases A, B and C for the whole measurement duration
(Averaged in each 15 minutes)

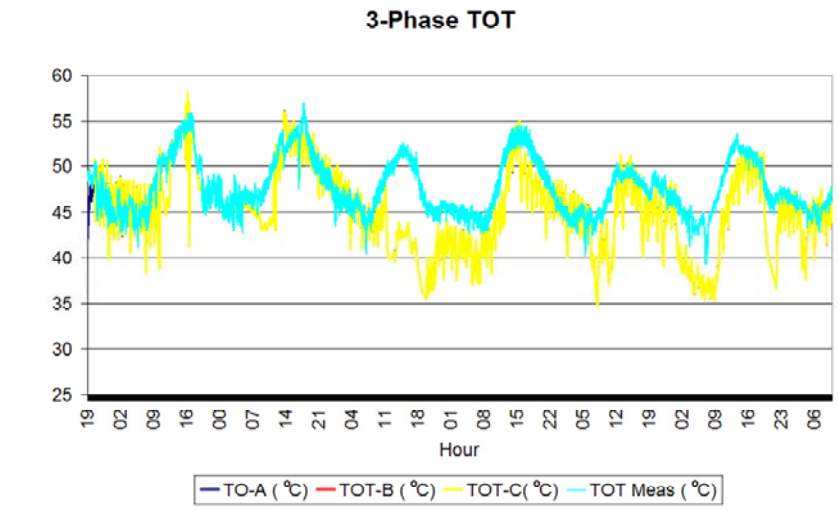

Figure 48 Alçuk-B, TOT calculated from the currents of Phases A, B and C (Averaged in each 20 seconds)

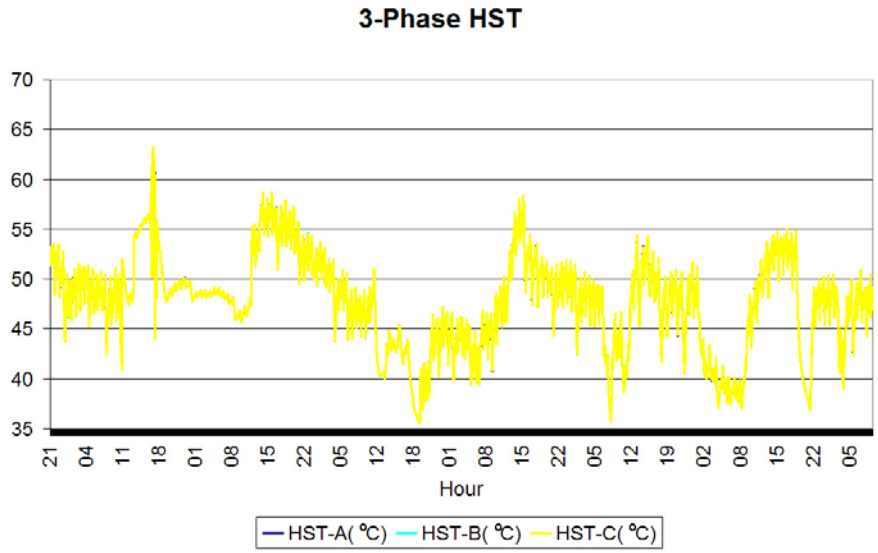

Figure 49 Alçuk-B, HST calculated from the currents of Phases A, B, C (Averaged in each 20 seconds)

Figures 48 and 49 show the Top-Oil and Hot-Spot temperatures calculated for all the 3 phases. The calculated temperatures are so inline for all 3 phases, the graphs seem to be identical.

The results are in near equal levels where they can not be distinguished from each other. To realize the differences, the deviations between phases have been shown below in Figures 50-53 for the differences of Phases B and C with respect to Phase A. The deviations are noted for the Top-Oil and Hot Spot temperatures.

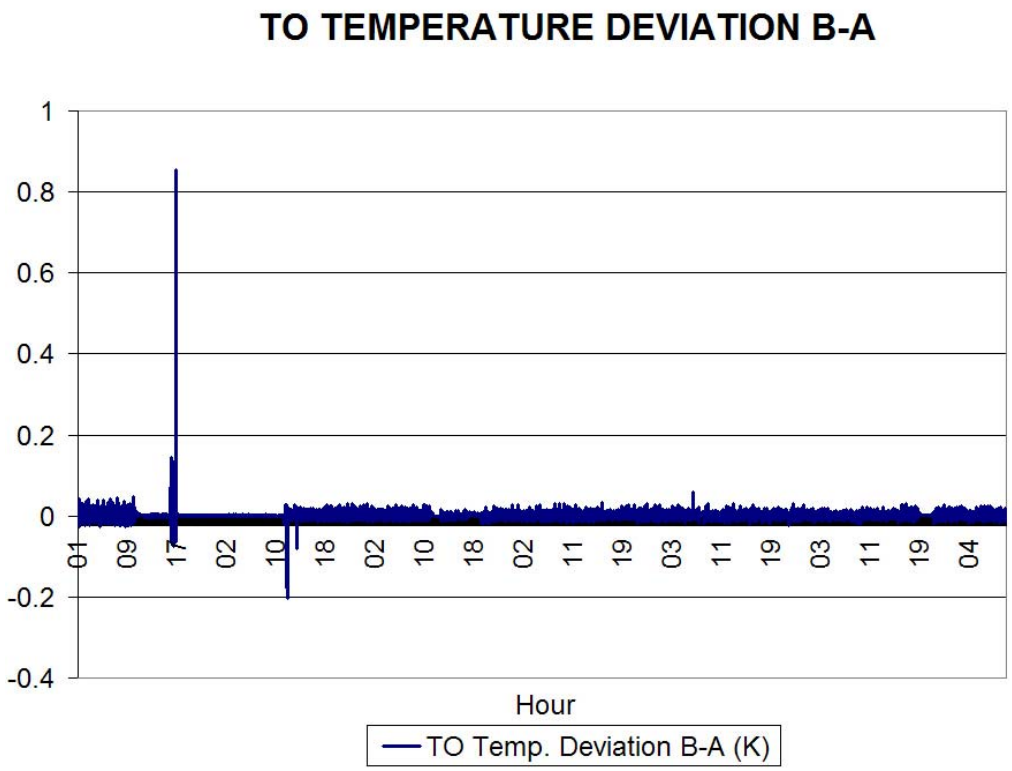

Figure 50 Alçuk-B, TOT Deviation between the Phases B and A (Averaged in each 20 seconds)

Figure 50 shows;

- The maximum deviation for the Top Oil temperatures between Phase B and Phase A is 0.85 ^{o}C.
- The average deviation for the Top Oil temperatures between Phase B and Phase A is 0.00003 ^{o}C.

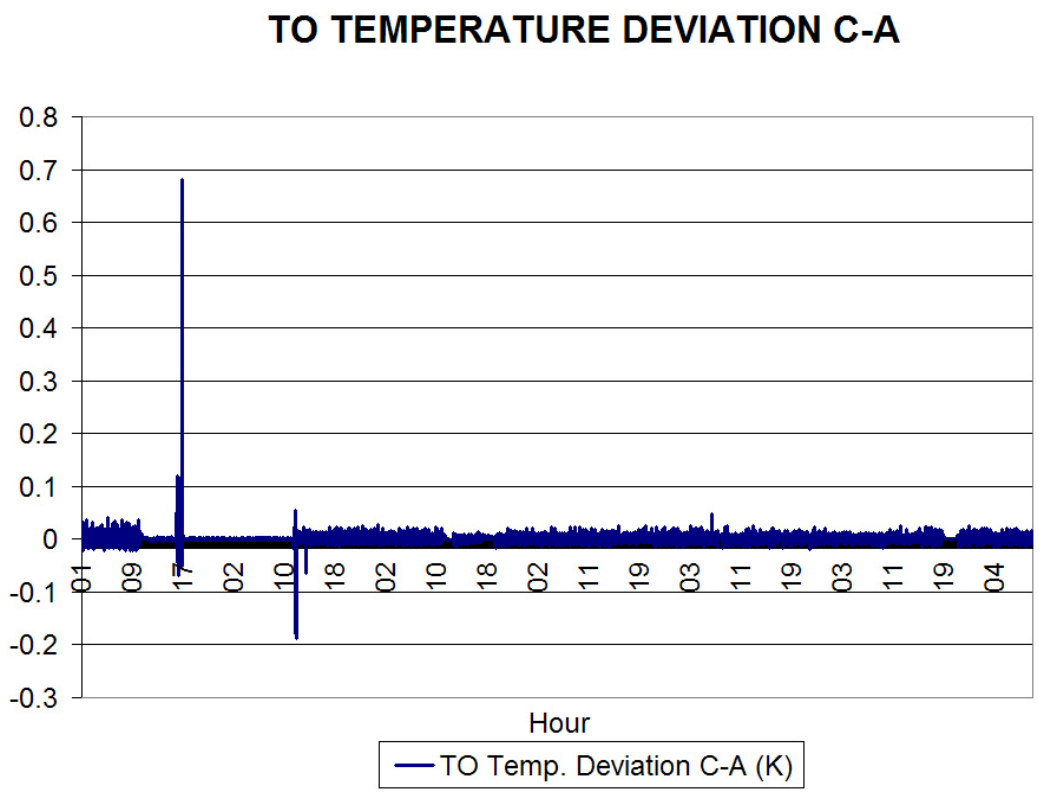

Figure 51 Alçuk-B, TOT Deviation between the Phases C and A (Averaged in each 20 seconds)

Figure 51 shows;

- The maximum deviation for the Top Oil temperatures between Phase C and Phase A is 0.68 ^{o}C.
- The average deviation for the Top Oil temperatures between Phase C and Phase A is 0.00010 ^{o}C.

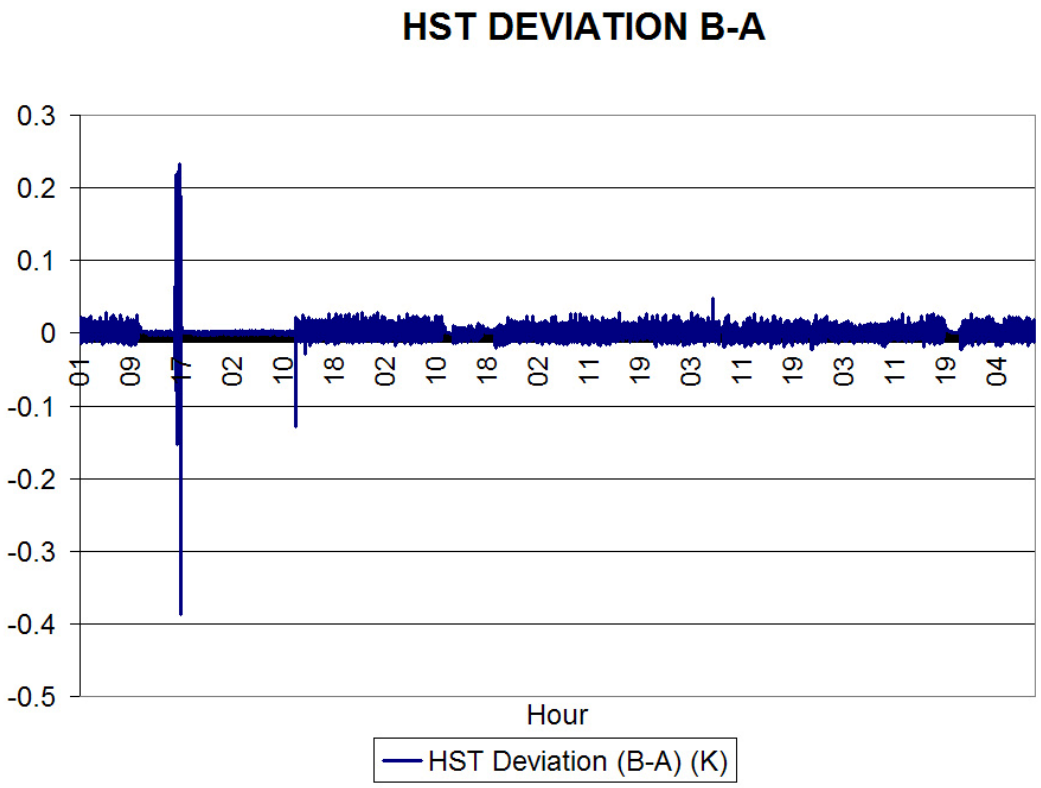

Figure 52 Alçuk-B, HST Deviation between the Phases B and A (Averaged in each 20 seconds)

Figure 52 shows;

- The maximum deviation for the Hot Spot temperatures between Phase B and Phase A is 0.23 ^{o}C.
- The average deviation for the Hot Spot temperatures between Phase B and Phase A is 0.00018 ^{o}C.

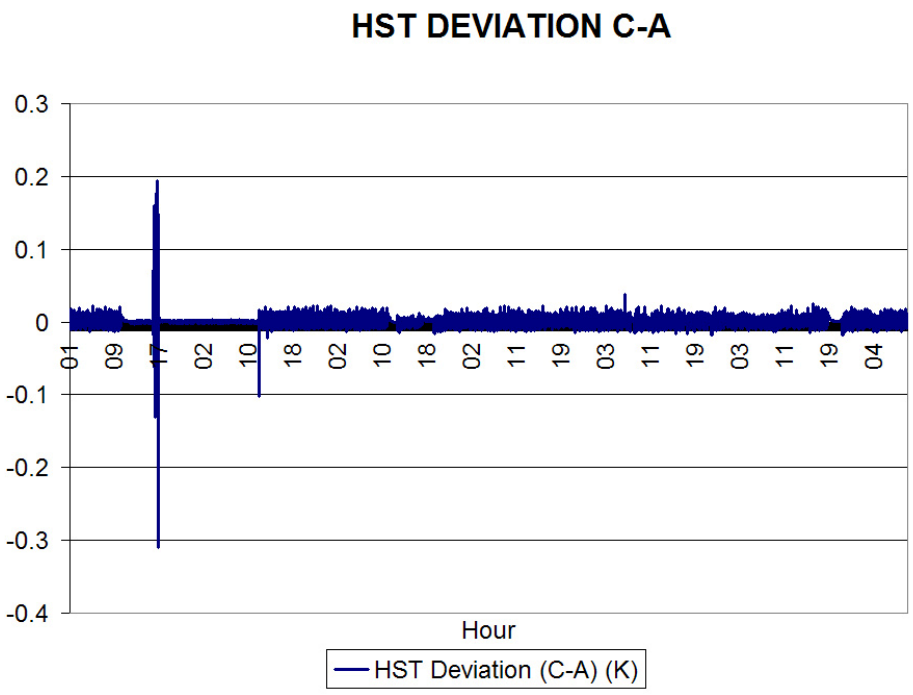

Figure 53 Alçuk-B, HST Deviation between the Phases C and A (Averaged in each 20 seconds)

Figure 53 shows;

- The maximum deviation for the Hot Spot temperatures between Phase C and Phase A is 0.19 ^{o}C.
- The average deviation for the Hot Spot temperatures between Phase C and Phase A is 0.00017 ^{o}C.

The maximum deviation during the measurement duration is 0.85 ^{o}C. The average deviation is less than 0.0002 ^{o}C. These data shows that the phase balance of the transformer loading is in acceptable values.

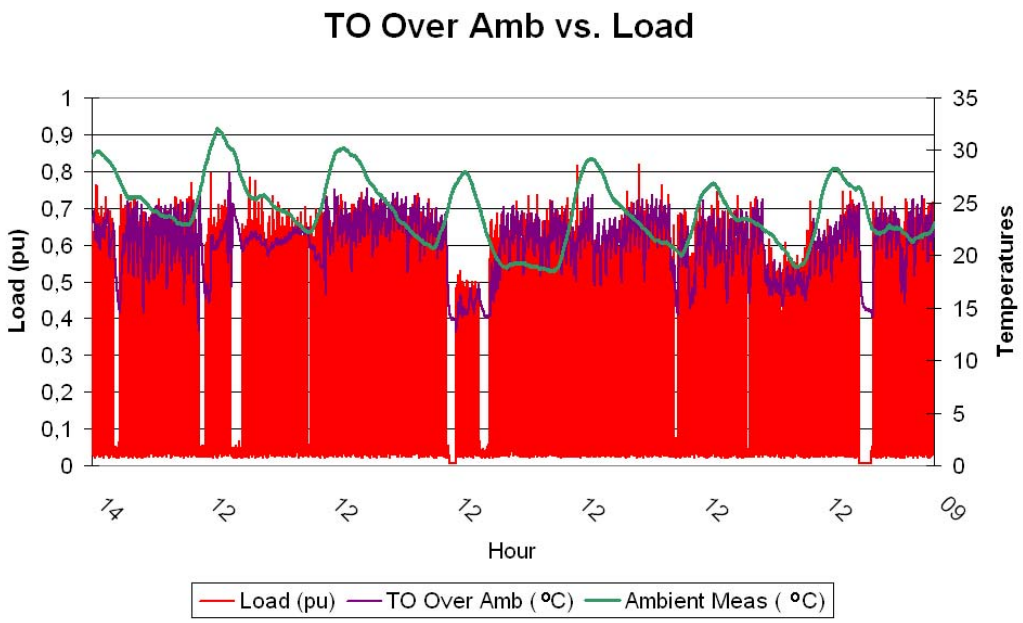

Figure 54 Alçuk-B, Top Oil rise over Ambient Temperature (Averaged in each 20 seconds)

The above figure shows the Top Oil Rise over Ambient Temperature. The Ambient Temperature and the per-unit load have been added to visualize the variations in accordance with these two most critical parameters.

As can be seen from the figure, the Top-Oil rise is only proportional to the load. As the load decreases or in some cases is approximately 0 pu, the Top-Oil rise decreases accordingly.

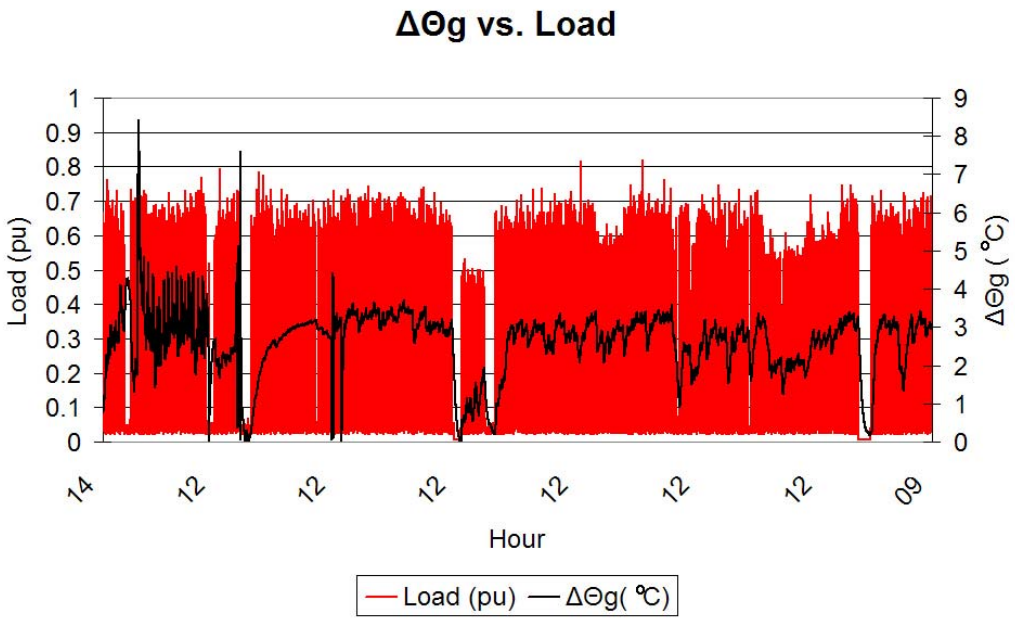

Figure 55 Alçuk-B, Hot Spot Conductor rise over Top Oil Temperature (Averaged in each 20 seconds)

The Hot-Spot conductor rise over Top-Oil temperature has been shown in Figure 55. It can be observed that loading is the major factor affecting the Hot-Spot temperature rise over Top-Oil temperature. Since all the losses are directly proportional to the load, as the loading is increased the Hot-Spot temperature is also increased. However the effect of harmonics is still another major factor affecting $\Delta\Theta_g$. The effect of harmonics can only be significant if they contribute to the losses, especially winding eddy current losses. A comparison of Figure 55 to Figures 35 and 36 show that harmonics can be more effective with higher loading.

4.1.5 Sample Temperature Calculation

Table 3 shows the harmonic distribution for a sample instant. The third column summation results in an rms current value of 1.006 pu. The fifth column summation results in a Harmonic Loss Factor for the winding eddy losses of 1.86, and the seventh column summation results in a Harmonic Loss Factor for the other stray losses of 1.04. The load at this instant is 0.7 pu.

Table 3 Harmonic distribution and parameter calculation for Alçuk-B

h	I_h/I_1	$(I_h/I_1)^2$	h^2	$(I_h/I_1)^2h^2$	$h^{0.8}$	$(I_h/I_1)^2h^{0.8}$
1	1	1	1	1	1	1
2	0,07	0,0049	4	0,0196	1,7411	0,008531
3	0,03	0,0009	9	0,0081	2,4082	0,002167
4	0,02	0,0004	16	0,0064	3,0314	0,001213
5	0,03	0,0009	25	0,0225	3,6239	0,003262
6	0,02	0,0004	36	0,0144	4,193	0,001677
7	0,016	0,000256	49	0,012544	4,7433	0,001214
8	0,02	0,0004	64	0,0256	5,278	0,002111
9	0,016	0,000256	81	0,020736	5,7995	0,001485
10	0,02	0,0004	100	0,04	6,3096	0,002524
11	0,02	0,0004	121	0,0484	6,8095	0,002724
12	0,02	0,0004	144	0,0576	7,3004	0,00292
13	0,018	0,000324	169	0,054756	7,7831	0,002522
14	0,016	0,000256	196	0,050176	8,2585	0,002114
15	0,017	0,000289	225	0,065025	8,7272	0,002522
16	0,014	0,000196	256	0,050176	9,1896	0,001801
17	0,014	0,000196	289	0,056644	9,6463	0,001891
18	0,014	0,000196	324	0,063504	10,098	0,001979
19	0,016	0,000256	361	0,092416	10,544	0,002699
20	0,015	0,000225	400	0,09	10,986	0,002472
21	0,014	0,000196	441	0,086436	11,423	0,002239
Σ	–	1,011746	–	1,885013		1,050067

Using the input data given earlier in Table 2, the other parameters can be calculated as follows.

The rated primary and secondary currents can be calculated from rated MVA and voltage values. Resistance values are taken from the test report.

$I_{1\text{-}R}$ (Primary Current) = 375.3 A

$I_{2\text{-}R}$ (Secondary Current) = 1675.5 A

R_1= 0.3 Ω

R_2= 0.0167 Ω

Using equation (2.15), the total stray losses can be found as;

$P_{TSL\text{-}R}$= 165000 – 1.5 x $[(375.3)^2$ x 0.3 + $(1675.5)^2$ x 0.0083] watts

$P_{TSL\text{-}R}$ = 31437 watts

$P_{EC\text{-}R}$=0.33 x $P_{TSL\text{-}R}$= 10374 watts

$P_{OSL\text{-}R}$= $P_{TSL\text{-}R}$ - $P_{EC\text{-}R}$ = 21063 watts

P_{LL}(pu)= I^2 x 0.7^2 = 1,011746 x 0.49 = 0,496

Table 4 shows the tabulated losses. The rated losses have been corrected to include the loading condition and the harmonic effect.

Table 4 Loss Separation for Alçuk-B

Type of Loss	Rated Losses	Load Corrected Losses	Harmonic Multiplier	Totally Corrected Losses
No-Load	32350 (%16.4)			32350 (% 27.2)
I2R	133562 (% 67.7)	66214		66214 (% 55.6)
EC	10374 (% 5.3)	5143	1,86	9582 (% 8.1)
OSL	21063 (% 10.7)	10442	1,04	10838 (% 9.1)
Total Losses	197350 (% 100)			118984 (% 100)

The Top-Oil temperature rise can be calculated as follows;

$$\Delta\Theta_{TO} = 55 \times \left(\frac{118984}{197350}\right)^{0.9} = 34.88 \ ^{o}C$$

The rated inner or LV winding losses can be calculated as follows:

$(I_{2\text{-}R})^2$ x R= 1.5 x 1675.5^2 x 0,0167= 70320 W

I_2^2 x R = 70320 x P_{LL} (pu)= 34860 W

$$\Delta\Theta_g = (65-55) \times \left(\frac{34860 + 9582 \times 2.4}{70320 + 10374 \times 2.4}\right)^{0.8} = 6 \ ^{o}C$$

The Hot-Spot rise is 6 ^{o}C in the presence of harmonics. To analyze the effect of the harmonics, the Hot-Spot rise can be calculated without taking into account the harmonic loss factor. The winding eddy current losses will therefore be 5143 W.

$$\Delta\Theta_g = (65-55)\times\left(\frac{34860+5143\times 2.4}{70320+10374\times 2.4}\right)^{0.8} = 5\ ^{o}\text{C}$$

The harmonic effect rises the Hot-Spot temperature by 1 ^{o}C. This value is lower than the examples shown in IEEE Std. C57.110-1998 because of the relatively lower harmonic content.

Also another important factor is the low per-unit load. This degraded load lowers the losses and the losses are one of the main factors to affect the Hot-Spot temperature.

4.2 25/32.5 MVA ONAN/ONAF Conventional Load

It is the desire of the author that TEMPEST can be applied to all transformers. Even the transformers without the manufacturers' certified test reports but only the nameplate of the transformer. The accuracy of the results will be highly decreased when compared to the measurements with more available data and it is highly recommended to acquire a certified test report for TEMPEST to operate effectively. Although few in number, it is reported that there are transformers without the manufacturer's certified test report. With some assumptions and data training, these transformers can be covered too.

Figure 56 Maltepe-2 Transformer

Maltepe GIS (Gaseous Isolated System) Transformer Center's Transformer-2 is chosen which also has a different power rating and LV voltage than the previously measured transformer. The transformer is located in the urban area where it is required to cover the smallest possible area. The SF_6 isolated circuit breakers takes up less space than the air isolated circuit breakers. Also these transformers are located inside a building (as seen in Figure 56) rather than the previously measured open area transformer. Table 5 shows the TEMPEST input data for transformer Maltepe-2. These values have been acquired from transformer's nameplate and making proper assumptions.

Table 5 TEMPEST Input data for Maltepe-2

MALTEPE-2 TRANSFORMER	
Rated Capacity	32,5 MVA
HV	154000 V
LV	6300 V
No-Load Losses	32500 W (Estimated)
Load Losses	227500 W (Estimated)
HV Connection	Wye
LV Connection	Delta
Base Current	2200 A
Top Oil Time Constant	1.6 hours
Winding Time Constant	9 minutes

4.21 Loading and Harmonic Content

This transformer does not posses a significant harmonic profile. Since the loading is steadier, the percentage of the harmonic content has been taken as constant. Only the 5. Harmonic is somehow significant. The high 5. Harmonic is caused by the slightly industrial effect on the load. Even with this effect, the load is nearly sinusoidal compared to an intermittent loaded transformer. The harmonic spectrum of the load is as seen in Figure 57. The harmonic content will not be further discussed for Maltepe-2 transformer. Also, for the steady loading, the phase balance can be achieved with ease. Therefore the unbalanced phase calculations have been omitted.

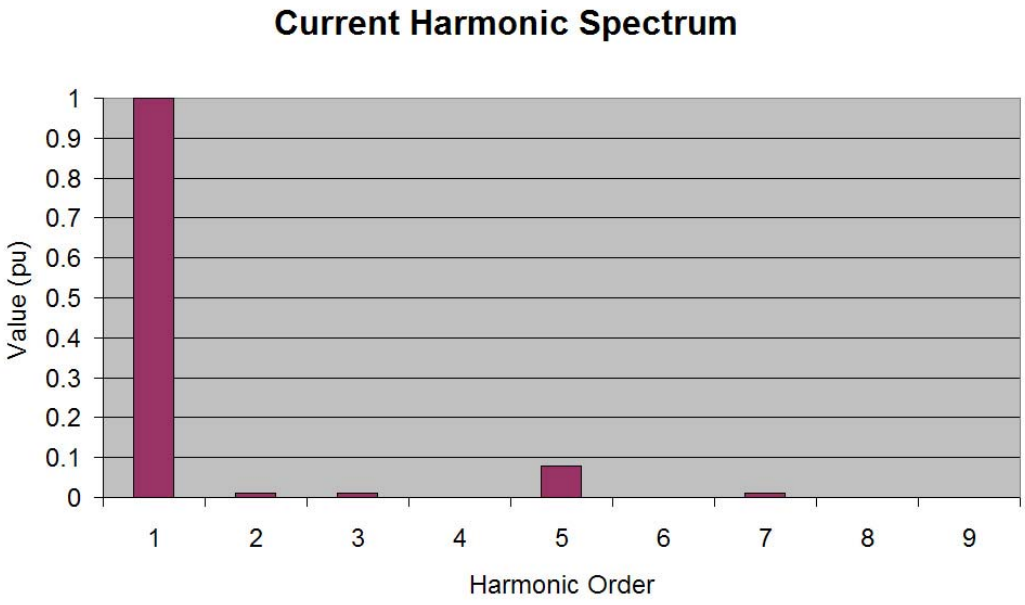

Figure 57 Maltepe-2 Harmonic Spectrum

4.2.2 Temperature Prediction

The results of the temperature measurements have been compared to the temperatures noted by the operators on duration noted every 3 hours. Since 3 hours period is too long considering the total measurement duration, only the new measured temperature at the beginning of 3 hours period shall be compared to the calculated temperatures. In the case of a rapid increase or decrease for the temperatures for more than 3 hours, the deviation between the measured and calculated temperatures is greatest just before the next measured value.

Figure 58 shows the Top-Oil temperature and Hot-Spot temperatures versus time. The Figure also shows the relatively steady power demanded by the load.

It shall be noted that the ambient temperature change on daily basis is relatively small compared to previous measurement. This is the result of constant rains during the week of the measurement. Since the humidity rose, the ambient temperature variation during night and day time has been minimized.

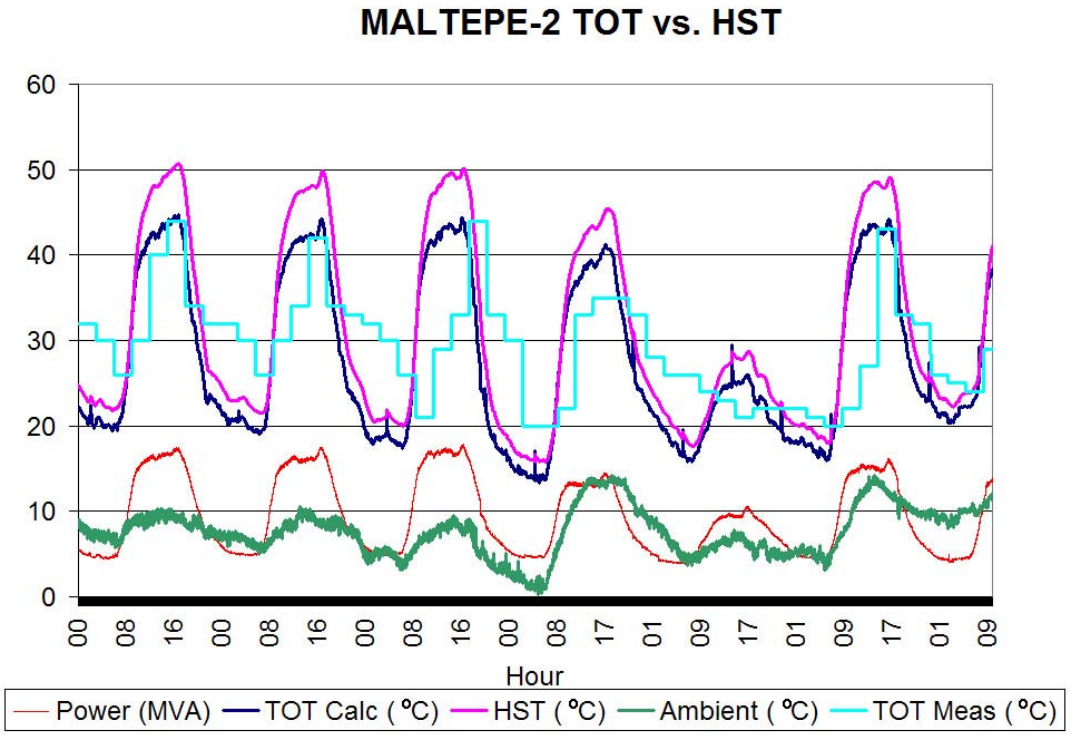

Figure 58 Maltepe-2 TOT vs. HST

The effects of loading and ambient changes have significant value in temperature calculations. However they shall be separately discussed to visualize their response. Figures 60 and 61 show the deviations between calculated and measured Top-Oil temperatures with respect to loading and ambient temperature respectively.

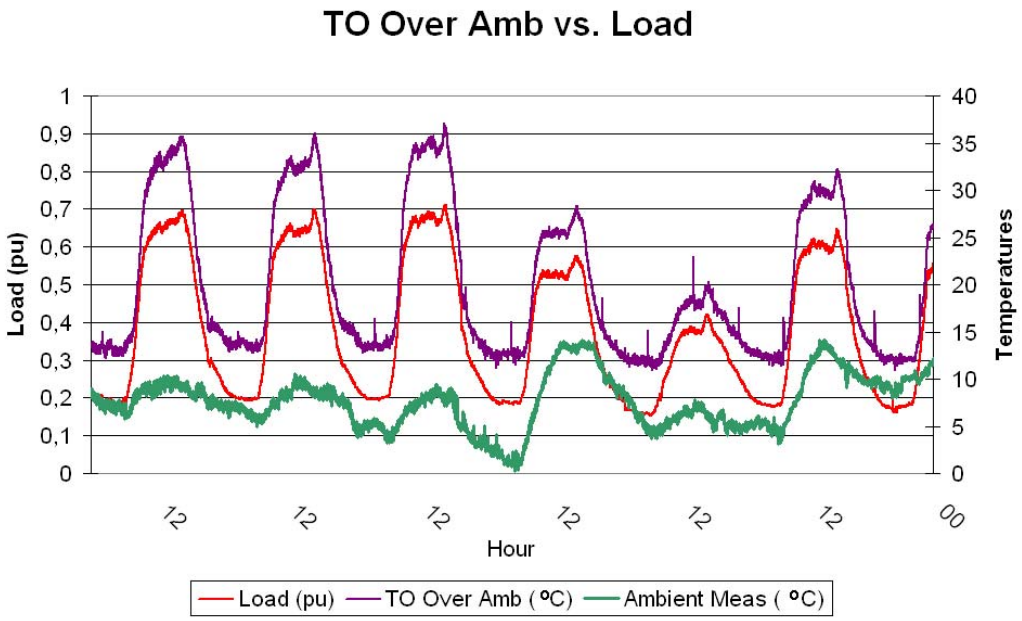

Figure 59 Maltepe-2, Top Oil rise over Ambient Temperature (Averaged in each 20 seconds)

The above figure shows the Top Oil Rise over Ambient Temperature. The Ambient Temperature and the per-unit load have been added to visualize the variations in accordance with these two most critical parameters.

As can be seen from the figure, the Top-Oil rise is only proportional to the load. The Top Oil Rise over Ambient Temperature is closely related to the daily load variations.

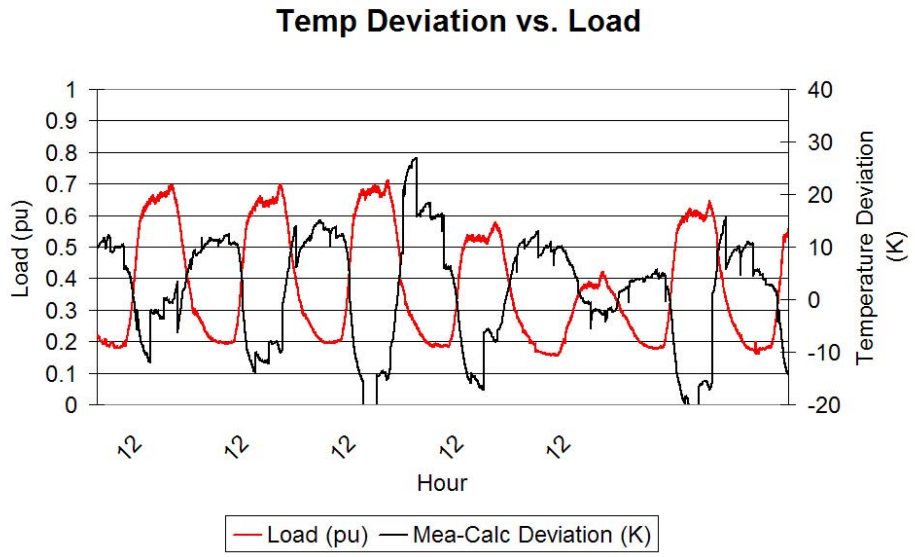

Figure 60 Maltepe-2, TOT deviations between Calculated and Measured Temperatures with respect to loading
(Averaged in each 20 seconds)

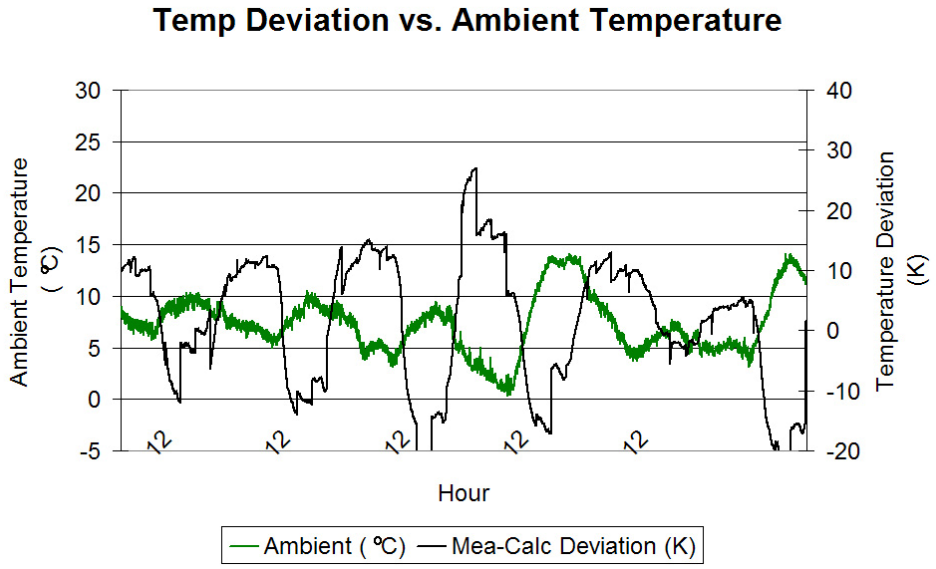

Figure 61 Maltepe-2, TOT deviations between Calculated and Measured Temperatures with respect to Ambient Temperature
(Averaged in each 20 seconds)

Figures 60 and 61 show the following properties;

- The maximum instantaneous deviation is -20 K.
- The maximum deviation with any duration longer than 1 hour is around -10 K.
- The average of all the deviations throughout the whole graph is 1.73 K.

These figures show that even without the data in manufacturer's test certificate, the temperatures can be predicted to some degree. The presented results show that system is able to follow the highest temperatures throughout the day, however it decreases rapidly during nighttime. This situation can be overcome with more input data to the prediction program.

4.2.3 Sample Temperature Calculation

Table 6 Harmonic distribution and parameter calculation for Maltepe-2

h	I_h/I_1	$(I_h/I_1)^2$	h^2	$(I_h/I_1)^2h^2$	$h^{0.8}$	$(I_h/I_1)^2h^{0.8}$
1	1	1	1	1	1	1
2	0,01	0,0001	4	0,0004	1,7411	0,000174
3	0,01	0,0001	9	0,0009	2,4082	0,000241
4	0,001	0,000001	16	0,000016	3,0314	3,03E-06
5	0,08	0,0064	25	0,16	3,6239	0,023193
6	0,001	0,000001	36	0,000036	4,193	4,19E-06
7	0,01	0,0001	49	0,0049	4,7433	0,000474
8	0,0001	0,00000001	64	6,4E-07	5,278	5,28E-08
9	0,0001	0,00000001	81	8,1E-07	5,7995	5,8E-08
Σ	–	1,00670202	–	1,1662535		1,02409

Table 6 shows the harmonic distribution for a sample instant. The third column summation results in an rms current value of 1.006 pu. The fifth column summation results in a Harmonic Loss Factor for the winding eddy losses of 1.15, and the seventh column summation results in a Harmonic Loss Factor for the other stray losses of 1.017. The load at this instant is 0.5 pu.

Using the input data given in Table 5, the other parameters can be calculated as follows.

The rated primary and secondary currents can be calculated from rated MVA and voltage values. Resistance values are taken from the test report.

$I_{1\text{-}R}$ (Primary Current) = 93.8 A

$I_{2\text{-}R}$ (Secondary Current) = 2294 A

R_1= 0.4 Ω

R_2= 0.01 Ω

Using equation (2.15), the total stray losses can be found as;

$P_{TSL\text{-}R}$= 227500 – 1.5 x $[(93.8)^2$ x 0.4 + $(2294)^2$ x 0.01] watts

$P_{TSL\text{-}R}$ = 101040 watts

$P_{EC\text{-}R}$=0.33 x $P_{TSL\text{-}R}$= 33343 watts

$P_{OSL\text{-}R}$= $P_{TSL\text{-}R}$ - $P_{EC\text{-}R}$ = 67697 watts

P_{LL}(pu)= I^2 x 0.5^2 = 1,007 x 0.25 = 0.252

Table 7 shows the tabulated losses. The rated losses have been corrected to include the loading condition and the harmonic effect.

Table 7 Loss Separation for Maltepe-2

Type of Loss	Rated Losses	Load Corrected Losses	Harmonic Multiplier	Totally Corrected Losses
No-Load	32350 (% 12.4)			32350 (%35.5)
I2R	126459 (% 48.7)	31827		31827 (% 34.9)
EC	33343 (% 12.8)	8392	1,16	9722 (% 10.7)
OSL	67697 (% 26.1)	17038	1,02	17332 (% 19)
Total Losses	259850 (% 100)			91230 (% 100)

The Top-Oil temperature rise can be calculated as follows;

$$\Delta\Theta_{TO} = 55 \times \left(\frac{91230}{259850} \right)^{0.9} = 21.4 \ ^{o}C$$

The rated inner or LV winding losses can be calculated as follows:

$(I_{2\text{-}R})^2$ x R= 1.5 x 2294^2 x 0.01= 131799 W

I_2^2 x R = 131799 x P_{LL} (pu)= 33170 W

$$\Delta\Theta_g = (65 - 55) \times \left(\frac{33170 + 9722 \times 2.4}{131799 + 33343 \times 2.4} \right)^{0.8} = 2.67 \ ^{o}C$$

The Hot-Spot rise is 2.67 ^{o}C in the presence of harmonics. To analyze the effect of the harmonics, the Hot-Spot rise can be calculated without taking into account the harmonic loss factor. The winding eddy current losses will therefore be 8392 W.

$$\Delta\Theta_g = (65-55)\times\left(\frac{34860+8392\times 2.4}{70320+10374\times 2.4}\right)^{0.8} = 2.5\ ^{o}\text{C}$$

The harmonic effect rises the Hot-Spot temperature by 0.1 ^{o}C. This value shows that the harmonic effect to the Hot-Spot temperature on this particular transformer is negligible.

Also the low Hot-Spot rise is because of the very low load factor.

CHAPTER 5

CONCLUSIONS

The various power transformers in use by TEİAŞ (Turkish Electricity Transmission Corporation,) have very simple thermometers to measure Top-Oil and Winding Temperatures. These thermometers show the Top-Oil temperature with a mechanical indicator. A coupling pipe transfers the Top-Oil temperature to the thermometer. Also in some transformers there are thermometers which show the winding temperature. However these winding temperature thermometers use the RMS current via a current transformer connected to the windings of the power transformer. After that it converts the current from the windings into heat. Meanwhile a coupling pipe transfers the Top-Oil temperature to the winding temperature thermometer. This coupling pipe and the current carrying cable are inserted into a liquid oil piston where they are used to heat the oil inside. The oil expands or shrinks according to the received heat and hence the temperature. This moves the indicator in the scope to the approximated temperature.

This type of measurement has critical problems. First, the result provided is totally an approximation. Second, the heat carrying Top-Oil temperature cable is in some cases 6m long and it is in direct contact with the ambient temperature. Lastly, the most critical problem is that the harmonic effect has been totally neglected. Considering a load demand with high harmonic content, the Hot-Spot temperatures will be greatly increased. And since the transformer protection equipment are switched on and off with the values defined by the Top-Oil and winding temperature scopes, the presence of harmonics will cause damage to the

transformers. These damages can be avoided using the calculations defined in IEEE Standards C57.110-1998 and C57.91-1995.

The work performed in this thesis has been accomplished by the utilization of the Mobile Power Quality Monitoring Devices used in National Power Quality Project (105G129).

Exact prediction of the Hot-Spot and Top-Oil temperatures can only be accomplished by the transformer manufacturer. This is because the required detailed knowledge such as the transformer structure, location of windings, insulating oil type etc. can only be acquired by the transformer manufacturer. For the verification activity, the best possible way to have the Hot-Spot data is through direct measurement via fiber optic sensors. The transformer manufacturers can perform these tests to be included in test reports. Since the cost of fiber optic sensor equipment has been decreasing rapidly during the last decade, this issue would bring the manufacturer a benefit rather than an extra cost.

Also the distribution companies may order transformers with fiber optic sensors already installed for the critical loads. Although this may seem to be an extra cost which is unnecessary, it will provide the safe operation for the transformers under risk. To validate the calculation of the Hot-Spot temperature on this thesis, the availability of the purchase of a transformer with fiber optic sensors has been discussed with TEİAŞ. Since such a purchase is unavailable during this time, the validation of Hot-Spot temperature measurements has been left as a further research activity.

The results of the TEMPEST have been logged on a MS Excel worksheet. However this technique showed incompatibility with Labview and resulted in erroneous data logging. Labview's own log files can be used to prevent this erroneous measurement which has also been left as a further study.

REFERENCES

[1] IEEE Std C57.12.80-2002, “IEEE Standard Terminology for Power and Distribution Transformers”.

[2] Asaad A. Elmoudi, “Evaluation of Power System Harmonic Effect on Transformers, Hot Spot Calculation and Loss of Life Estimation”, Doctoral Dissertation, http://lib.tkk.fi/Diss/ , November 2007.

[3] IEEE Std C57.110-1998, “IEEE Recommended Practice for Establishing Transformer Capability When Supplying Nonsinusoidal Load Currents”.

[4] IEEE Std C57.91-1995, “IEEE Guide for Loading Mineral-Oil- Immersed Transformers”.

[5] IEEE Std C57.91™-1995/Cor 1-2002, “IEEE Guide for Loading Mineral-Oil- Immersed Transformers Corrigendum 1”.

[6] S. N. Makarov, A. E. Emanual, “Corrected Harmonic Loss Factor For Transformers supplying Non-sinusoidal Load current,” Proc. of the 9th International conference on Harmonics and Power Quality, vol. 1, pp.87-90 Oct. 2000,

[7] M. K. Pradhan and T. S. Ramu, “Prediction of Hottest Spot Temperature (HST) in Power and Station Transformers”, IEEE Transaction on Power Delivery, vol. 18, iss. 4, October 2003.

[8] Lesieutre B.C., Hagman W.H., Kirtley J.L. Jr., "An improved transformer top oil temperature model for use in an on-line monitoring and diagnostic system", IEEE Transactions on Power Delivery, vol. 12 , iss. 1, pp. 249 – 256, January 1997.

[9] G. W. Swift et al., “Adaptive Transformer Thermal Overload Protection", IEEE Transactions on Power Delivery , vol. 16, iss. 4, pp. 516-521, Oct 2001.

[10] Dejan Susa, “Dynamic Thermal Modeling of Power Transformers”, Doctoral Dissertation, http://lib.tkk.fi/Diss/ , November 2007.

[11] Lida Jauregui Rivera, Daniel J. Tylavsky, “Acceptability of Four Transformer Top-Oil, Thermal Models: Pt. 1: Defining Metrics”, www.pserc.org/ecow/get/publicatio/2007public/, November 2007.

[12] Lida Jauregui Rivera, Daniel J. Tylavsky, “Acceptability of Four Transformer Top-Oil Thermal Models: Pt. 2: Comparing Metrics”, www.pserc.org/ecow/get/publicatio/2007public/ , November 2007.

[13] Yong Liang, “Simulation of Top Oil Temperature for Transformers”, Masters Thesis and Final Project Report, www.pserc.org/ecow/get/publicatio/2001public/, November 2007.

[14] Rummiya Vilaithong, Stefan Tenbohlen, Tobias Stirl, “Investigation of Different Top-oil Temperature Models for On-line Monitoring System of Power Transformer”, www.uni-stuttgart.de/ieh/forschung/veroeffentlichungen, November 2007.

[15] S. Tenbohlen et. al., “Experienced-based Evaluation of Economic Benefits of On-line Monitoring Systems for Power Transformers”, www.uni-stuttgart.de/ieh/forschung/veroeffentlichungen/, November 2007.

[16] Daniel J. Tylavsky and Xiaolin Mao, “Transformer Thermal Modeling: Improving Reliability Using Data Quality Control”, IEEE Transactions on Power Delivery, Publication Date: July 2006, vol. 21, iss. 3, pp. 1357-1366.

[17] IEC 61000-4-30, “Testing and Measurement Techniques- Power Quality Measurement Methods”.

[18] IEC 61000-4-7, “Testing and Measurement Techniques- General Guide on harmonics and interharmonics measurements and instrumentation, for power supply systems and equipment connected thereto”.

[19] IEC 61000-4-15, “Testing and Measurement Techniques- Flickermeter-Functional and Design Specifications”.

[20] IEEE Std-519, “Recommended Practices and Requirements for Harmonic Control in Electrical Power Systems”.

.

[21] IMO (Independent Electricity Market Operator), “Market Manual 3: Metering, Part 3.5: Site-Specific Loss Adjustments”, iss. 6.0.

[22] IEEE Std C57.123-2002, “IEEE Guide for Transformer Loss Measurement”.

[23] Vivian Ohis, Tadeusz Czaszejko, “Techniques for estimation of hot spot temperatures in transformers”, www.itee.uq.edu.au/~aupec/aupec02/ Final-Papers/V-Ohis1.pdf, November 2007.

[24] IEC (International Electrotechnical Commission), “Loading guide for oil-immersed power transformers”, Standard 354:1991-09, Second ed.

[25] M. Ermiş et.al, “Mobile Monitoring System to Take PQ Snapshots of Turkish Electricity Transmission System”, Instrumentation and Measurement Technology Conference – IMTC 2007 Warsaw, Poland, May 2007.

[26] National Instruments, “Analog Signal Conditioning Accessories”, http://sine.ni.com/nips/cds/view/p/lang/en/nid/1728, November 2007.

[27] National Instruments, "NI DAQCard-6036E (for PCMCIA)", http://sine.ni.com/nips/cds/view/p/lang/en/nid/11914, November 2007.

[28] LabVIEW™ 8.0, National Instruments, 2005

[29] José Antonio Jardin et. al., "Power Transformer Temperature Evaluation for Overloading Conditions", IEEE Transactions on Power Delivery, vol. 20, iss. 1, January 2005.

[30] M. K. Pradhan and T. S. Ramu, "Estimation of the Hottest Spot Temperature (HST) in Power Transformers Considering Thermal Inhomogeneity of the Windings", IEEE Transactions on Power Delivery, vol. 19, iss. 4, October 2004.

[31] IEEE Std C57.12.90-2006, "IEEE Standard Test Code for Liquid-Immersed Distribution, Power, and Regulating Transformers".

[32] IEEE Std C57.12.91-2001, "IEEE Standard Test Code for Dry-Type Distribution and Power Transformers".

[33] Sheldon P. Kennedy, C.L. Ivey, "Application, Design and Rating of Transformers Containing Harmonic Currents", Conference Record of 1990 Annual Pulp and Paper Industry Technical Conference, 1990, pp. 19-31, 18-22 Jun 1990.

[34] Del Vecchio et. al., "Transformer Design Principles: With Applications to Core Form Transformers", Gordon and Breach Science Publishers, c2001, TK2551 .T73 2001.

[35] D. Pavlik, D. C. Jdvlson, R. S. Girgis, "Calculation and Reduction of Stray and Eddy Losses in Core-Form Transformers using a highly accurate finite element modeling technique", IEEE Transactions on Power Delivery, vol. 8, iss. 1, pp. 239-245, January 1993.

[36] O.W. Andersen, “Transformer leakage flux program based on the finite element method”, IEEE Transactions on Power Apparatus and Systems, vol. PAS-92, iss. 2, pp. 682-689, March 1973.

[37] S.V. Kulkarni and S.A. Khaparde, “Transformer Engineering-Design and Practice”, New York: Marcel Dekker, Inc., c2004, TK2551 .K96 2004.

[38] O.W. Andersen, “Transformer leakage flux program based on the finite element method”, IEEE Transactions on Power Apparatus and Systems, vol. PAS-92, iss. 2, pp. 682-689, March 1973.

[39] A. Kara, Ö. Kalenderl, K. Mardikyan, “Effect of dielectric barriers to the electric field of rod-plane air gap”, www2.humusoft.cz/ www/akce/comsol06/, November 2007.

[40] MATLAB 7.0, the language of technical computing, Matworks Inc., 2005

[41] Edward Simonson, The National Grid Company plc., “Transformer Ratings and Transformer Life”, IEE Colloquium on Transformer Life Management (Ref. No. 1998/510), pp. 7/1-7/6, Oct 1998

[42] Working Group 09 of Study Committee 12, “Direct Measurement of Hot-Spot Temperature of Transformers,” CIGRE Electra no. 129, pp. 48–51, March 1990.

[43] Jean-Noël Bérubé, Jacques Aubin – Neoptix Inc. & W. McDermid – Manitoba Hydro, “Transformer winding Hot Spot Temperature Determination”, http://electricenergyonline.com/MAGArchives.asp?m=55, November 2007.

APPENDIX A

TRANSFORMER LOSSES AND TEMPERATURE RISE

A.1 Transformer Losses

A.1.1 Introduction

IEEE Std C57.12.90-2006 [31] and IEEE Std C57.12.91-2001 [32] categorize transformer losses as no-load loss (excitation loss); load loss (impedance loss); and total loss (the sum of no-load loss and load loss). Figure 62 shows the hierarchy of the transformer losses. Load loss is subdivided into I^2R loss and stray loss. Stray loss is determined by subtracting the I^2R loss (calculated from the measured resistance) from the measured load loss (impedance loss) [3]. Stray losses can be particularly high in power transformers with large ratings [2].

A.1.2 No-Load Losses

No-load or core loss can be broken down into core eddy loss, hysteresis loss and a very small winding excitation loss. These core eddy losses are not same as the winding eddy-current losses. These losses vary on a Watt per pound basis.

The harmonics flowing in the load current may also create harmonic distortions in the voltage waveforms. Due to saturation, the higher the core induction the more these effects will be.

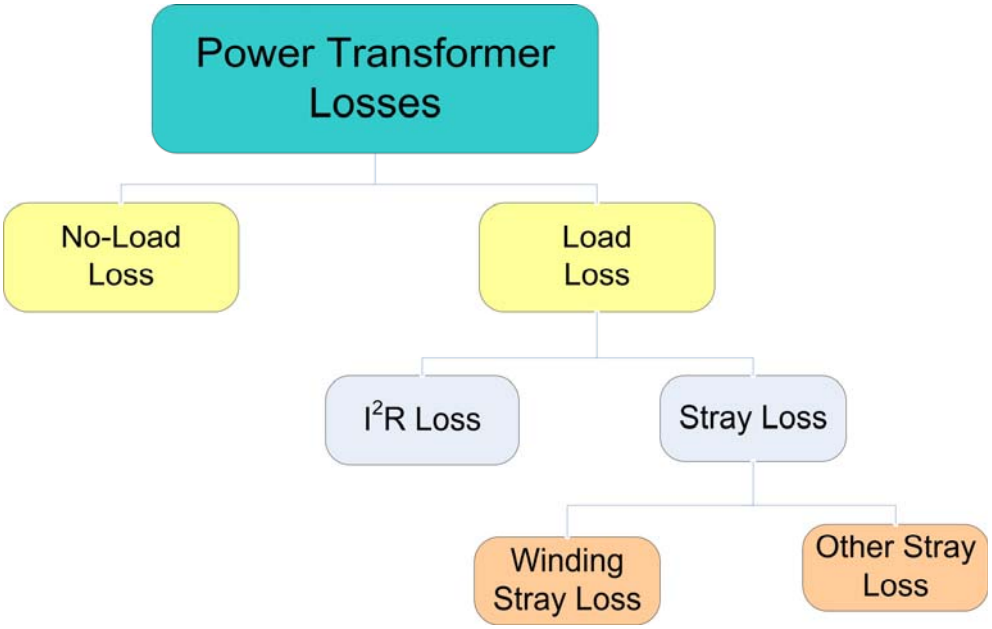

Figure 62 Types of Transformer Losses

Another important concern is the usage of variable frequency output transformers which may result in increased Volts per Hertz. This may lead to an extreme situation of core saturation and exciting current values in the level of short-circuit type [3, 33].

A.1.3 Load Losses

Load loss is subdivided into I^2R loss and stray loss. Stray loss is determined by subtracting the I^2R loss (calculated from the measured resistance) from the measured load loss (impedance loss). Stray loss can be defined as the loss due to stray electromagnetic flux in the windings, core, core clamps, magnetic shields,

enclosure or tank walls, etc. Thus, the stray loss is subdivided into winding stray loss and stray loss in components other than the windings (P_{OSL}) [3, 33]. The winding stray loss includes winding conductor strand eddy-current loss and loss due to circulating currents between strands or parallel winding circuits. All of this loss may be considered to constitute winding eddy-current loss, P_{EC}. The relationships can then be stated as;

$$P_{LL} = P_{I^2R} + P_{stray} \tag{A.1}$$

$$P_{TSL} = P_{EC} + P_{OSL} \tag{A.2}$$

$$P_{LL} = P_{I^2R} + P_{EC} + P_{OSL} \tag{A.3}$$

Load losses are measured by applying a short circuit across either the high-voltage winding or the low-voltage winding and applying sufficient voltage across the other winding to cause a specified current to flow in the windings. The power loss within the transformer under these conditions equals the load losses of the transformer at the temperature of test for the specified load current. [31]

A.1.4 Voltage Harmonic Effect

$$N_1 . \frac{d\phi}{dt} \cong u_1(t) \tag{A.4}$$

$$N_1 . j(hw) . \phi_h \cong U_h \quad \text{h=1,3,…} \tag{A.5}$$

These equation shows that the flux magnitude is proportional to the voltage harmonic and inversely proportional to the harmonic order h. Furthermore, within most power systems the harmonic distortion of the system voltage THD. is well below 5% and the magnitudes of the voltage harmonics components are small compared to the fundamental component, rarely exceeding a level of 2-3%. This is determined by the low internal impedance of most supply systems carrying harmonics. Therefore neglecting the effect of harmonic voltage and considering the no load losses caused by the fundamental voltage component will only give rise to an insignificant error [2].

A.1.5 Current Harmonic Effect

A.1.5.1 Harmonic current effect on I^2R loss

If the RMS value of the load current is increased due to harmonic components, the I^2R loss will be increased accordingly [3].

A.1.5.2 Harmonic current effect on P_{EC} and solution of P_{EC} using FEM

Winding eddy-current loss (P_{EC}) in the power frequency spectrum tends to be proportional to the square of the load current and the square of frequency. It is this characteristic that can cause excessive winding loss and hence abnormal winding temperature rise in transformers supplying nonsinusoidal load currents. [2, 34]

$$P_{EC} = \frac{w^2 B_0^2 t^2}{24\rho} \tag{A.6}$$

where;

$$(P_{EC})_{axial} = \frac{w^2 B_y^2 T^2}{24\rho} \tag{A.7}$$

$$(P_{EC})radial = \frac{w^2 B_x^2 l^2}{24\rho} \tag{A.8}$$

For strand dimensions that are small compared to skin depth

$$P_{EC} \cong \frac{\pi^2 f^2 T^2 B^2}{3\rho} \text{ W/m}^3 \quad \text{for Rectangular Conductor} \tag{A.9}$$

$$P_{EC} \cong \frac{\pi^2 f^2 d^2 B^2}{4\rho} \text{ W/m}^3 \quad \text{for Round Conductor} \tag{A.10}$$

The assumption that the eddy current losses in a winding are proportional to the square of the harmonic order is only reasonable for transformers with small conductors.

FEM (Finite Element Method) shall be used to calculate the B component of the Eddy Current Losses [34, 35, 36, 37, 38]. A detailed modeling shall be established such as in Figure 63.

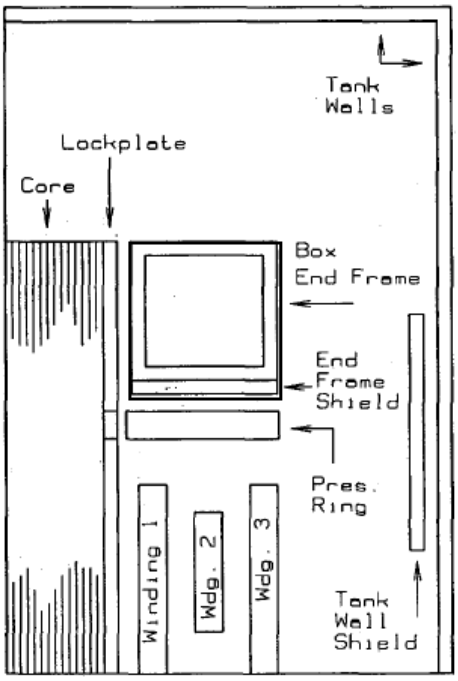

Figure 63 View of a transformer leakage flux region modeling

One of the mainly used programs for the calculation of FEM is the COMSOL Multiphysics [2, 39] (a stand alone program formerly called FEMLAB). Figure 64 and Figure 65 show the stages of a sample modeling of using COMSOL.

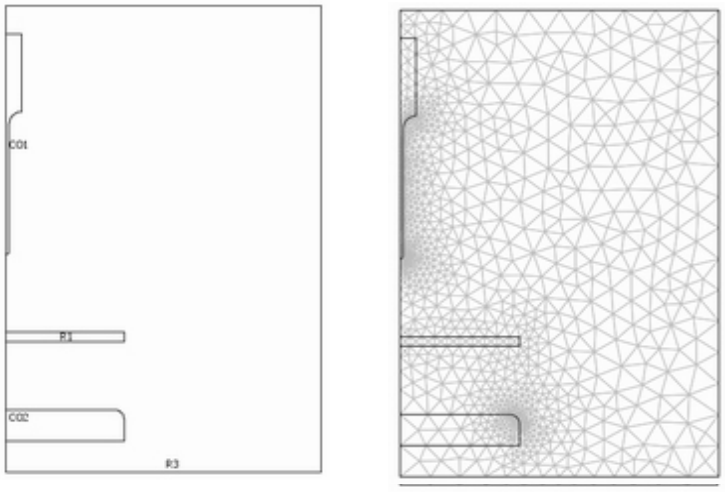

Figure 64 Problem definition in COMSOL software and the obtained electric field and potential distributions (Draw Mode and Mesh Solution)

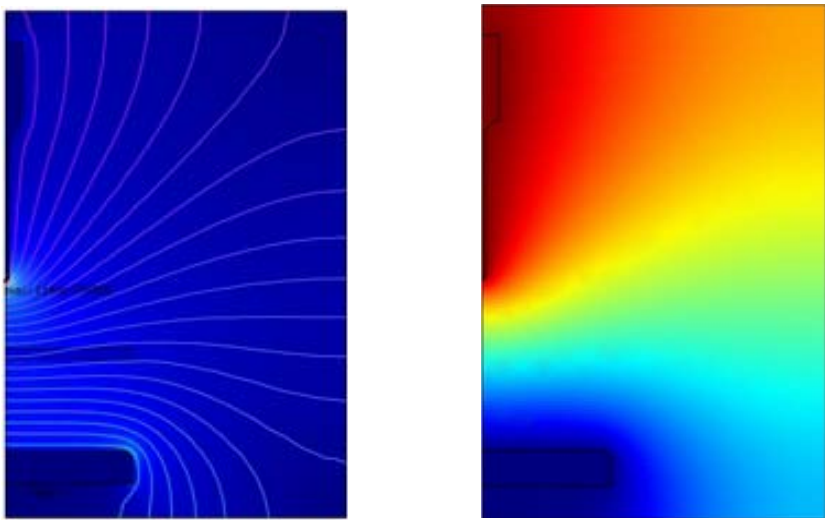

Figure 65 Problem definition in COMSOL software and the obtained electric field and potential distributions (Counter and Color Solutions)

However the usage of a more familiar and widely used program, MATLAB (in association with Partial Differential Equation (PDA) Toolbox which is also powered by COMSOL), can provide similar results [40]. The availability of FEM calculations with MATLAB has been investigated prior to the finalization of the TEMPEST program. It was concluded that due to the impracticality of the application of FEM on the site, the winding eddy current loss calculation using FEM is unsuitable for online calculations such as the one performed on this thesis. However, as an example, the following work has been performed before this conclusion and it can be accepted that MATLAB is a sufficient tool for the calculations of FEM using PDA tool. Figure 66 shows the results performed by using MATLAB at the draw mode view of a transformer with the specifications as depicted in Table 8 [2]. Figure 67 shows the combined solution of counter and color mode.

Table 8 Input data for PDA Toolbox

Input data for 31.5 MVA			
Sub domain	Sig σ	μ_r	Current density
LV Winding	0	1	-2.67A/mm2
HV Winding	0	1	1.98 A/mm2
Reg. Winding	0	1	0
Core	0	2000	0

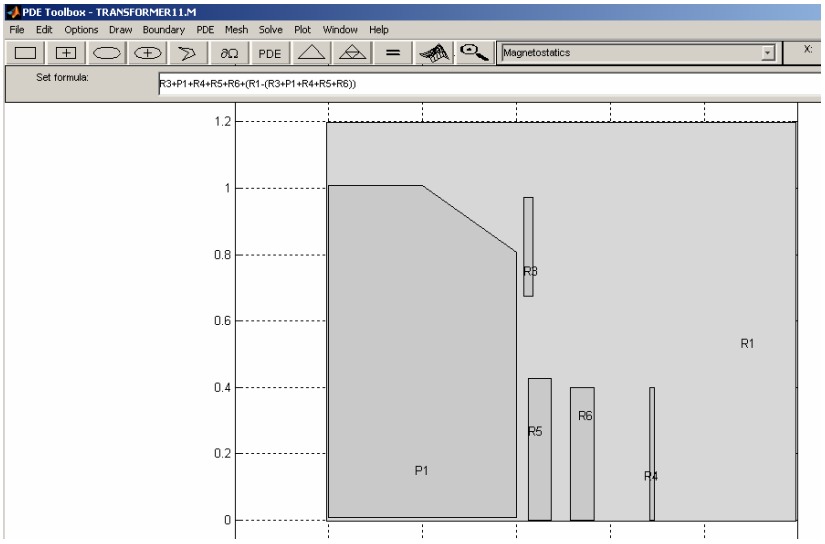

Figure 66 Draw mode view of a FEM analysis using MATLAB PDA Toolbox

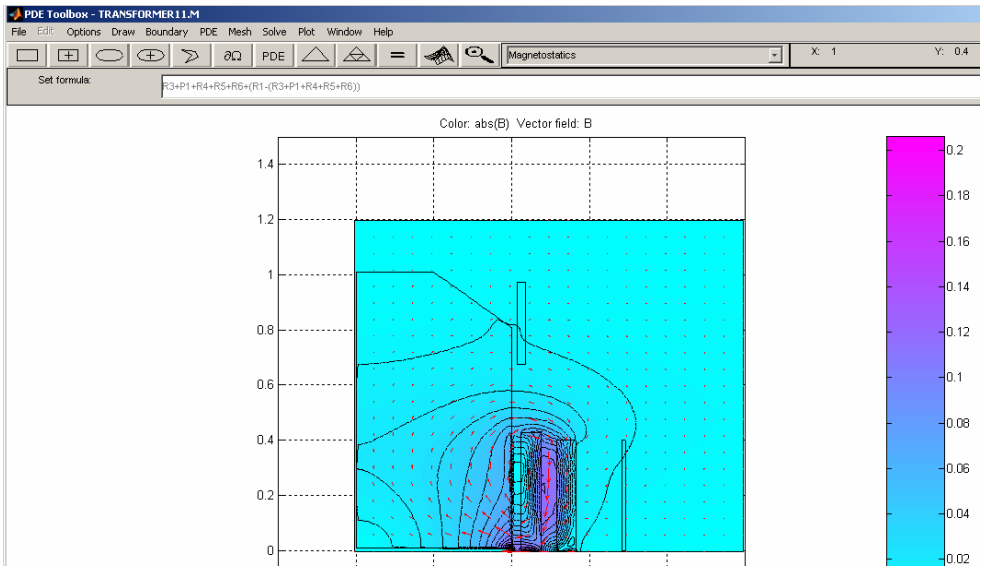

Figure 67 Counter and Color mode solutions of a FEM analysis using MATLAB PDA Toolbox

A.1.5.3 Harmonic Current Effect on P_{OSL}

It is recognized that other stray loss (P_{OSL}) in the core, clamps, and structural parts will also increase at a rate proportional to the square of the load current. However, these losses will not increase at a rate proportional to the square of the frequency, as in the winding eddy losses. Studies by manufacturers and other researchers have shown that the eddy-current losses in bus bars, connections and structural parts increase by a harmonic exponent factor of 0.8 or less. Temperature rise in these regions will be less critical than in the windings for dry-type transformers. However, these losses must be properly accounted for in liquid filled transformers [3].

A.1.5.4 Harmonic Current Effect on Transformer

The increased eddy current losses produced by a non-sinusoidal load current can cause excessive winding losses and hence abnormal temperature rise. Therefore the influence of the current harmonics is more important, not only because of the assumed square of the harmonic order but also because of the relatively large harmonic currents present in the power system [3].

A.2. Temperature Rise

A.2.1 Introduction

The most common used method model for Top-Oil and Hot-Spot temperature calculations is the method described in Clause 7 of the IEEE Guide [4]. A pictorial description of the steady-state relationships is shown in Figure 68, similar to Figure of the IEC Standard [25].

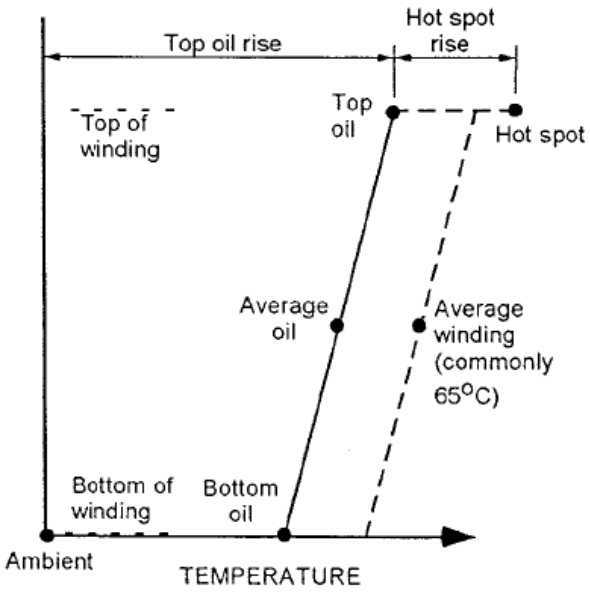

Figure 68 Steady-state temperature relationships

Aging or deterioration of insulation is a time function of temperature, moisture content, and oxygen content. It is defined as; for a given Hot-Spot temperature, the rate at which transformer insulation aging is accelerated compared with the aging rate at a reference hot -spot temperature. The reference Hot-Spot temperature is 110 °C for 65 °C average winding rise and 95 °C for 55 °C average winding rise transformers (without thermally upgraded insulation). For Hot-Spot temperatures in excess of the reference Hot-Spot temperature the aging acceleration factor is greater than 1. For Hot-Spot temperatures lower than the reference Hot-Spot temperature, the aging acceleration factor is less than 1.

With modern oil preservation systems, the moisture and oxygen contributions to insulation deterioration can be minimized, leaving insulation temperature as the

controlling parameter. Since, in most apparatus, the temperature distribution is not uniform, the part that is operating at the highest temperature will ordinarily undergo the greatest deterioration. Therefore, in aging studies it is usual to consider the aging effects produced by the highest (Hot-Spot) temperature. Because many factors influence the cumulative effect of temperature over time in causing deterioration of transformer insulation, it is not possible to predict with any great degree of accuracy the useful life of the insulation in a transformer, even under constant or closely controlled conditions, much less under widely varying service conditions [4].

The transformer per unit insulation life curve of Figure 69 relates per unit transformer insulation life to winding Hot-Spot temperature. This curve should be used for both distribution and power transformers because both are manufactured using the same cellulose conductor insulation. The use of this curve isolates temperature as the principal variable affecting thermal life. It also indicates the degree to which the rate of aging is accelerated beyond normal for temperature above a reference temperature of 110 °C and is reduced below normal for temperature below 110 °C.

The per unit transformer insulation life curve (Figure 69) can be used in the following two ways. It is the basis for calculation of an aging acceleration factor (F_{AA}) for a given load and temperature or for a varying load and temperature profile over a 24 h period. A curve of F_{AA} vs. Hot-Spot temperature for a 65 °C rise insulation system is shown in Figure 70 [4].

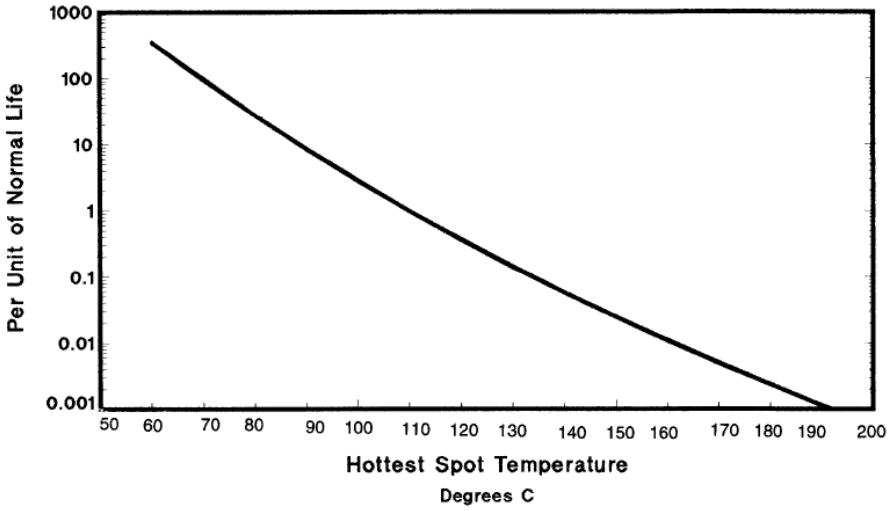

Figure 69 Transformer Insulation Life [12]

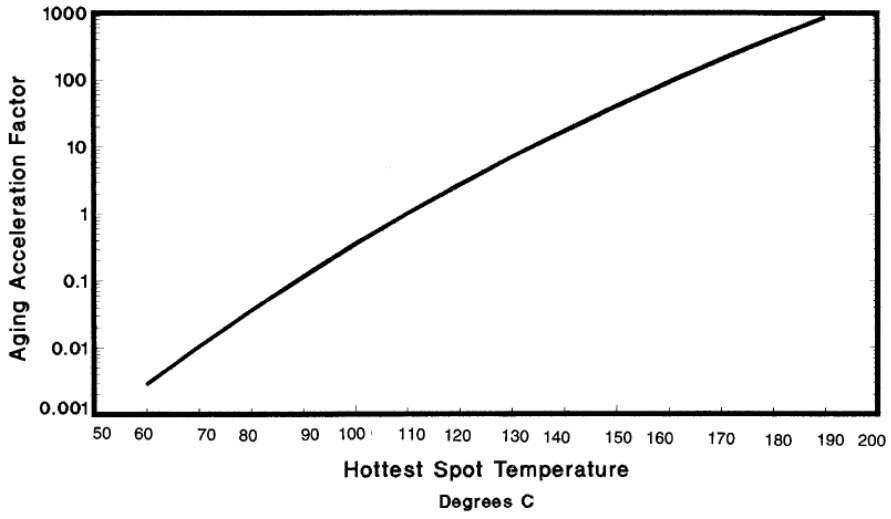

Figure 70 Aging acceleration factor (relative to 110 ^{o}C) [12]

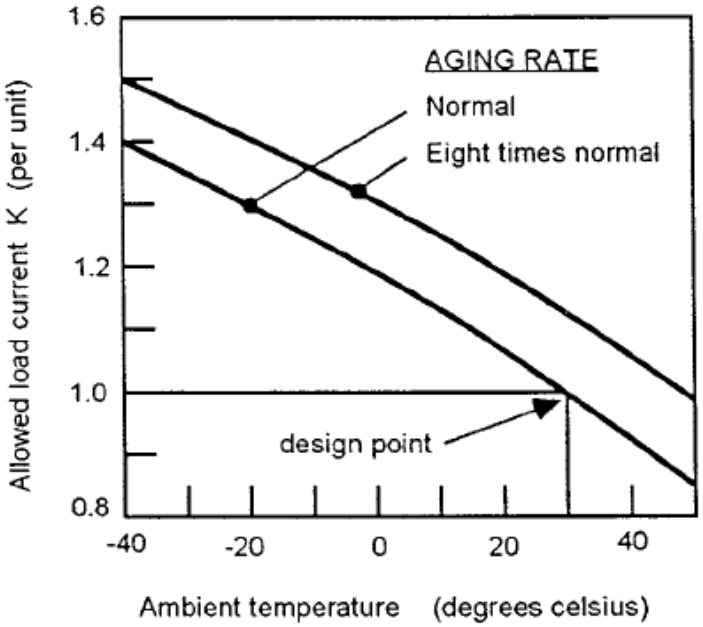

Figure 71 Allowable load currents at different ambient temperatures [15]

A specified aging rate of "normal," i.e., 1.0, determines the pickup level of one per unit current, meaning nameplate current. A higher pickup level is chosen by simply increasing the specified aging rate. As seen in Figure 71, at an ambient temperature of 30 ^{o}C, the pickup would increase from 1.0 per unit to about 1.1 per unit, for that transformer, for an eight-fold increase in allowable steady-state aging rate [9].

A.2.2 Effects of temperature rise

A.2.2.1 Effects on Paper Insulation

It is usually accepted that the ageing of the paper insulation system is such that the stated transformer life can be achieved for a continuous maximum Hot-Spot temperature of 98°C. Beyond this, it is assumed that the rate of ageing doubles for every increase of 6°C. At temperatures of the order of 150°C, accelerated ageing tests in the laboratory demonstrate that the useful life of the paper may only be a few days. The mechanical strength of the paper arises from long chain cellulose polymers. The chain length can be characterized by a degree of polymerization (DP) measurement that gives values of 1000 or more for new paper.

The cellulose structure of the paper degrades at high temperatures until at a DP of about 200, the paper has no remaining mechanical strength. This clearly limits the life of the transformer and is one of the governing factors on the maximum load that should be used [9, 41].

A.2.2.2 Gas Formation

There are also other effects of the temperature on the transformer; one such factor is the production of gas in the oil. Significant gassing can start to occur at temperatures in the region of 140°C to 160°C and above. For transformers with moisture levels of 0.5% or less, bubbles may not form until the temperature is above 200 ^{o}C. This can seriously compromise the dielectric strength of the insulation system and lead to premature failure. However, gas bubbles produced in the windings will tend to occur in the hot regions nearer the top and may quickly be drawn off into the cooling system. Likewise, bubbles resulting from high temperatures caused by stray loss heating of the core or other metal parts

need not pass through areas of high electrical stress at all and may thus offer a lower risk of failure. Of course, unless the gas is removed in some way or re-dissolves before circulating out of the coolers, there is scope for serious problems when it re-enters the transformer at the bottom of the windings. The rate of gas production could thus be as important as the total amount produced, but either way, although such considerations provide another limit on transformer ratings, they need not have any direct effect on transformer life [9, 41].

A.2.2.3 Insulation Oil

The other major transformer component to be considered is the insulating oil. Oil is subject to degradation due to direct thermal effects and enhanced oil temperatures are likely to accelerate other ageing processes. The condition of the oil can affect the ability of a transformer to withstand emergency overloading. The concentrations of moisture, gases and impurities due to ageing are all important. However, unlike the paper insulation, the oil can be reclaimed or changed where this is deemed beneficial. Oil condition can have an effect on loading [9, 41].

A.2.3 Measurement method of Winding Hot-Spot temperature in transformers used in Turkish Electricity Transmission System

There are two types of temperature thermometers used in Turkish Electricity Transmission System as shown in Figure 72; oil and winding thermometers.

The oil thermometer measuring range is designated as -20 to 130 ^{o}C. This range corresponds to an accuracy value of ± 3 ^{o}C. There are 4 micro switching contacts on the device. A 6m long coupling pipe connects the Top-Oil temperature measurement bulb to the thermometer. The coupling pipe is used to transfer the

temperature to the thermometer. Here the thermal heat is used to warm a piston so that the pointer moves as the Top-Oil temperature varies.

Usually the Hot-Spot temperature cannot be directly measured on commercial designs because of the voltage hazard when placing a temperature detector at the proper location. The Hot-Spot temperature for commercial designs may be determined by the manufacturers from analytical studies verified by thermal tests on coils with imbedded temperature detectors.

Figure 72 Oil and Winding Thermometers

Hot-Spot temperature devices are supplied, when specified, and usually indicate a simulated Hot-Spot temperature. The simulated devices are calibrated for use with specific transformers and simulate the Hot-Spot temperature by taking into account the Top-Oil temperature and the load. The simulated Hot-Spot indicators may be used to control cooling equipment and give alarms at a predetermined Hot-Spot temperature in order to limit overloading [4]. The winding temperature monitoring thermometers found on transformers in Turkish Electricity Transmission System utilizes the above mentioned simulation technique.

The winding temperature measuring range is designated as 0 to 150 ^{o}C. This range corresponds to an accuracy value of ± 3 ^{o}C. There are 4 micro switching contacts on the device.

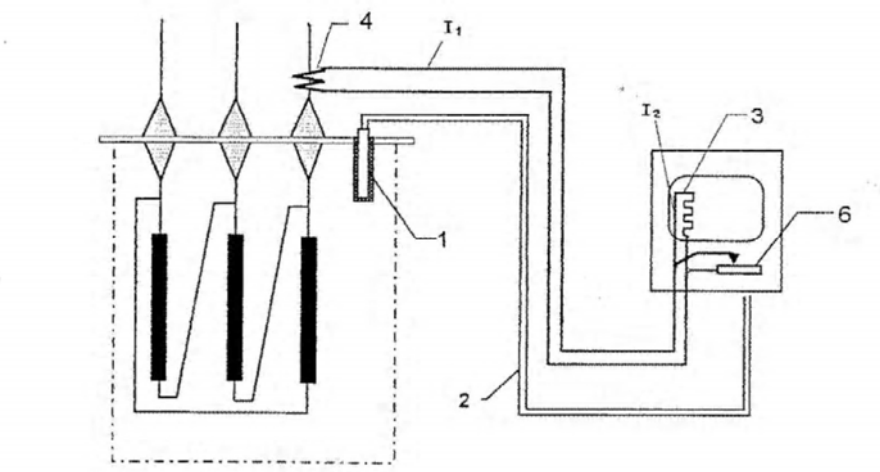

Figure 73 Winding thermometer principal diagram

Instead of direct measurement of winding temperature, winding thermometers use the RMS current via a current transformer (indicated by “4”) connected to the windings of the power transformer as shown in Figure 73. Later, it converts the current from the windings into heat by the thermal component (indicated by “3”). Meanwhile a coupling pipe (indicated by “2”) transfers the Top-Oil temperature (indicated by “1”) to the winding thermometer.

Inside the winding thermometer, the temperature coupled by “2” and generated by “3” is added together in a liquid oil piston where they are used to heat the piston’s oil. The oil expands or shrinks according to the received heat. This effect moves the indicator in the thermometer, which shows the approximated temperature.

The above mentioned temperature measurement has critical problems. First, the result provided is totally an approximation. Second, the heat carrying coupling pipe is 6m long and it is in direct contact with the ambient temperature. Finally, the most critical problem is the harmonic effect which has been totally neglected. Considering a load demand with high harmonic content, the Hot-Spot temperatures will be greatly increased. And since the transformer protection equipment are switched on and off with the values defined by the contacts positioned inside the Top-Oil and winding temperature thermometers, the presence of harmonics will be neglected. This situation may cause damage to the transformers. These damages can be avoided using the calculations defined in IEEE Standards C57.110-1998 and C57.91-1995.

A.2.4 Determination of Winding Hot-Spot temperature by direct measurement

The best method to measure the Hot-Spot would be the direct measurement of the actual Hot-Spot with fiber optic sensors [2, 3 and 10]. This kind of direct measurement technique has been increasingly used since the mid-1980s [10]. Due to the poor reliability, redundant probes must be used. Experience indicates that even with extreme care in installation about 25%-33% of the probes can be expected to fail due to damage. Reported data indicates that the location of the Hot-Spot is difficult to determine. A survey reported that two to eight sensors would be adequate if placed in the winding where the higher temperature is expected but for prototype transformers it was estimated that twenty to thirty sensors would be required [4, 42].

These devices are capable of indicating the temperature only at the spots where sensors are located. The proper choice of location for the sensors in the transformer windings is crucial to accurately determine the Hot-Spot temperature. Therefore, their accuracy in measuring the winding Hot-Spot is dependent on the ability to predict the Hot-Spot location prior to the sensors' placement. However, even with these disadvantages, many consider fiber optic sensors the best tool available for measuring winding Hot-Spot temperatures [5, 10, 13].

Figure 74 shows an example of sensor directly in contact with a continuously transposed cable (CTC). The insulation must be removed locally and restored after sensor installation [43]. However, this method may not be practical for existing transformers, also added difficulty in justifying the added costs, has limited its use on new transformers. On existing transformers, the most common method is to simulate the Hot-Spot temperature [2].

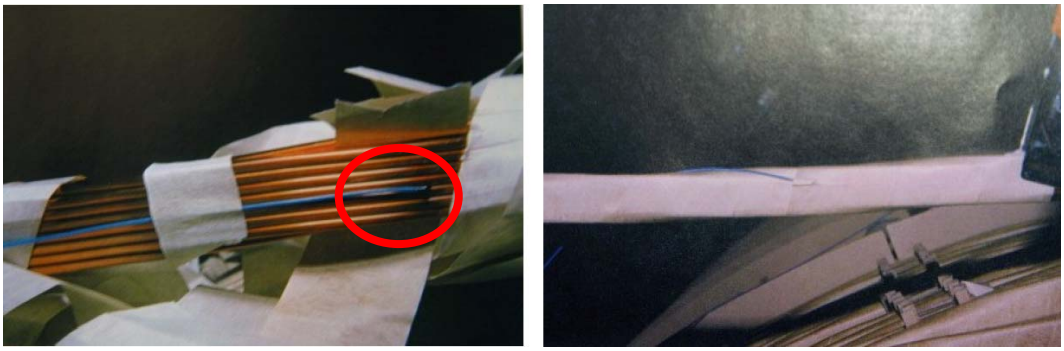

Figure 74 Fiber optic sensor directly in contact with CTC cable [43]

A.3. Application Examples

Apart from the 2 Power Transformer measurements presented in Chapter 4, measurements have been performed on 4 different locations. The first two transformer measurements mentioned below are performed on transformer with high harmonic content and intermittent loads while the latter two transformers supplies conventional loads.

A.3.1 80/100 MVA ONAN/ONAF Intermittent Load

Figure 75 Transformer Almak-A

A measurement has been performed on a transformer located in Almak Transformer Center with the same ratings but with a different loading than the one in Alçuk-B.

Table 9 shows the TEMPEST input data for transformer Almak-A. These values have been acquired from manufacturer's certified test report.

Also in this transformer, the calculated Hot-Spot temperature's response to an excessive initial value has been examined. An initial value of 80 ^{o}C has been given to the Hot-Spot temperature. The Hot-Spot temperature's response to settle at steady state has been examined.

Table 9 TEMPEST Input data for Almak-A

ALMAK-A TRANSFORMER	
Rated Capacity	100 MVA
HV	154000 V
LV	34500 V
No-Load Losses	32350 W
Load Losses	165000 W
HV Connection	Wye
LV Connection	Wye
Base Current	1718.3 A
Top Oil Time Constant	3 hours
Winding Time Constant	7 minutes

A.3.1.1 Loading and Harmonic Content

Figure 76 shows the Total Demand Distortion graph for the full scale measurement. On the general, the TDD's maximum value is around 10% and the average value is around 6%.

Figures 77-97 show the fundamental and harmonic components of the load current from 2nd to 21st for all of the 3 phases. It can be seen that the required harmonic content for Hot-Spot temperature calculation is present for this transformer. The acceptable harmonic limits defined by the "Electricity Transmission Demand Safety and Quality Regulations" have been marked as "Standard Limit".

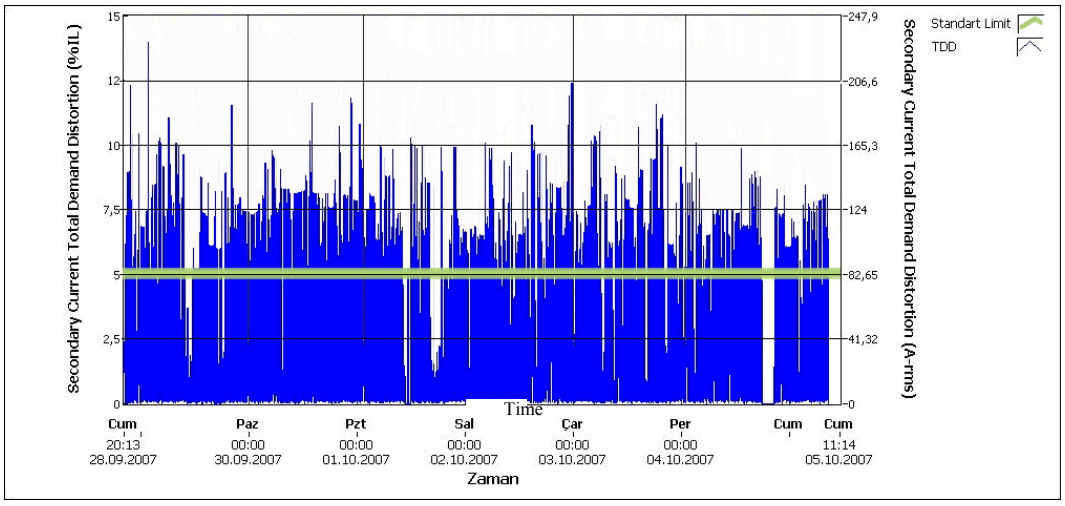

Figure 76 Almak-A, TDD
(Averaged in each 3 seconds)

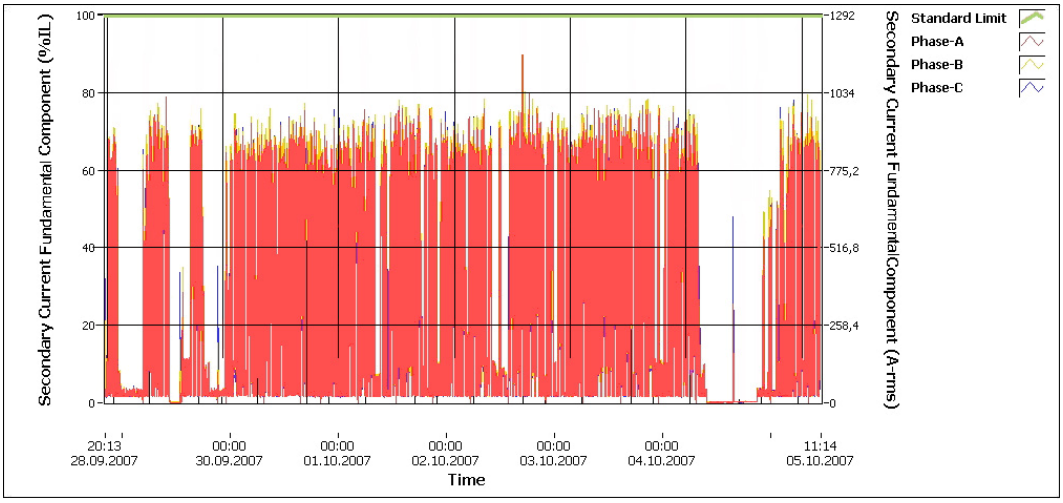

Figure 77 Almak-A, Fundamental Component of the Secondary Current (Averaged in each 3 seconds)

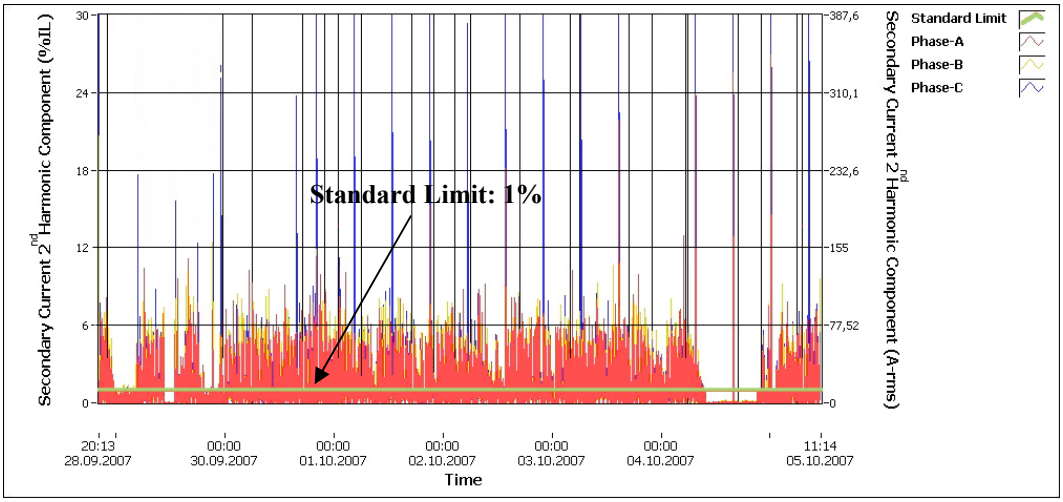

Figure 78 Almak-A, 2nd Harmonic Component of the Secondary Current (Averaged in each 3 seconds)

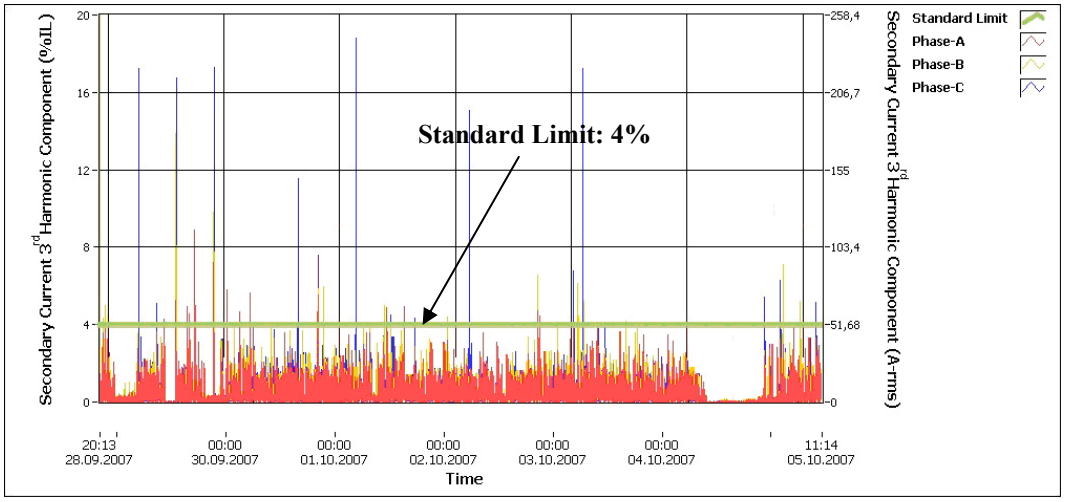

Figure 79 Almak-A, 3rd Harmonic Component of the Secondary Current (Averaged in each 3 seconds)

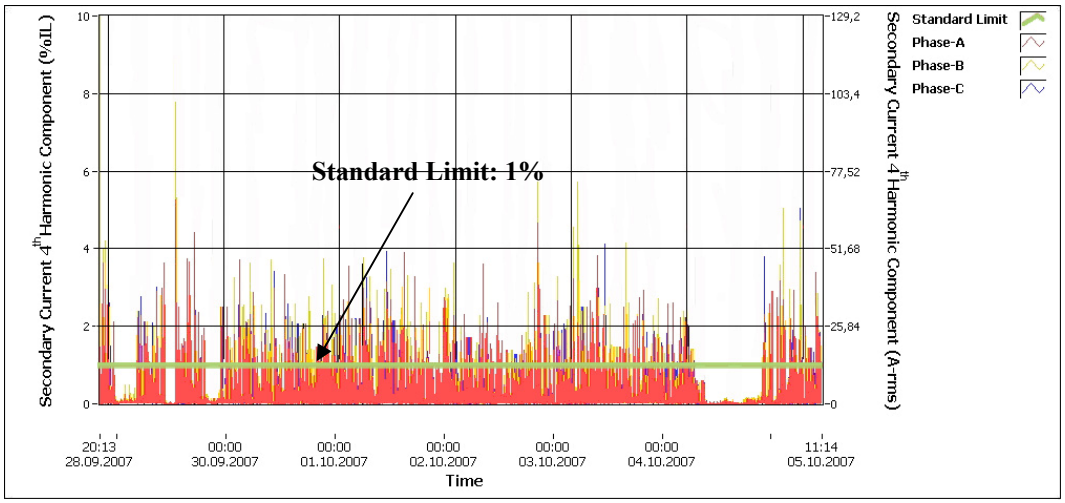

Figure 80 Almak-A, 4th Harmonic Component of the Secondary Current (Averaged in each 3 seconds)

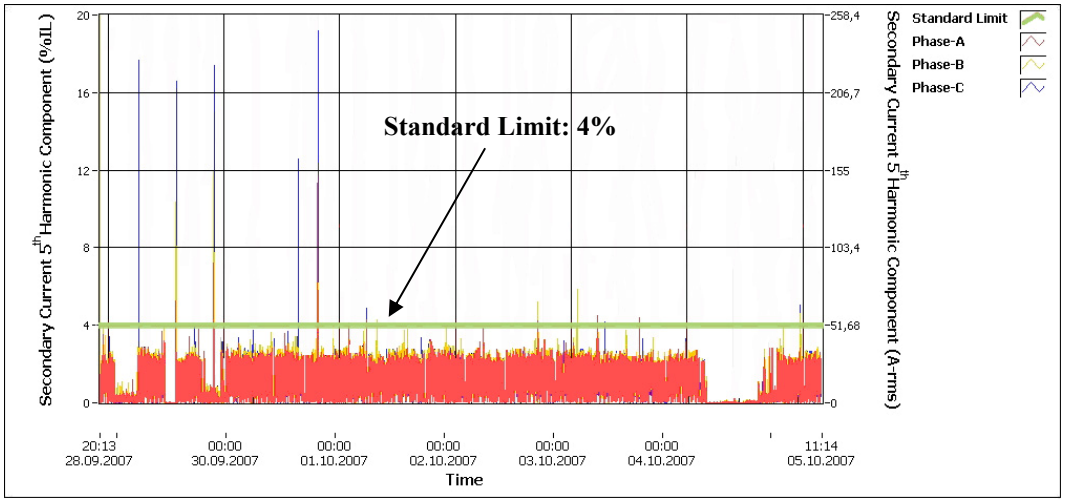

Figure 81 Almak-A, 5th Harmonic Component of the Secondary Current (Averaged in each 3 seconds)

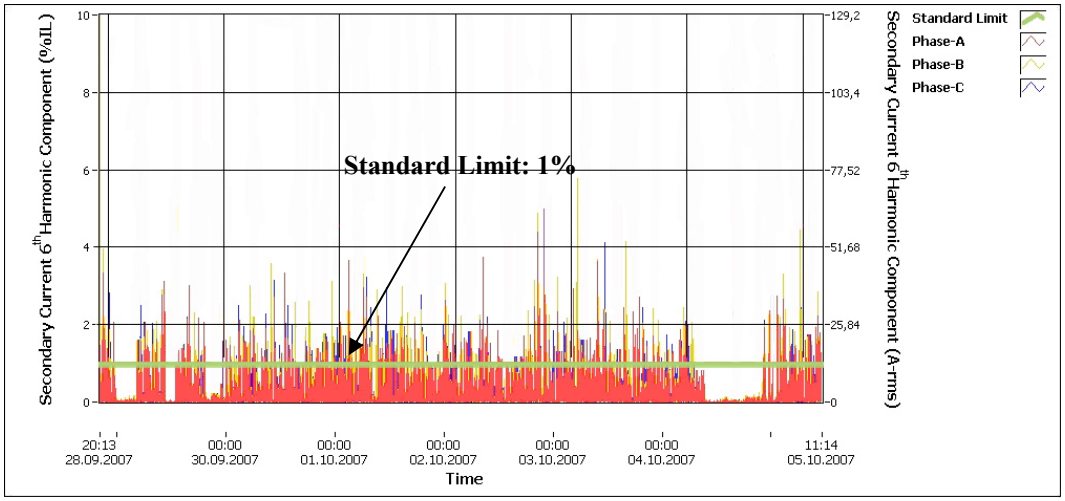

Figure 82 Almak-A, 6th Harmonic Component of the Secondary Current (Averaged in each 3 seconds)

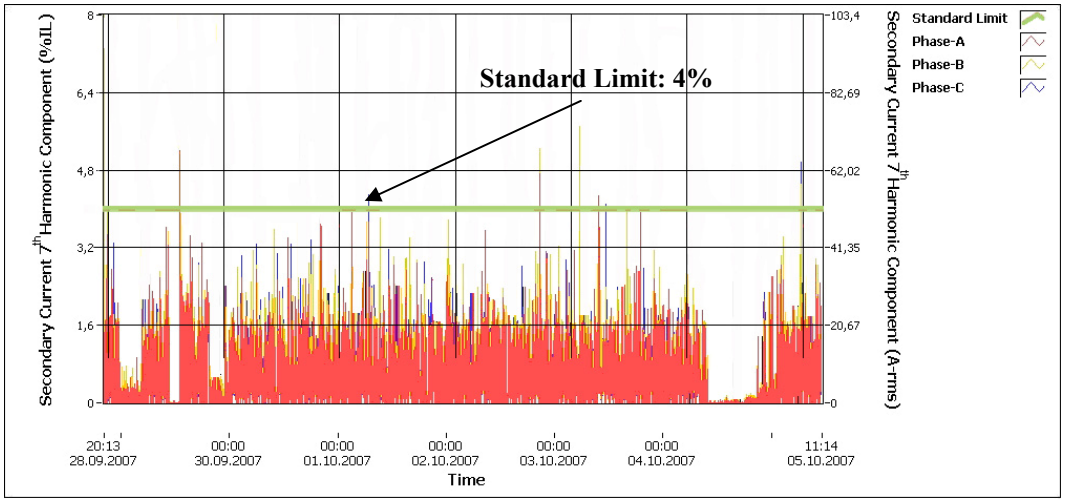

Figure 83 Almak-A, 7th Harmonic Component of the Secondary Current (Averaged in each 3 seconds)

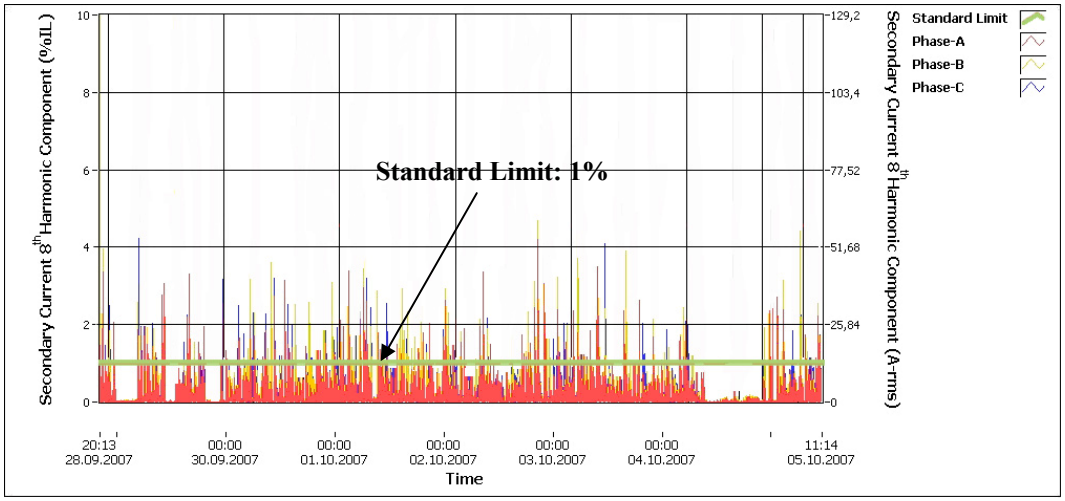

Figure 84 Almak-A, 8th Harmonic Component of the Secondary Current (Averaged in each 3 seconds)

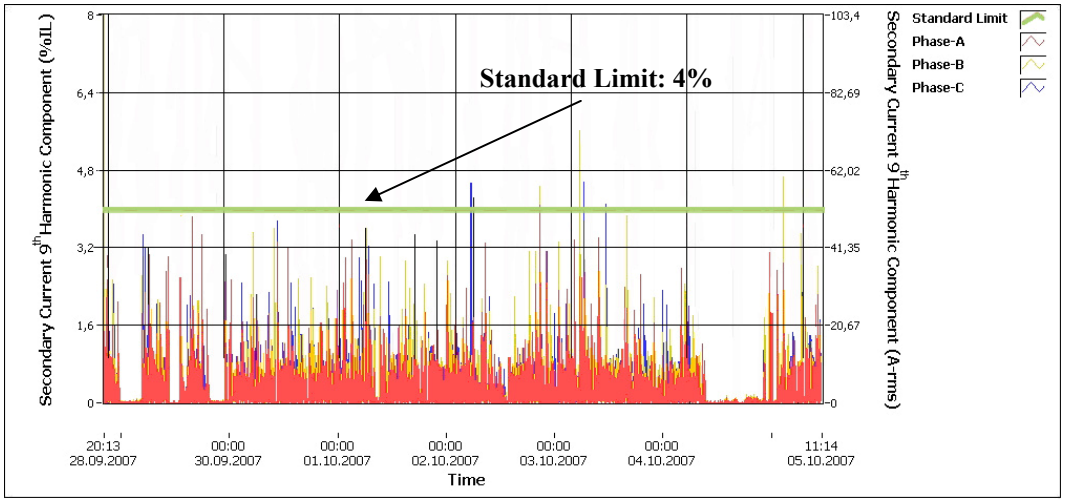

Figure 85 Almak-A, 9th Harmonic Component of the Secondary Current (Averaged in each 3 seconds)

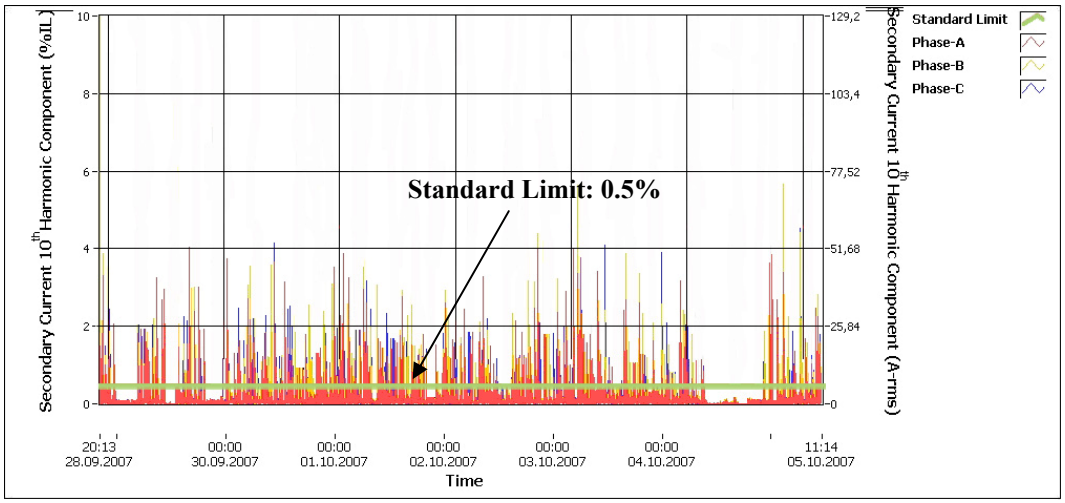

Figure 86 Almak-A, 10th Harmonic Component of the Secondary Current (Averaged in each 3 seconds)

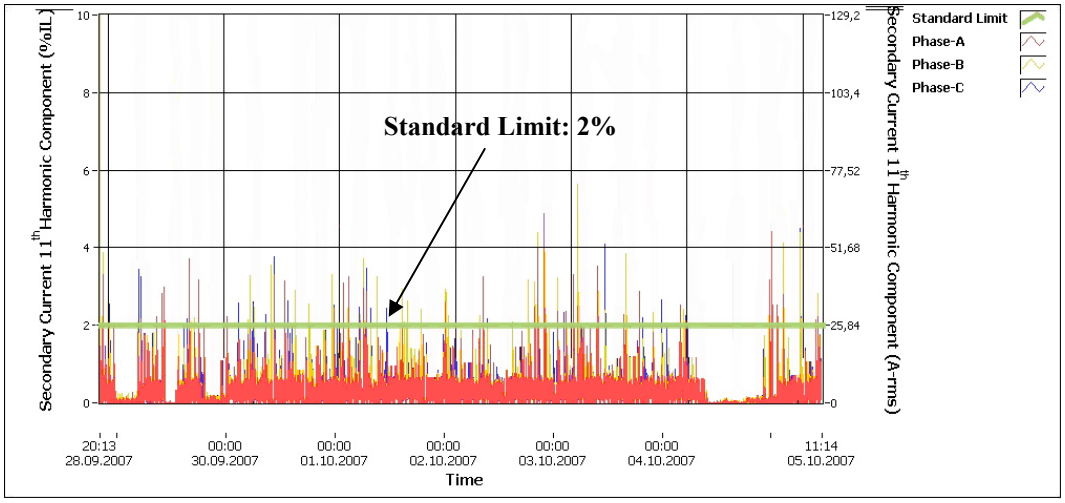

Figure 87 Almak-A, 11th Harmonic Component of the Secondary Current (Averaged in each 3 seconds)

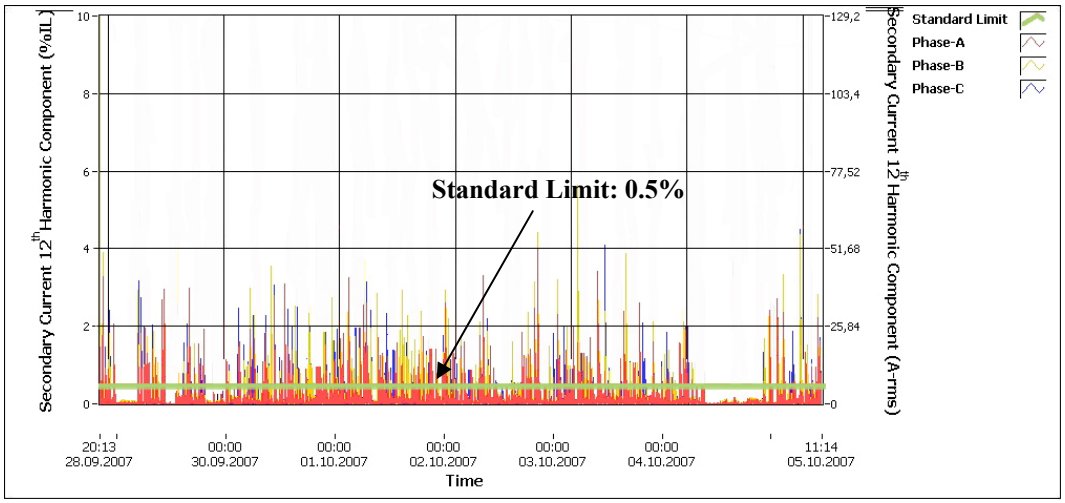

Figure 88 Almak-A, 12th Harmonic Component of the Secondary Current (Averaged in each 3 seconds)

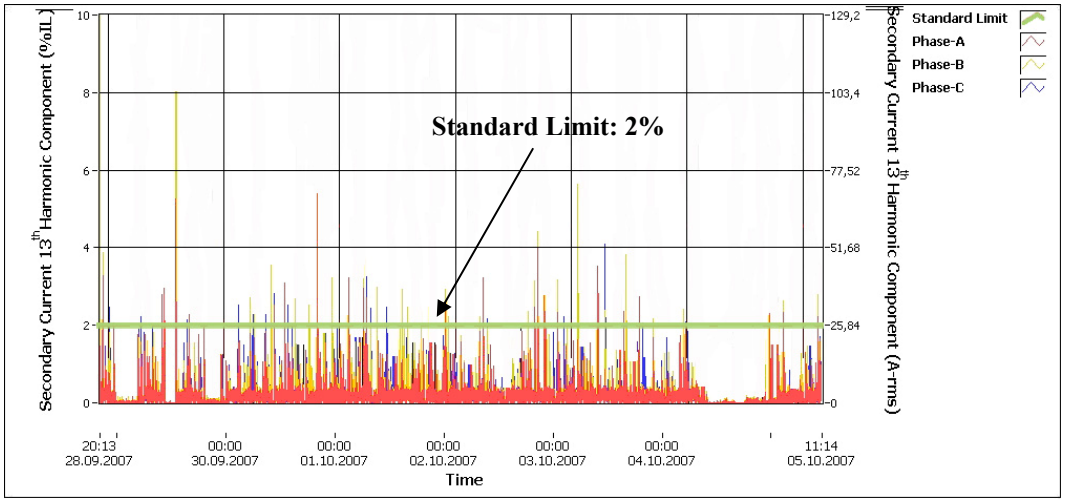

Figure 89 Almak-A, 13th Harmonic Component of the Secondary Current (Averaged in each 3 seconds)

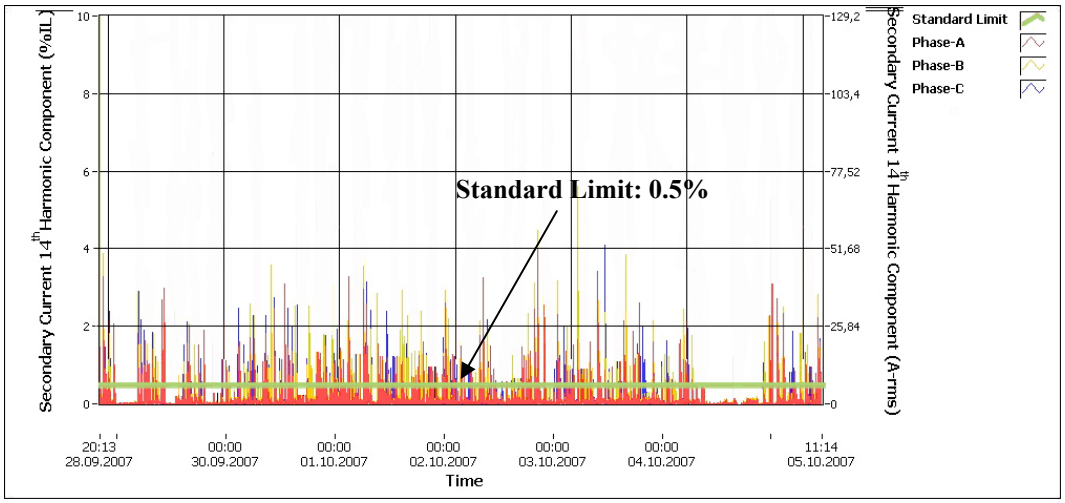

Figure 90 Almak-A, 14th Harmonic Component of the Secondary Current (Averaged in each 3 seconds)

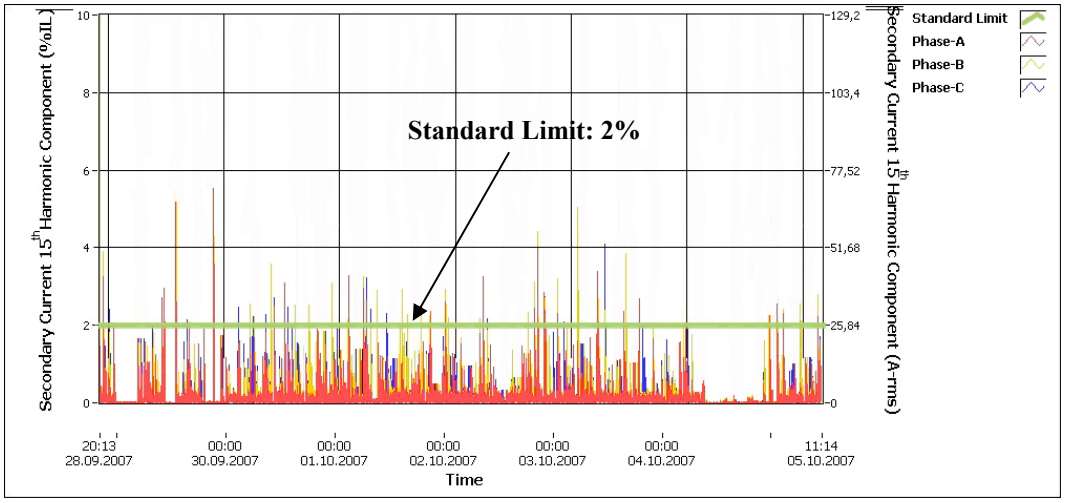

Figure 91 Almak-A, 15th Harmonic Component of the Secondary Current (Averaged in each 3 seconds)

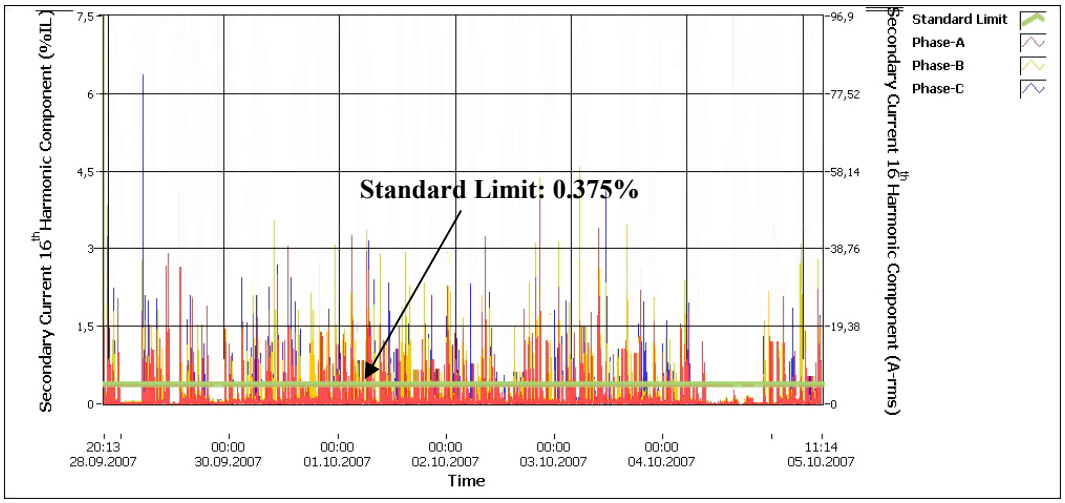

Figure 92 Almak-A, 16th Harmonic Component of the Secondary Current (Averaged in each 3 seconds)

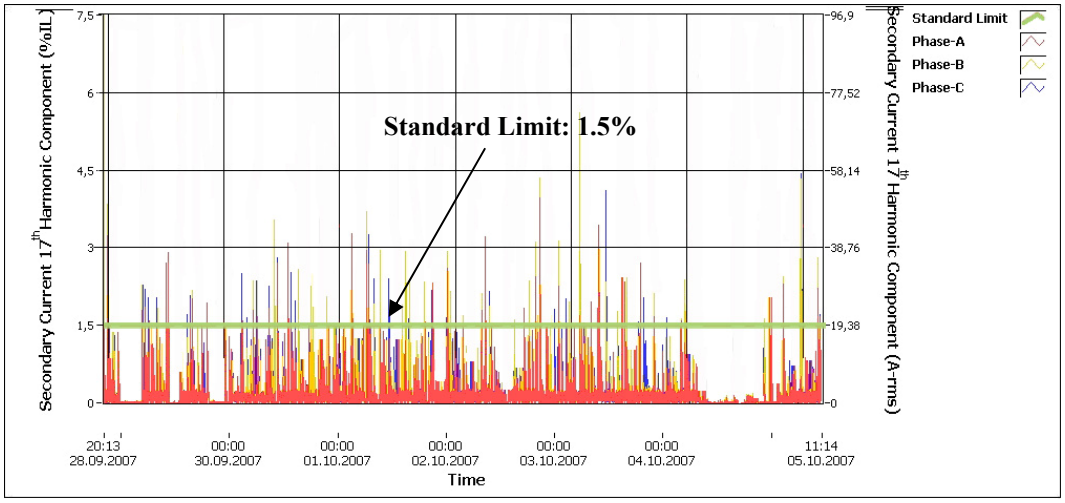

Figure 93 Almak-A, 17th Harmonic Component of the Secondary Current (Averaged in each 3 seconds)

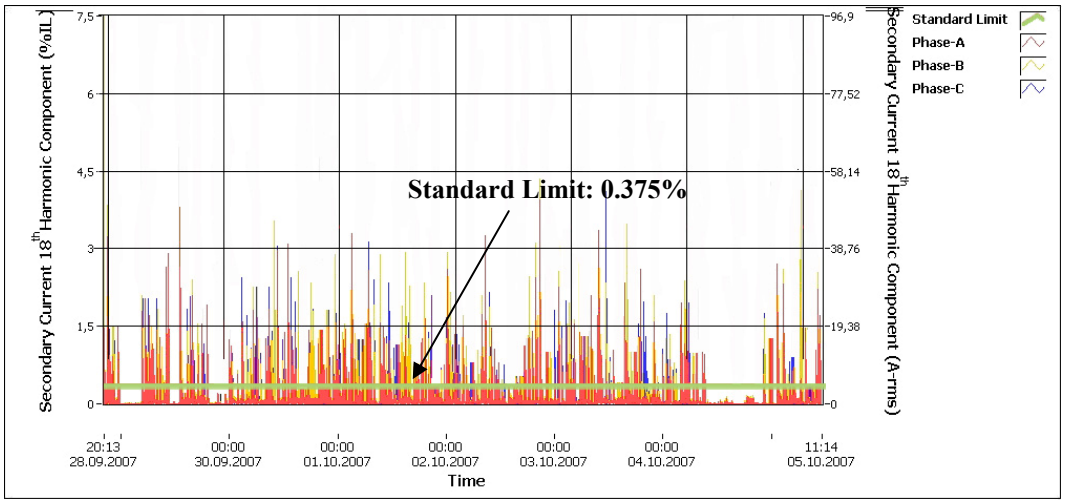

Figure 94 Almak-A, 18th Harmonic Component of the Secondary Current (Averaged in each 3 seconds)

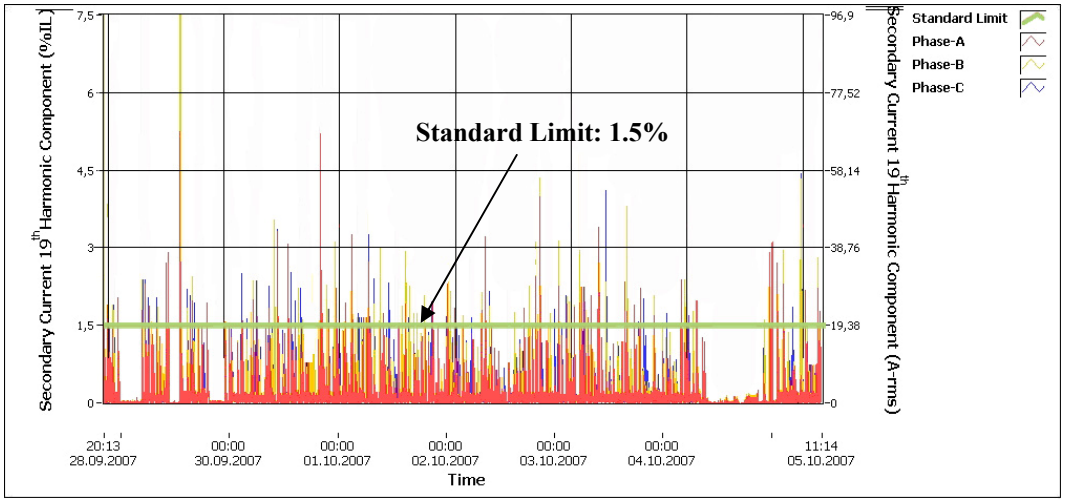

Figure 95 Almak-A, 19th Harmonic Component of the Secondary Current (Averaged in each 3 seconds)

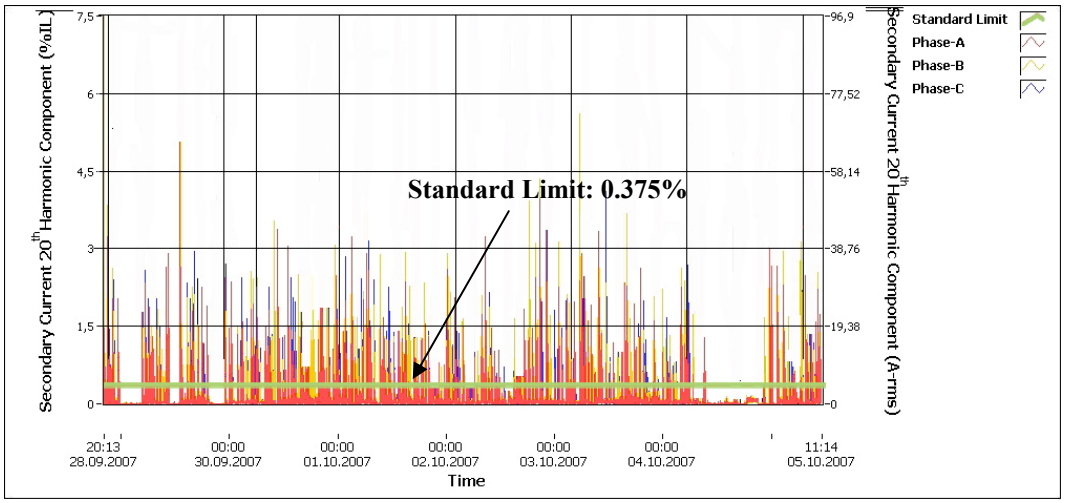

Figure 96 Almak-A, 20th Harmonic Component of the Secondary Current (Averaged in each 3 seconds)

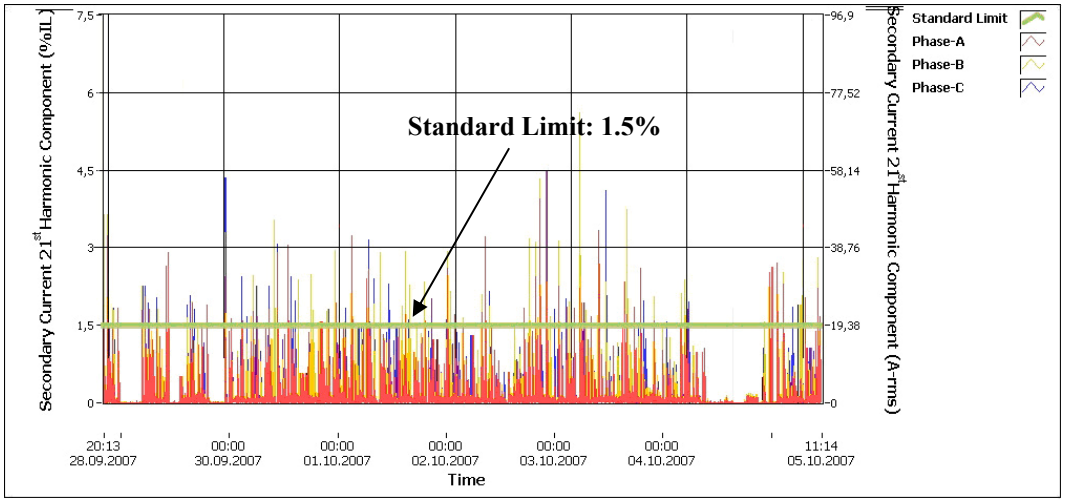

Figure 97 Almak-A, 21st Harmonic Component of the Secondary Current (Averaged in each 3 seconds)

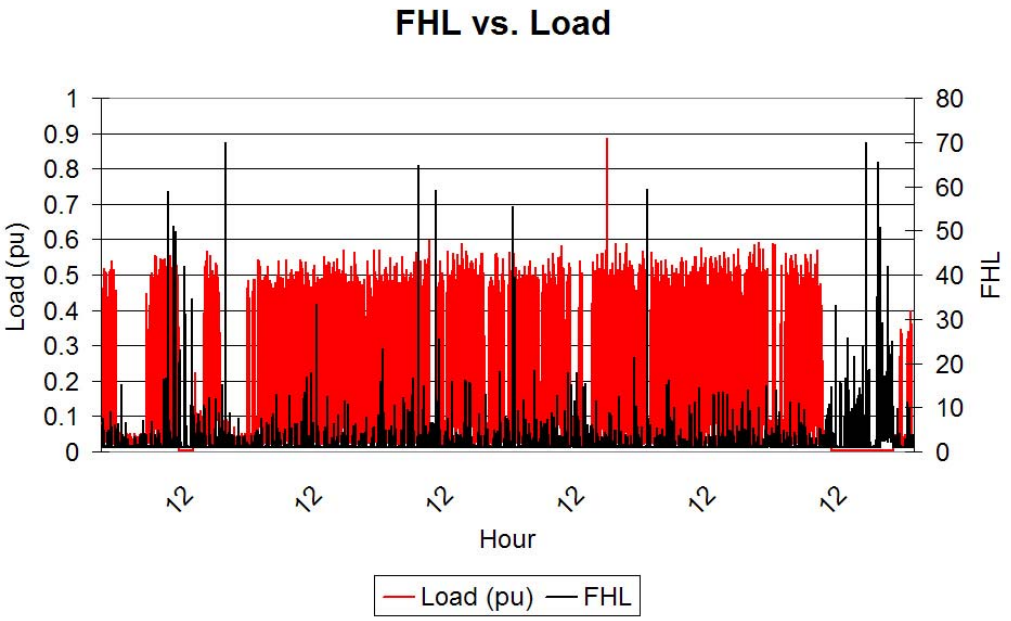

Figure 98 Almak-A, FHL vs. Load (Averaged in each 20 seconds)

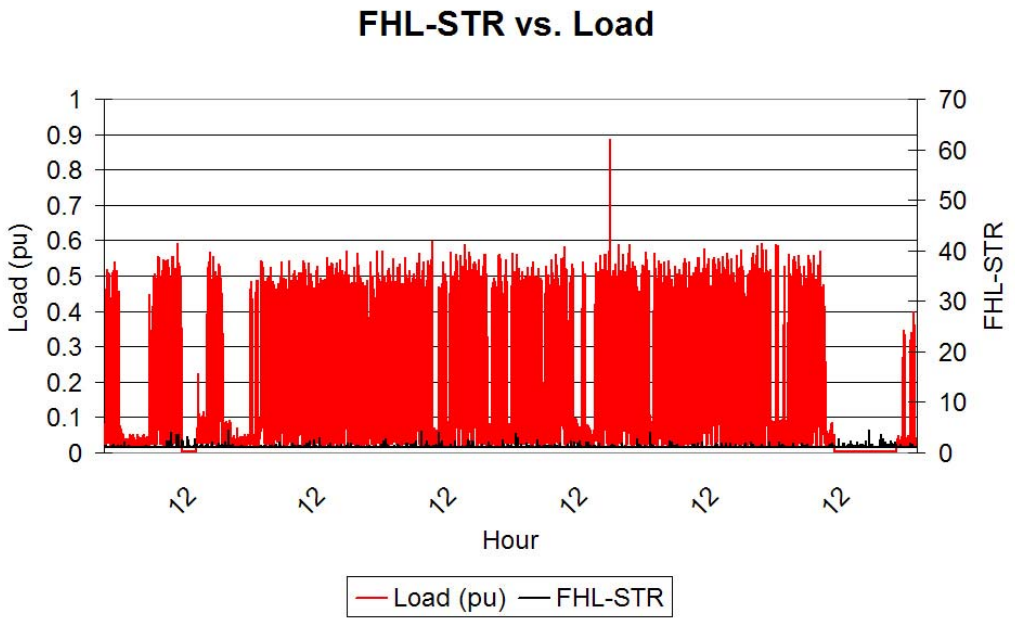

Figure 99 Almak-A, FHL-STR vs. Load
(Averaged in each 20 seconds)

Detailed analysis of Figure 98 shows the following properties;

- The average of the F_{HL} is 1.68.
- The maximum F_{HL} value during measurement is as high as 70.

Also, analysis of Figure 99 shows the following properties;

- The average of the $F_{HL\text{-}STR}$ is 1.057.
- The maximum $F_{HL\text{-}STR}$ value during measurement is as high as 4.57.

The difference between the maximum values of F_{HL} and $F_{HL\text{-}STR}$ indicates that the degree of harmonics is relatively high. This situation is because of the fact that F_{HL} is proportional to the harmonic level by a power of 2, whereas the $F_{HL\text{-}STR}$ is proportional to the harmonic level by a power of 0.8.

If, only the effect of the RMS value of the current has been taken into account, as in the case of the traditional measurement devices located on the present transformers, the effect of the harmonics would have been neglected. However for this particular transformer and its load, the effect of the harmonics is significant.

In addition to these, the harmonic levels in this transformer are higher than the one used for transformer #1. However the loading is lower so the difference is somewhat balanced.

A.3.1.2 Temperature Prediction

Since there was no free oil pocket to insert the Top-Oil temperature thermometer during the measurement duration, the measured Top-Oil temperature was taken from the Top-Oil temperature thermometer installed by the manufacturer on the transformer. The temperature measurement from manufacturers' thermometers has a tolerance value of ±3 ^{o}C which must be taken into account. Also the temperature values are noted by an operator at the start of each hour. The values in the graphs show the variations in only hourly intervals rather than instantaneous values. The resultant Figures 100 and 101 are as follows;

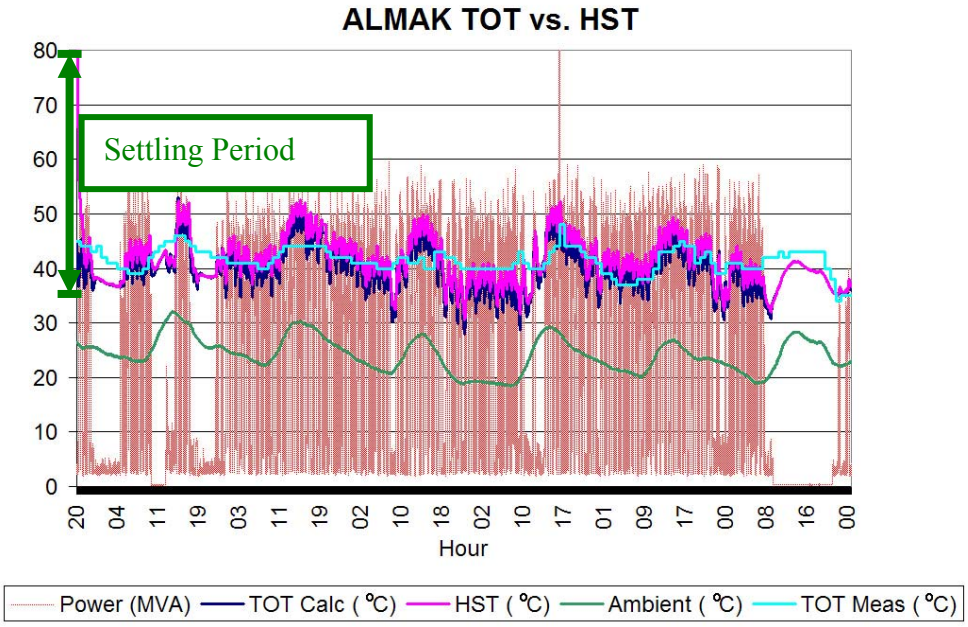

Figure 100 Almak-A, Calculated vs. Measured TOT with respect to Loading

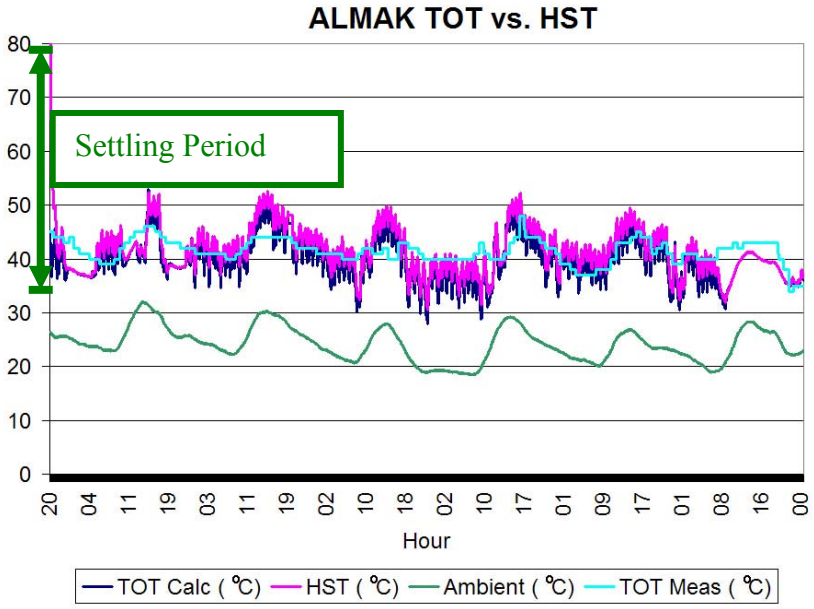

Figure 101 Almak-A, Calculated vs. Measured TOT excluding Loading

As seen from Figures 100 and 101, the time needed to have the 80 ^{o}C Hot-Spot temperature to settle in its steady state value is a around 1/2 hour. Considering that this requires $5\tau_w$ time, the results are inline with the assumptions.

To analyze the deviations between the measured and the calculated temperature values more efficiently, Figures 102 and 103 have been prepared showing the deviation between the calculated and measured data with respect to the pu loading and the Ambient temperature respectively.

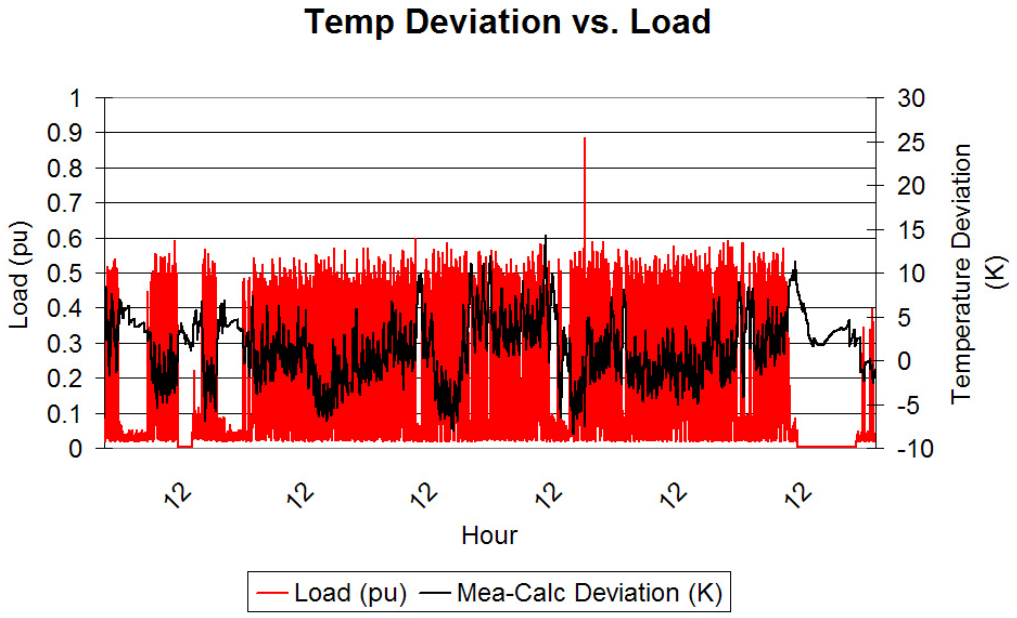

Figure 102 Almak-A, TOT deviations between Calculated and Measured Temperatures with respect to Loading

It shall be noted that when there is loading, the deviations are generally in ±5 °C tolerance band. However when the transformer enters the shut-down operation, the deviations increase as described in section 4.1.2.2.

Also the same measurement on the Top-Oil and Hot-Spot temperature calculation on all 3 phases has been performed. The results are shown in Figures 104 and 105.

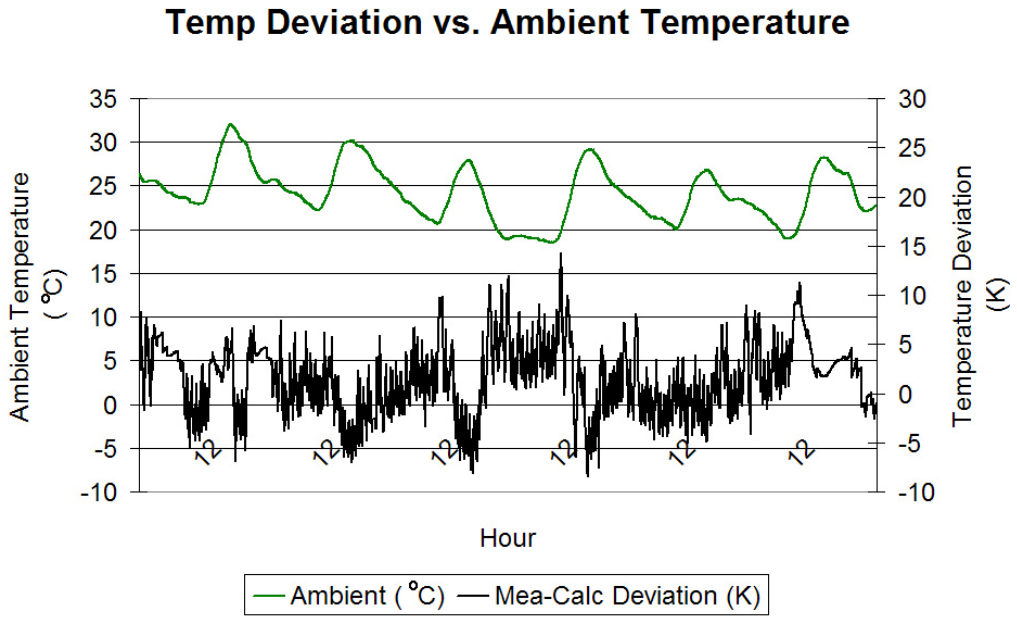

Figure 103 Almak-A, TOT deviations between Calculated and Measured Temperatures with respect to Ambient Temperature

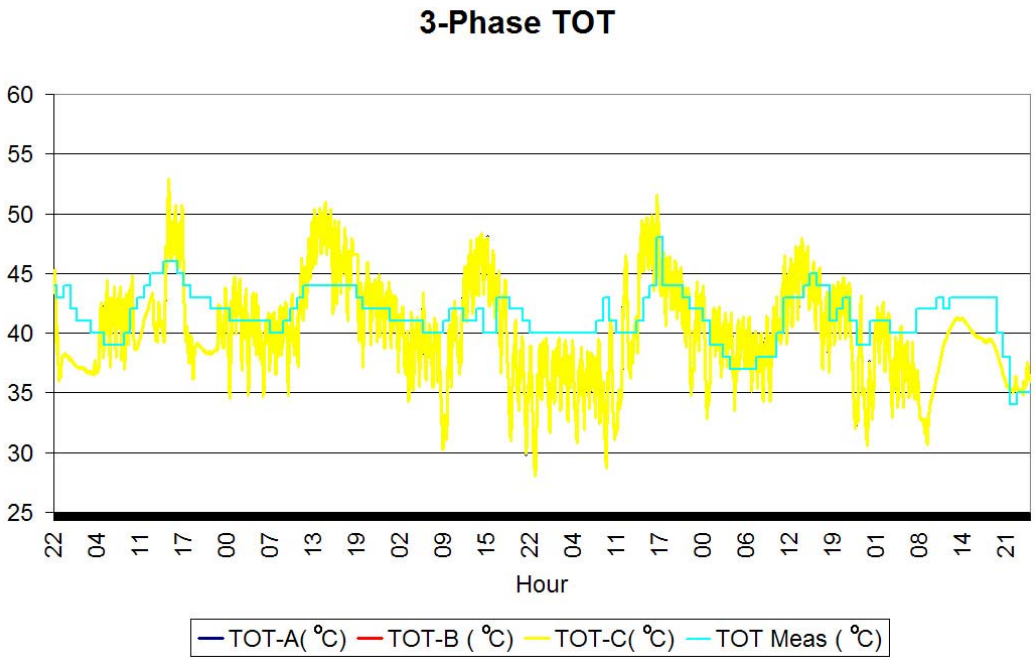

Figure 104 Almak-A, TOT calculated from the currents of Phases A, B and C

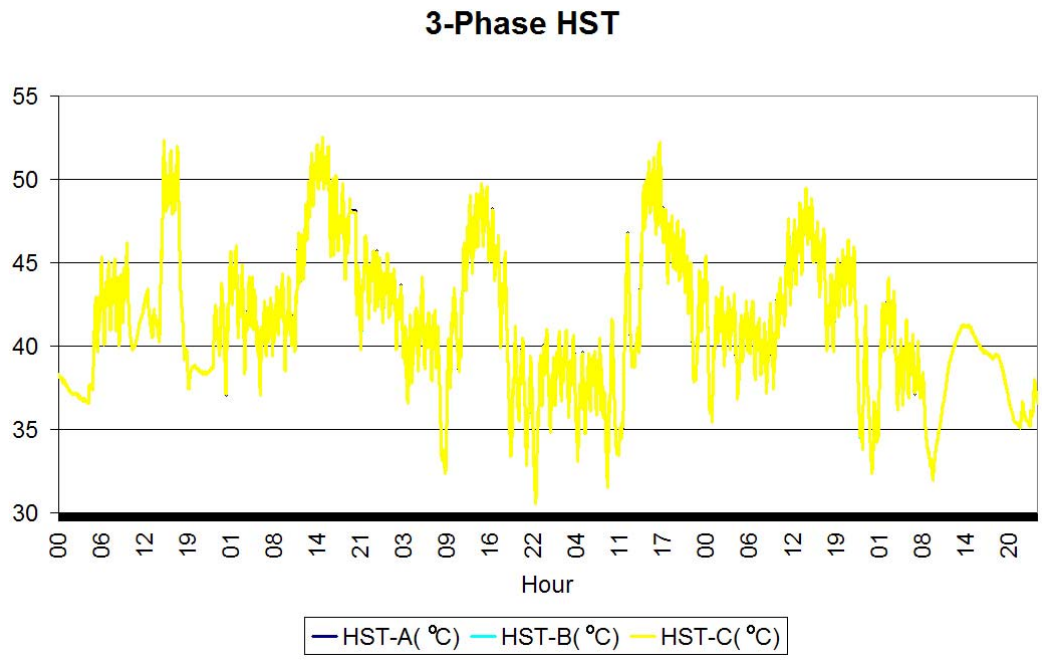

Figure 105 Almak-A, HST calculated from the currents of Phases A, B and C

The differences between phases have been calculated. Figures 107 through 109 show the deviations of Top Oil and Hot Spot temperatures between phases C and B with respect to phase A.

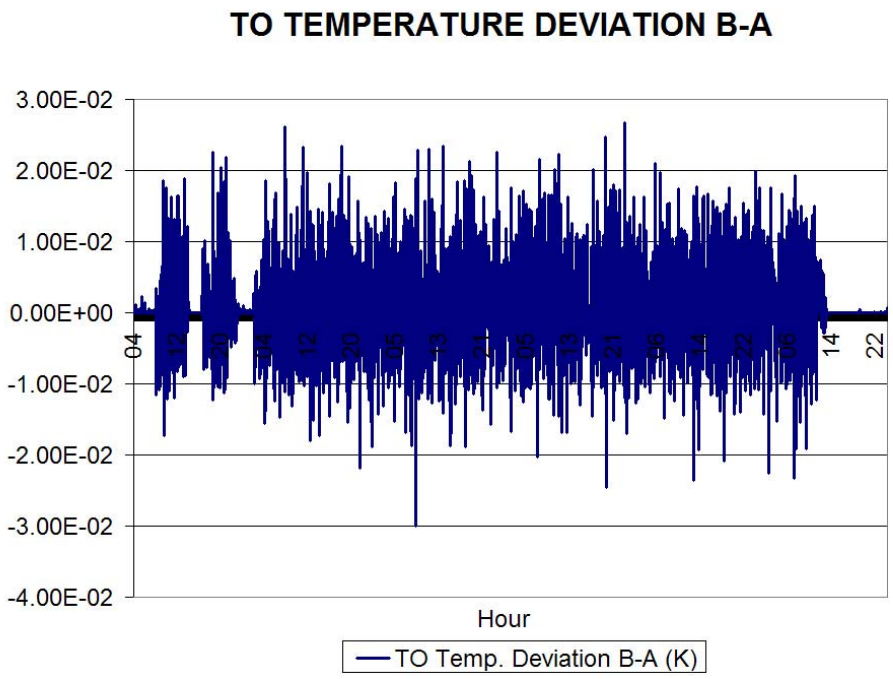

Figure 106 Almak-A, TOT Deviation between the Phases B and A

Figure 106 shows;

- The maximum deviation for the Top Oil temperatures between Phase B and Phase A is 0.03 ^{o}C.
- The average deviation for the Top Oil temperatures between Phase B and Phase A is -0.000002 ^{o}C.

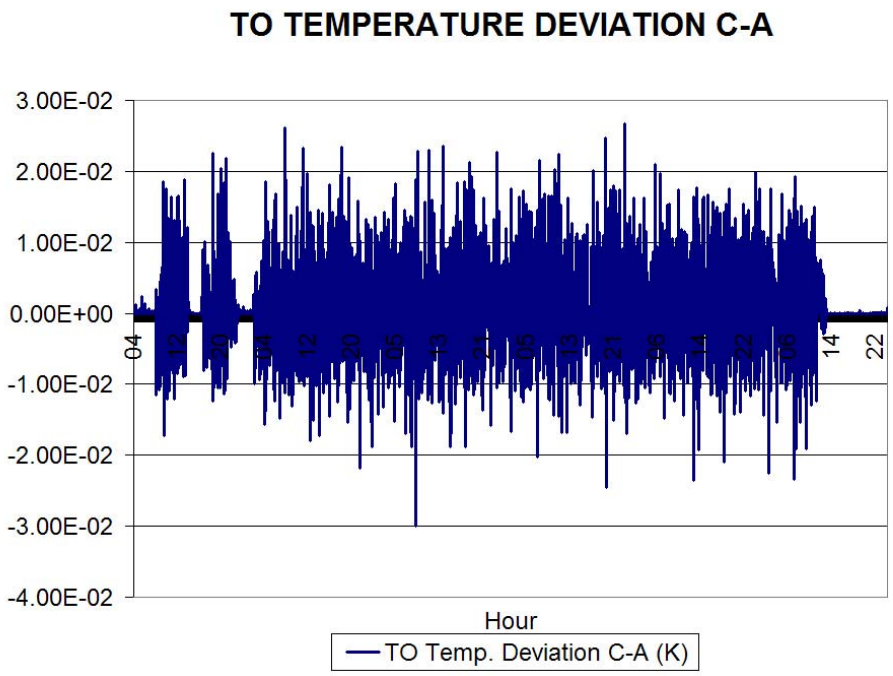

Figure 107 Almak-A, TOT Deviation between the Phases C and A

Figure 107 shows;

- The maximum deviation for the Top Oil temperatures between Phase C and Phase A is 0.027 ^{o}C.
- The average deviation for the Top Oil temperatures between Phase C and Phase A is -0.000015 ^{o}C.

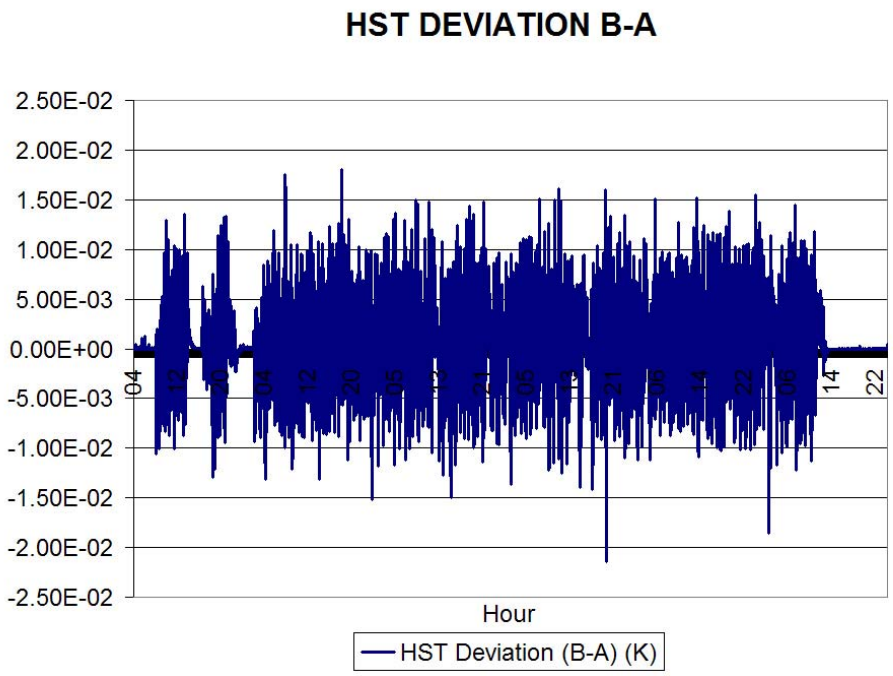

Figure 108 Almak-A, HST Deviation between the Phases B and A

Figure 108 shows;

- The maximum deviation for the Hot Spot temperatures between Phase B and Phase A is 0.06 ^{o}C.
- The average deviation for the Hot Spot temperatures between Phase B and Phase A is 0.00011 ^{o}C.

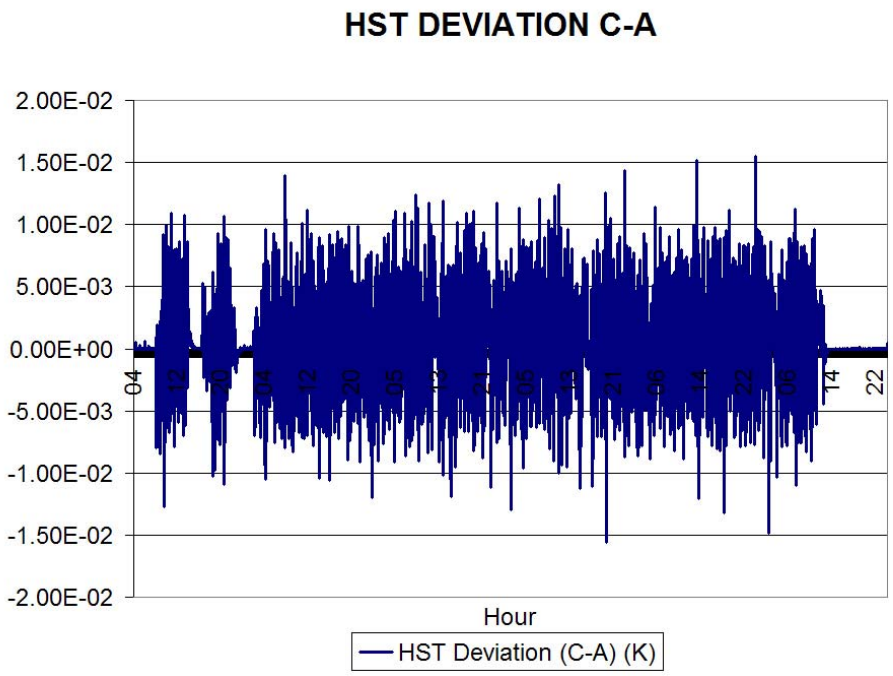

Figure 109 Almak-A, HST Deviation between the Phases C and A

Figure 109 shows;

- The maximum deviation for the Hot Spot temperatures between Phase C and Phase A is 0.06 ^{o}C.
- The average deviation for the Hot Spot temperatures between Phase C and Phase A is 0.00017 ^{o}C.

The maximum deviation during the measurement duration is 0.06 ^{o}C. The average deviation is less than 0.0002 ^{o}C. These data shows that the phase balance of the transformer loading is in acceptable values.

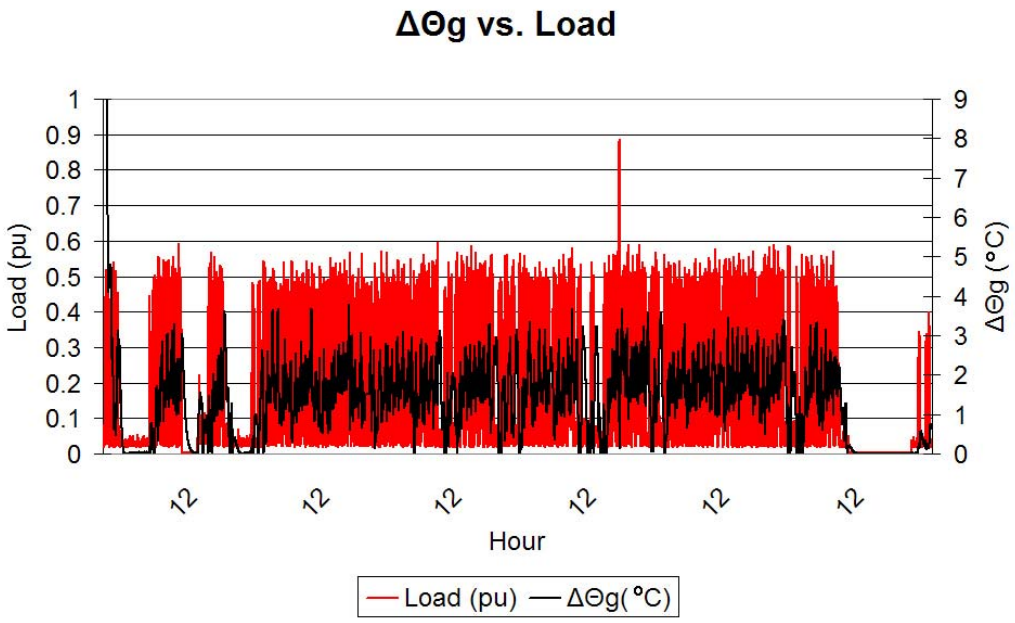

Figure 110 Almak-A, Hot Spot Conductor rise over Top Oil Temperature (Averaged in each 20 seconds)

The Hot-Spot conductor rise over Top-Oil temperature has been shown in Figure 110. A comparison of Figure 110 to Figures 98 and 99 shows that harmonics can be more effective with higher loading.

A.3.2 80/100 MVA ONAN/ONAF Intermittent Load

Figure 111 Transformer Habaş-C

An additional measurement has been performed in Habaş Transformer Center (shown in Figure 111). This transformer, too, supplies a factory with arc furnaces thus the loading is intermittent.

Table 10 TEMPEST Input data for Habaş-C

HABAŞ-C TRANSFORMER	
Rated Capacity	100 MVA
HV	154000 V
LV	34500 V
No-Load Losses	32350 W
Load Losses	165000 W
HV Connection	Wye
LV Connection	Wye
Base Current	1718.3
Top Oil Time Constant	3.4 hours
Winding Time Constant	7 minutes

Table 10 shows the TEMPEST input data for transformer Habaş-C. These values have been acquired from manufacturer's certified test report.

A.3.2.1 Loading and Harmonic Content

Figure 112 shows the Total Demand Distortion (TDD) graph for the full scale measurement. The overshoots in the graph are the results of erroneous measurements. On the general, the TDD's maximum value is around 15% and the average value is around 10%.

Figures 113-133 show the fundamental and harmonic components of the load current from 2nd to 21st, for all of the 3 phases. It can be seen that the required harmonic content for Hot-Spot temperature calculation is present for this transformer. The acceptable harmonic limits defined by the "Electricity Transmission Demand Safety and Quality Regulations" have been marked as "Standard Limit".

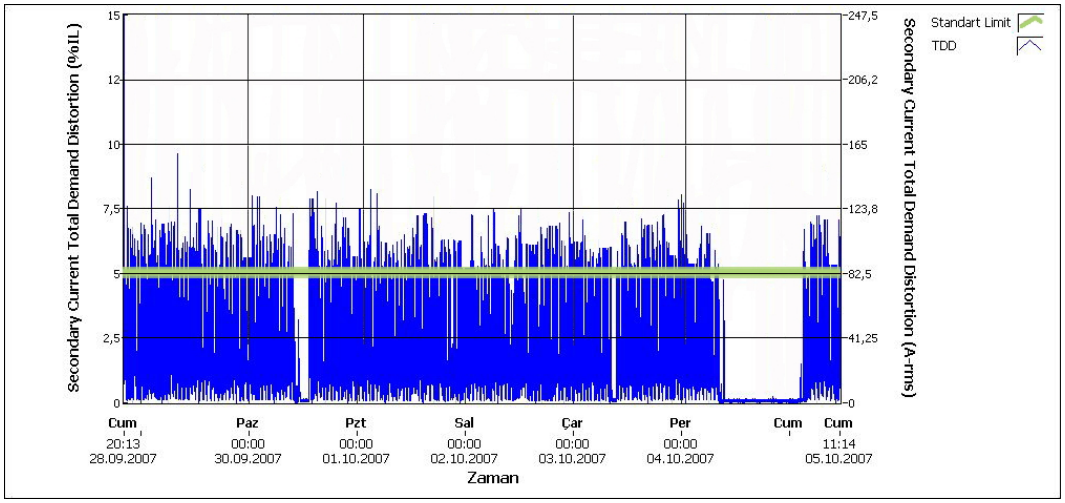

Figure 112 Habaş-C, TDD

Figure 113 Habaş-C, Fundamental Component of the Secondary Current (Averaged in each 3 seconds)

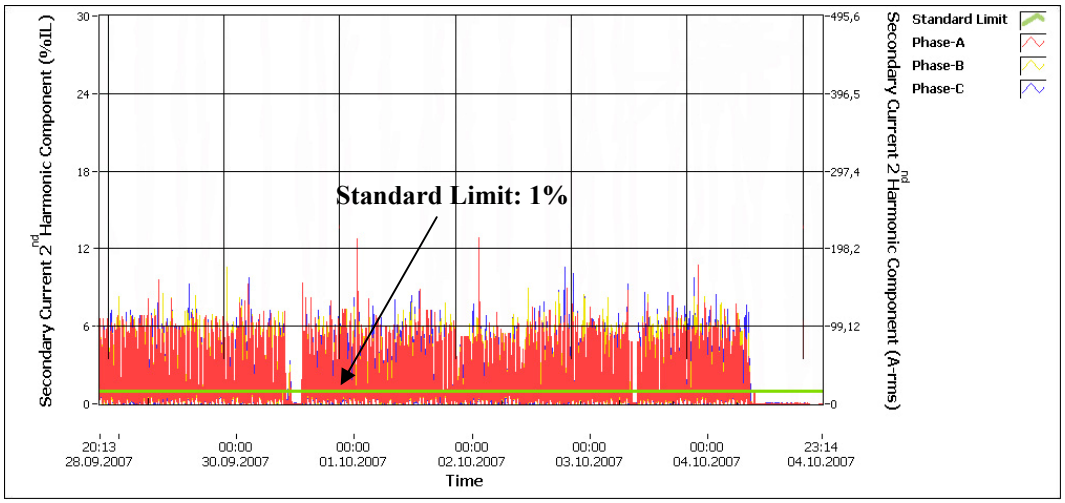

Figure 114 Habaş-C, 2nd Harmonic Component of the Secondary Current (Averaged in each 3 seconds)

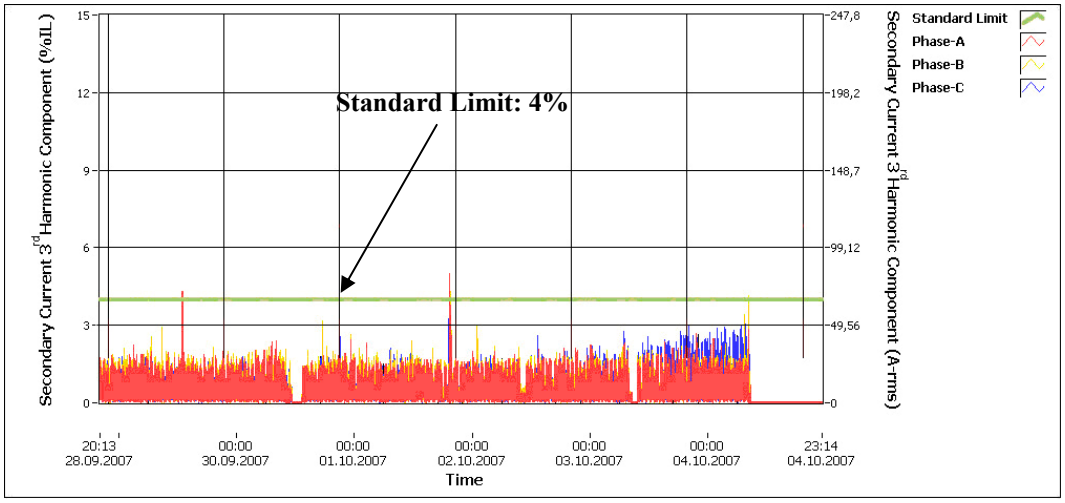

Figure 115 Habaş-C, 3rd Harmonic Component of the Secondary Current (Averaged in each 3 seconds)

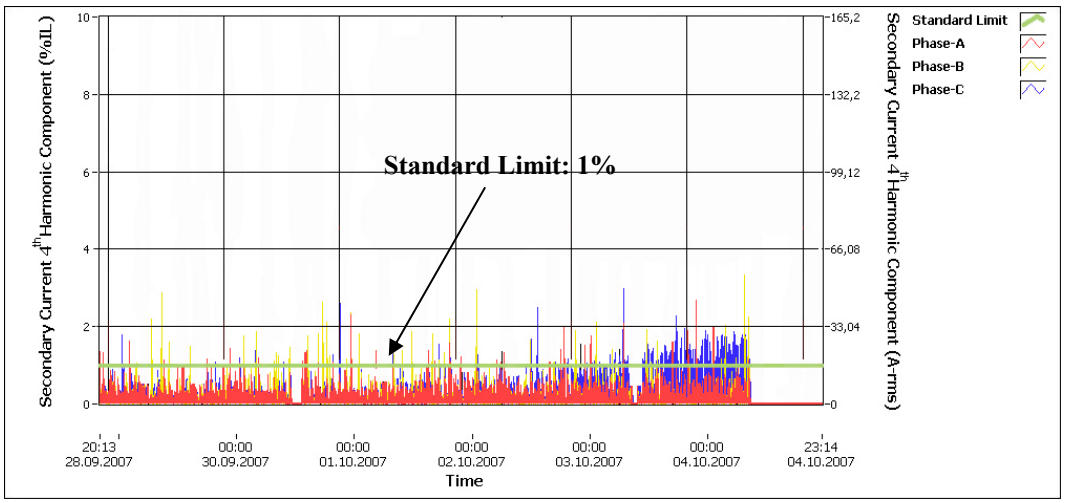

Figure 116 Habaş-C, 4th Harmonic Component of the Secondary Current (Averaged in each 3 seconds)

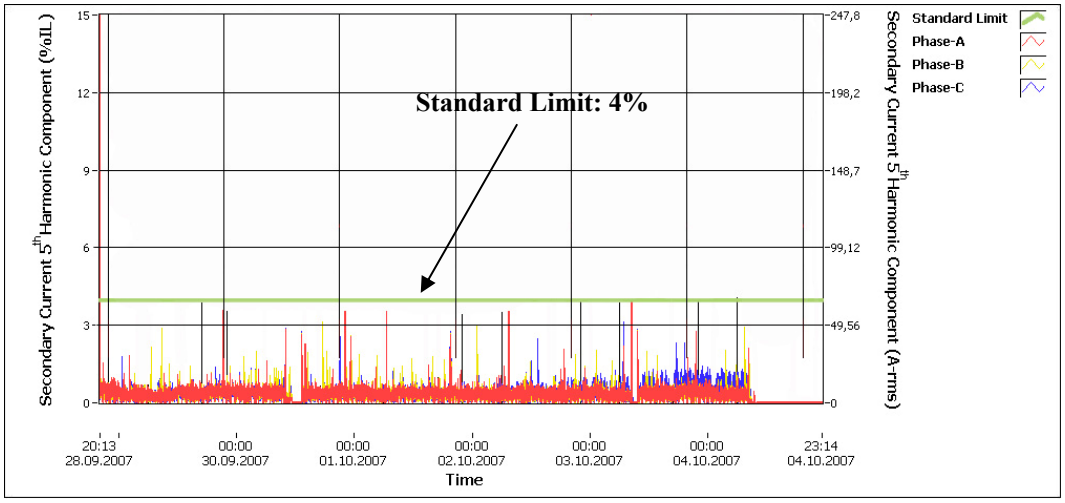

Figure 117 Habaş-C, 5th Harmonic Component of the Secondary Current (Averaged in each 3 seconds)

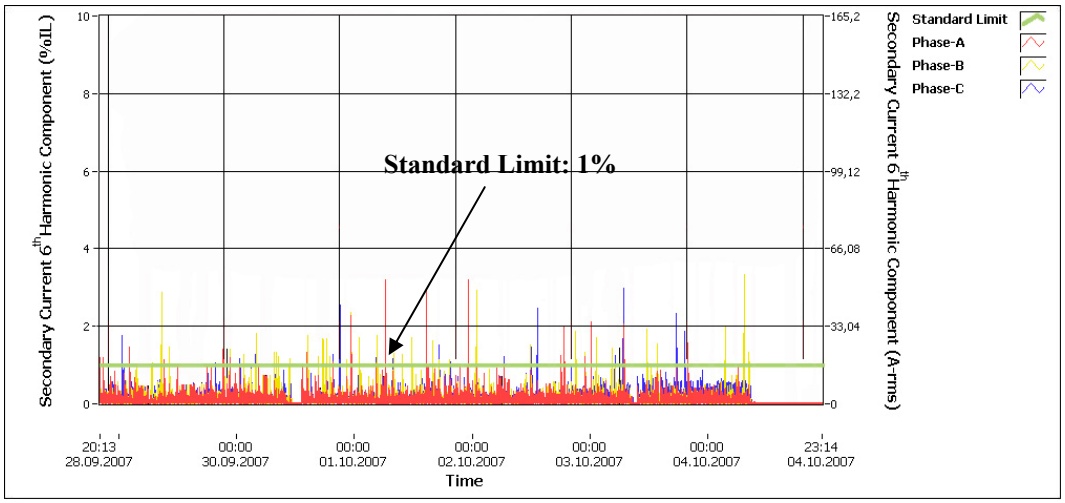

Figure 118 Habaş-C, 6th Harmonic Component of the Secondary Current (Averaged in each 3 seconds)

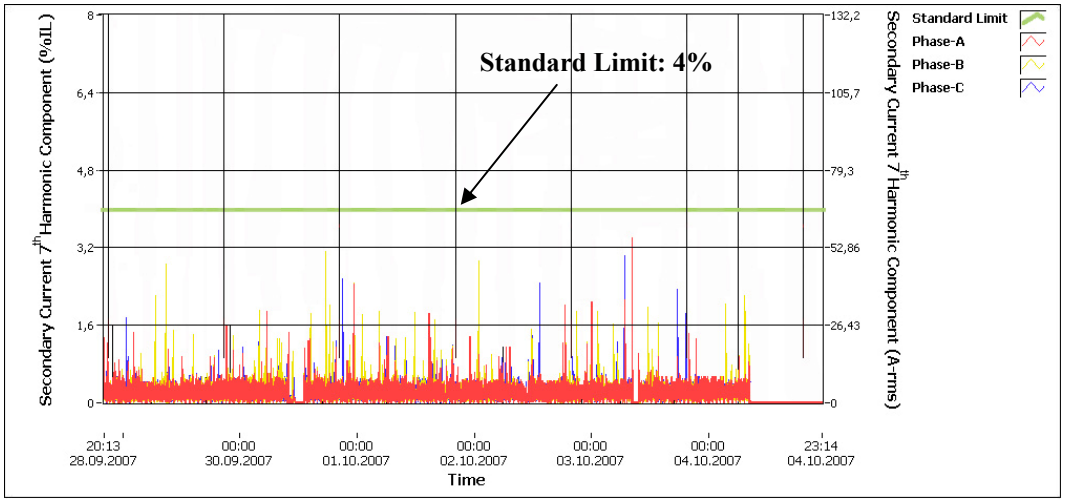

Figure 119 Habaş-C, 7th Harmonic Component of the Secondary Current (Averaged in each 3 seconds)

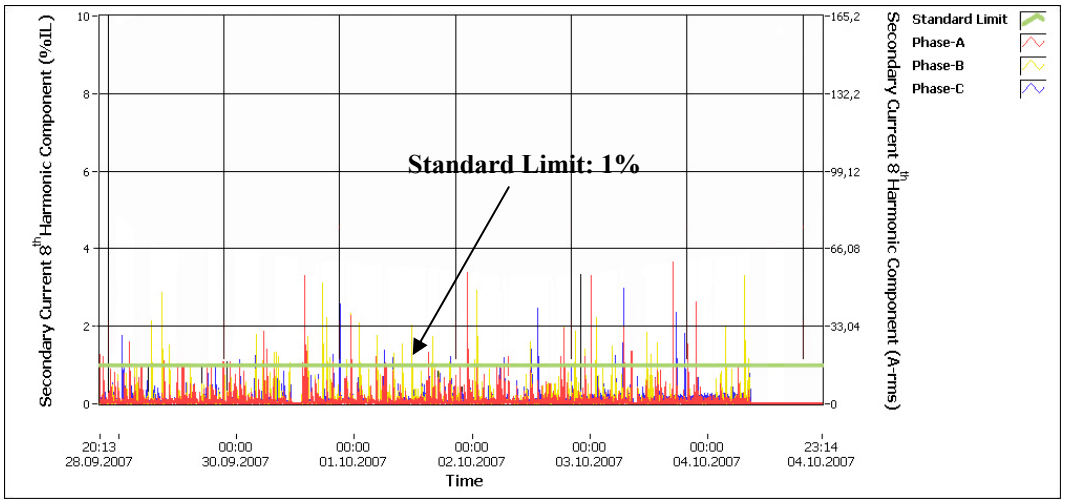

Figure 120 Habaş-C, 8th Harmonic Component of the Secondary Current (Averaged in each 3 seconds)

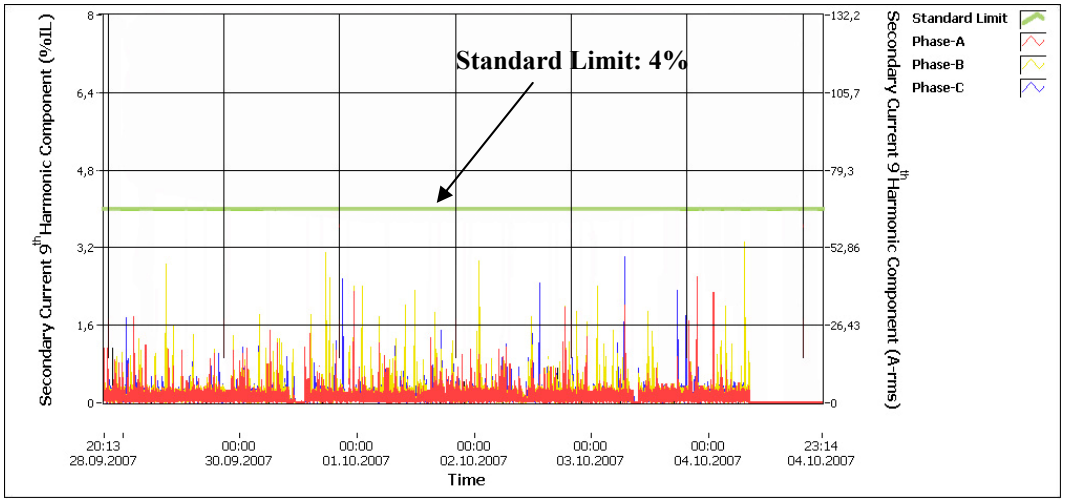

Figure 121 Habaş-C, 9th Harmonic Component of the Secondary Current (Averaged in each 3 seconds)

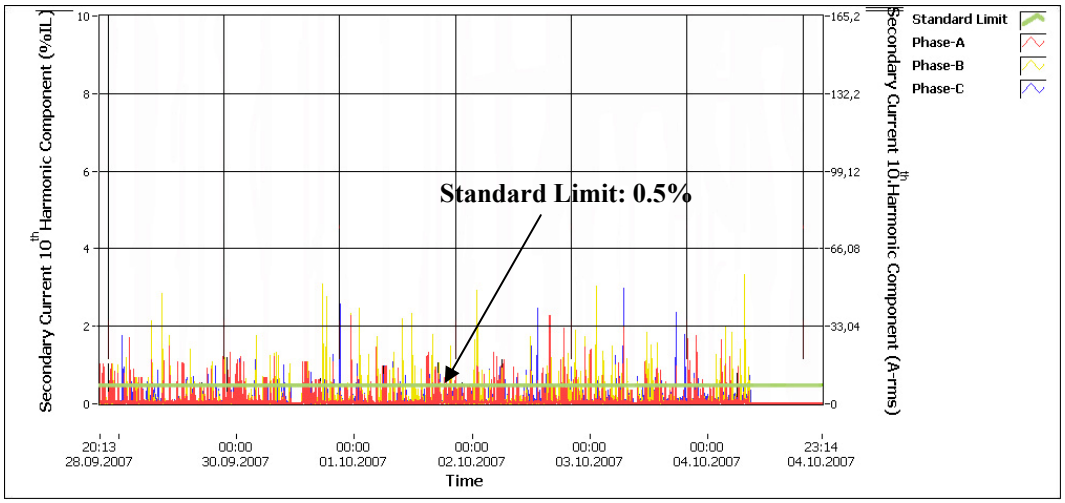

Figure 122 Habaş-C, 10th Harmonic Component of the Secondary Current (Averaged in each 3 seconds)

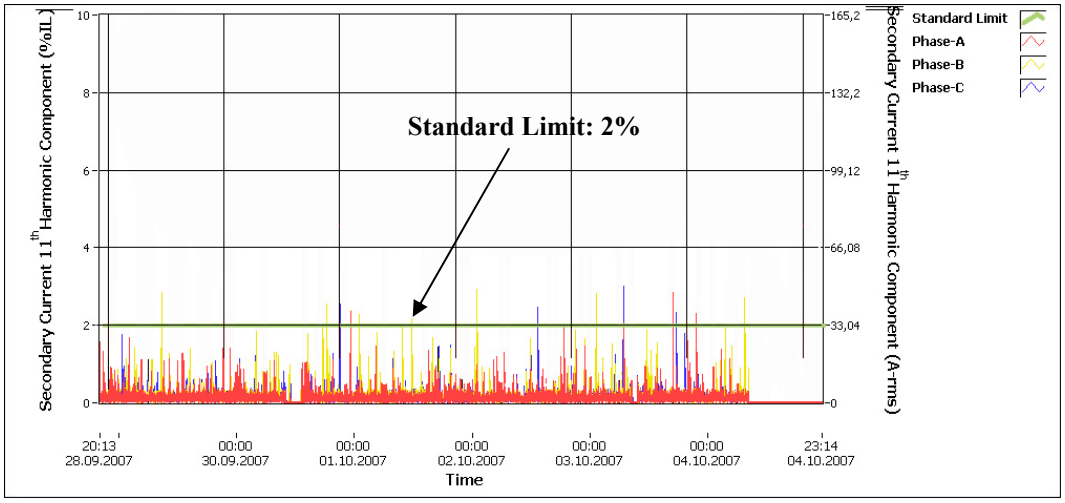

Figure 123 Habaş-C, 11th Harmonic Component of the Secondary Current (Averaged in each 3 seconds)

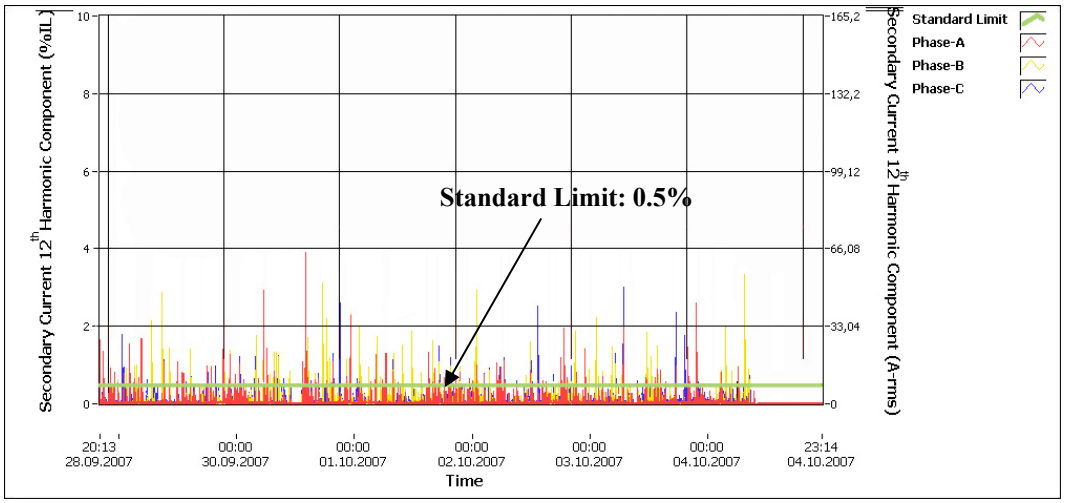

Figure 124 Habaş-C, 12th Harmonic Component of the Secondary Current (Averaged in each 3 seconds)

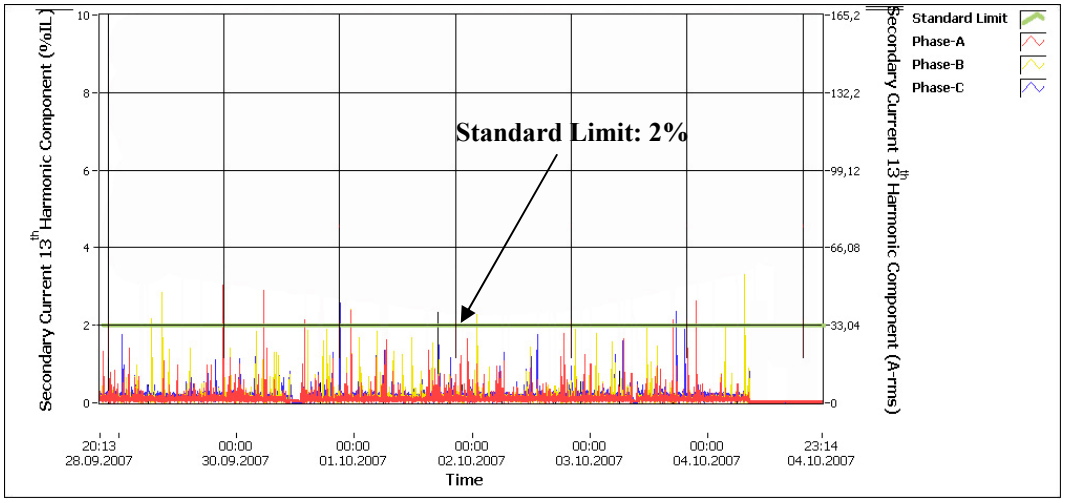

Figure 125 Habaş-C, 13th Harmonic Component of the Secondary Current (Averaged in each 3 seconds)

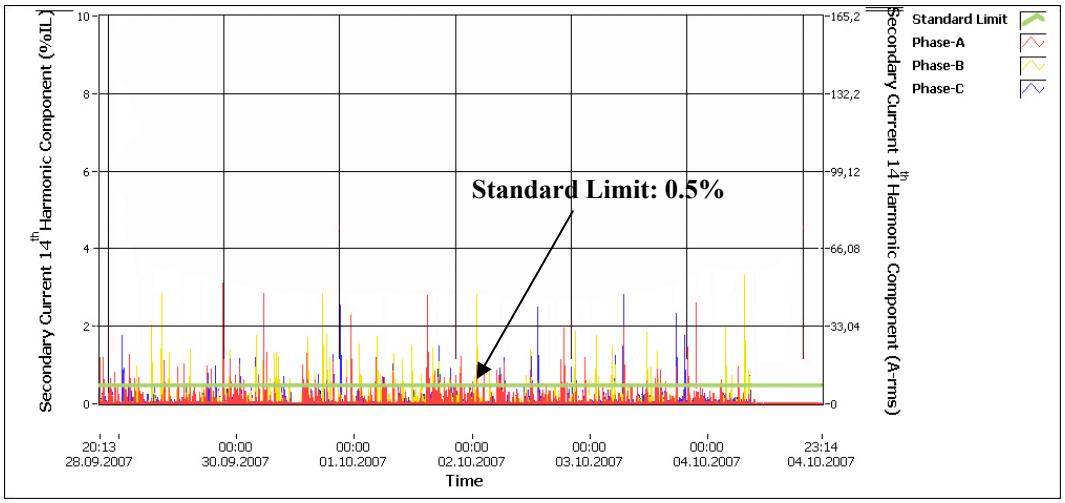

Figure 126 Habaş-C, 14th Harmonic Component of the Secondary Current (Averaged in each 3 seconds)

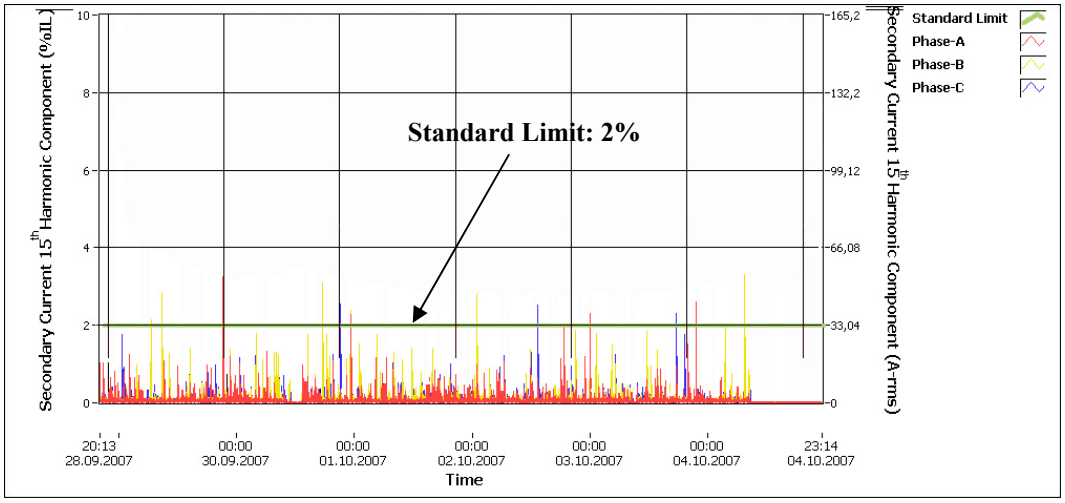

Figure 127 Habaş-C, 15th Harmonic Component of the Secondary Current (Averaged in each 3 seconds)

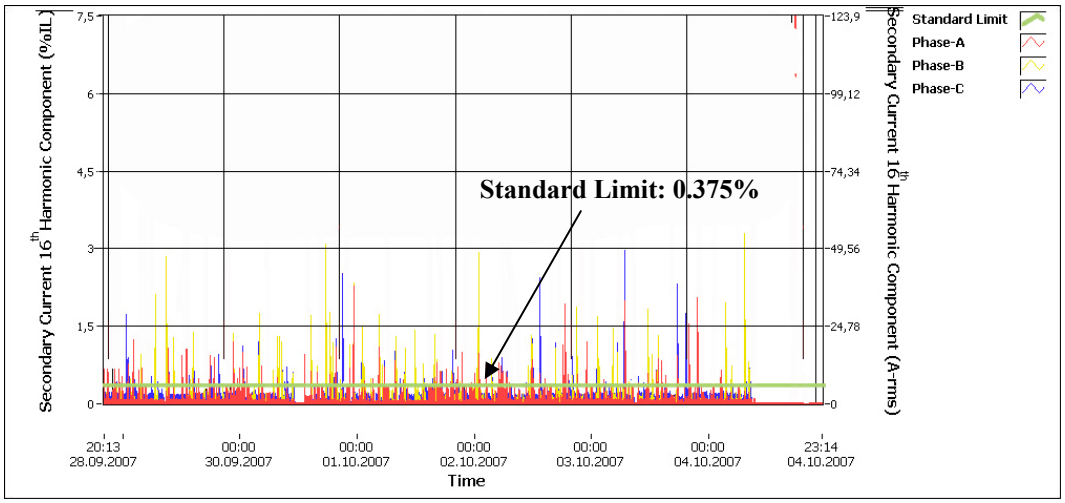

Figure 128 Habaş-C, 16th Harmonic Component of the Secondary Current (Averaged in each 3 seconds)

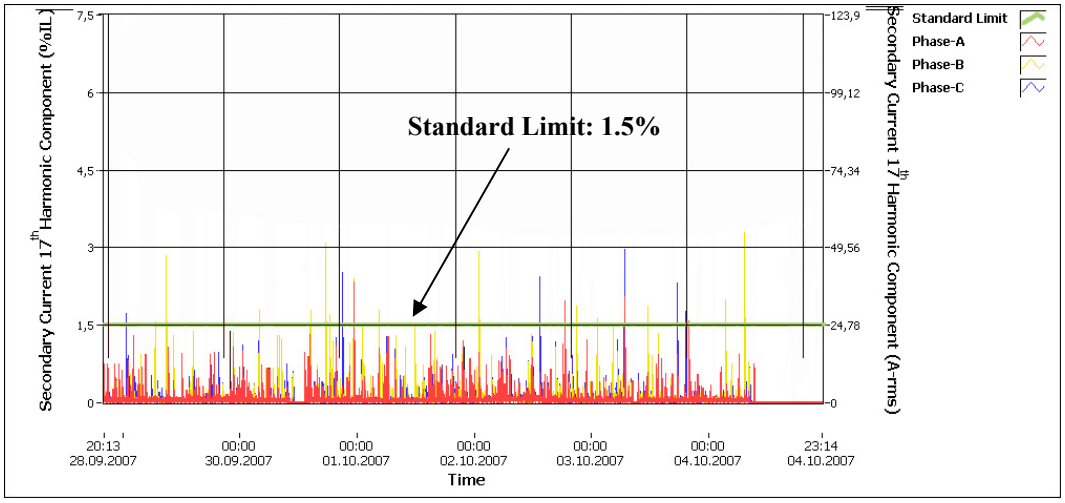

Figure 129 Habaş-C, 17th Harmonic Component of the Secondary Current (Averaged in each 3 seconds)

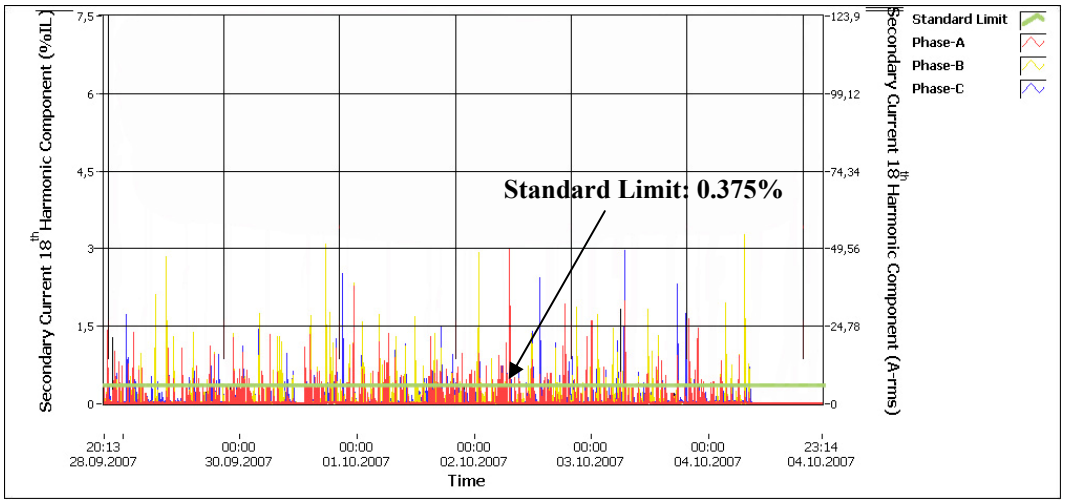

Figure 130 Habaş-C, 18th Harmonic Component of the Secondary Current (Averaged in each 3 seconds)

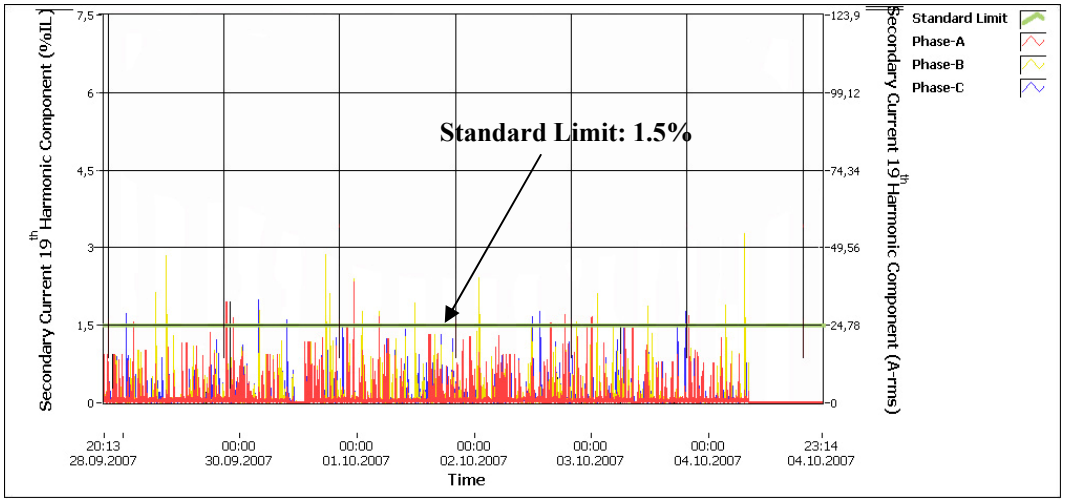

Figure 131 Habaş-C, 19th Harmonic Component of the Secondary Current (Averaged in each 3 seconds)

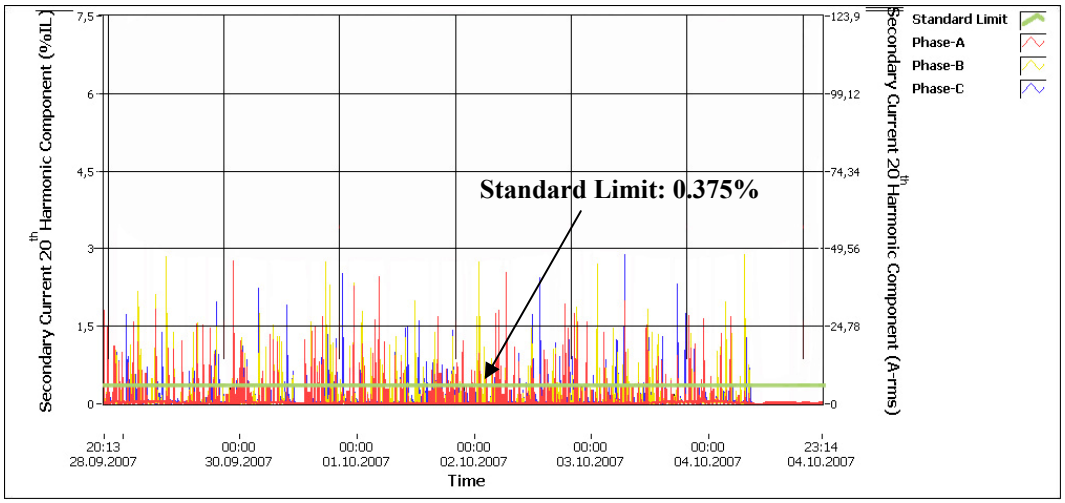

Figure 132 Habaş-C, 20th Harmonic Component of the Secondary Current (Averaged in each 3 seconds)

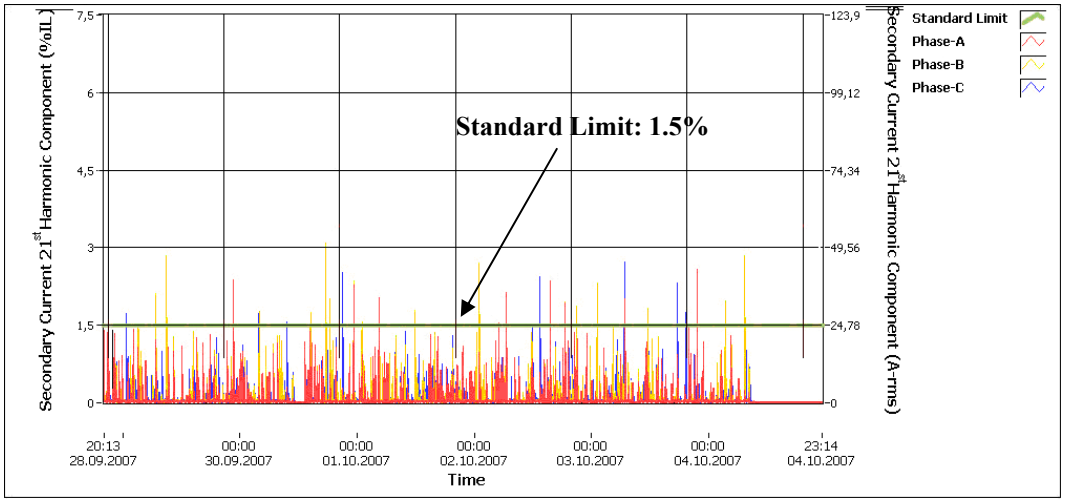

Figure 133 Habaş-C, 21st Harmonic Component of the Secondary Current (Averaged in each 3 seconds)

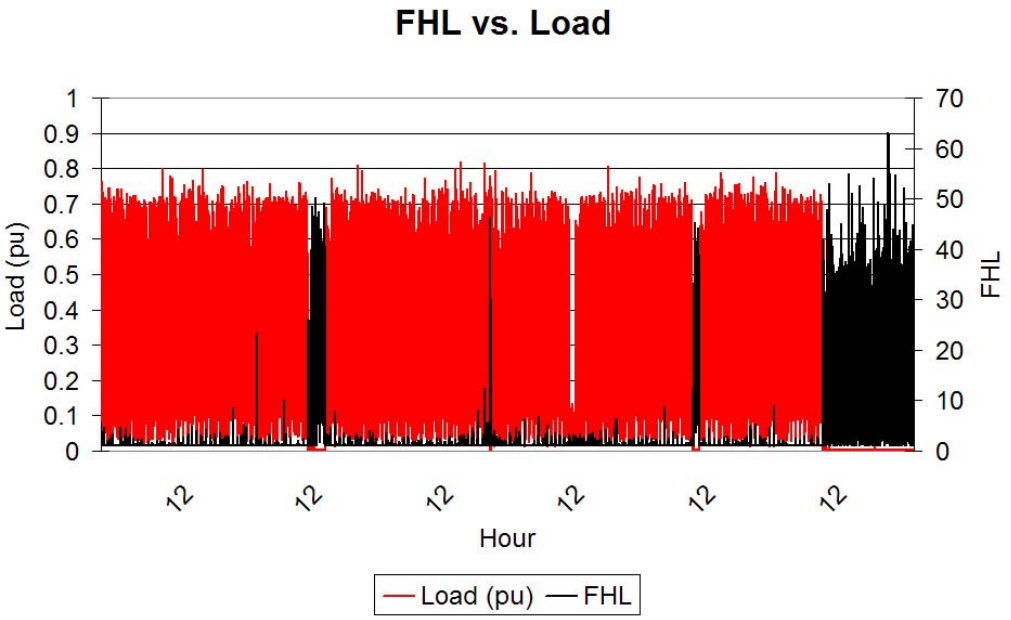

Figure 134 Habaş-C, FHL vs. Load (Averaged in each 20 seconds)

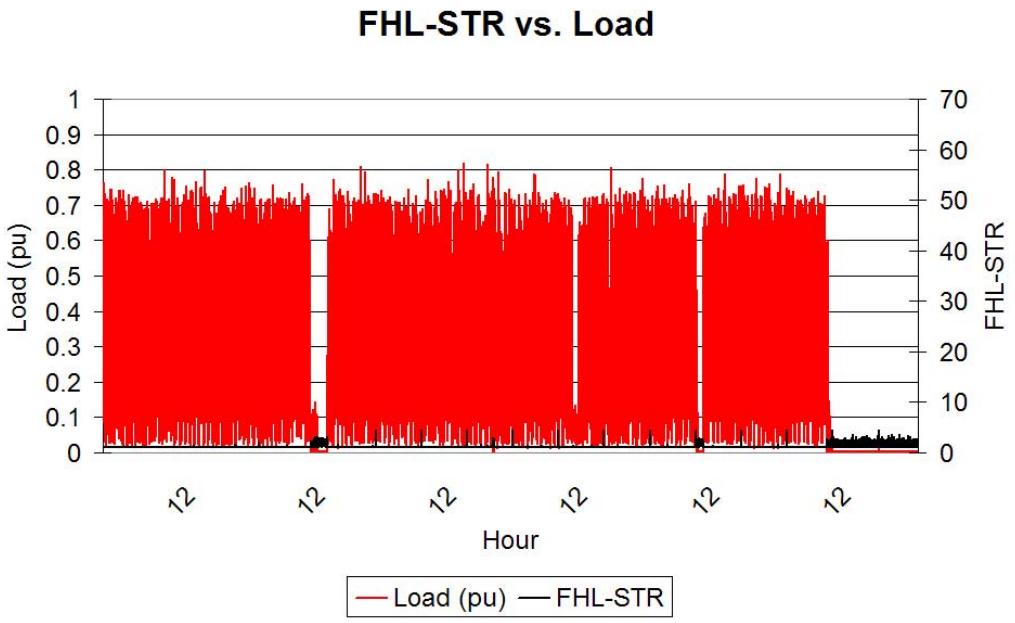

Figure 135 Habaş-C, FHL-STR vs. Load
(Averaged in each 20 seconds)

Detailed analysis of Figure 134 shows the following properties;

- The average of the F_{HL} is 3.33.
- The maximum F_{HL} value during measurement is as high as 60.

Also, analysis of Figure 135 shows the following properties;

- The average of the $F_{HL\text{-}STR}$ is 1.114.
- The maximum $F_{HL\text{-}STR}$ value during measurement is as high as 4.57.

The difference between the maximum values of F_{HL} and $F_{HL\text{-}STR}$ indicates that the degree of harmonics is relatively high. This situation is because of the fact that F_{HL} is proportional to the harmonic level by a power of 2, whereas the $F_{HL\text{-}STR}$ is proportional to the harmonic level by a power of 0.8.

If, only the effect of the RMS value of the current has been taken into account, as in the case of the traditional measurement devices located on the present transformers, the effect of the harmonics would have been neglected. However for this particular transformer and its load, the effect of the harmonics is significant.

Of the 3 transformer with the same ratings, this transformer has the highest F_{HL} and $F_{HL\text{-}STR}$ values thus it may seem to be that it had been affected by the harmonics more than the other two transformers. However this first impression may lead to false results since the F_{HL} is only the harmonic loss factor and it does not include the effect of the loading.

Careful examination of Figures 134 and 135 shows that the major effect of the harmonics had been where the load has decreased to nearly “0”. In the presence of a load, the harmonic loss factor is much lower than the average values. Actually, when loaded, the F_{HL} value is not greater than 1.2. This value is much lower than the previously determined “average” value of 3.33. Therefore it can be concluded that, the harmonic loss factor can not be accepted as the major factor effecting temperature rise. It shall be considered in conjunction with the loading factor.

A.3.2.2 Temperature Prediction

Since there was no free oil pocket to insert the Top-Oil temperature thermometer, the measured Top-Oil temperature was read from the Top-Oil temperature thermometer on the transformer during the measurement duration. The temperature measurement from thermometers has a tolerance value of 3 ^{o}C which must be taken account. The measured Top-Oil temperatures could not be acquired from operators so a partial measured temperature has been provided as shown in Figures 136 and 137.

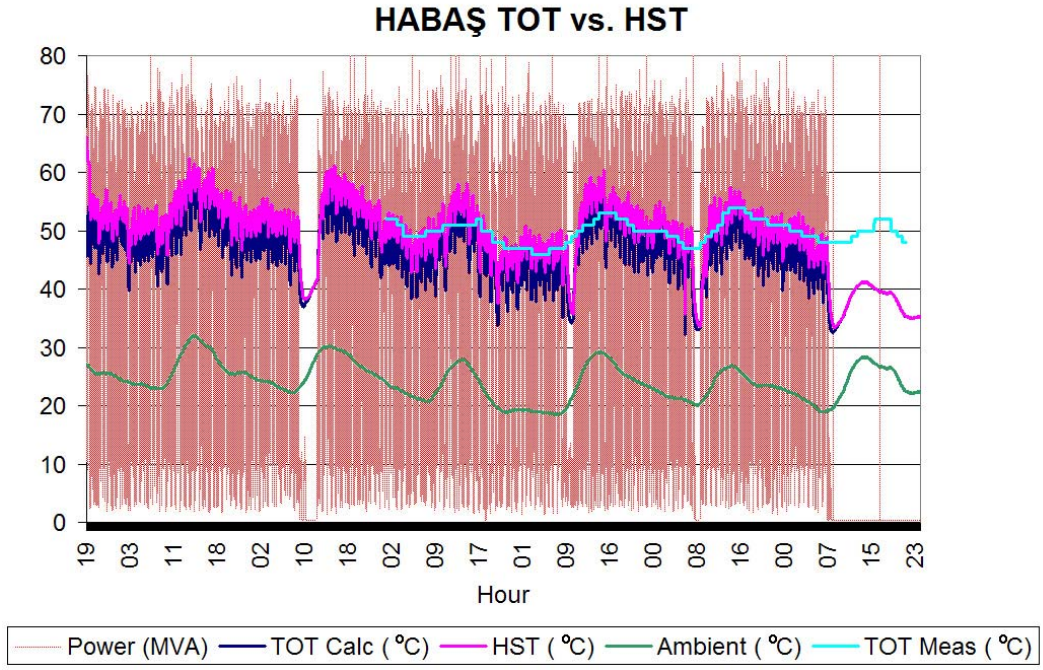

Figure 136 Habaş-C, Calculated vs. Measured TOT with respect to Loading (Averaged in each 20 seconds)

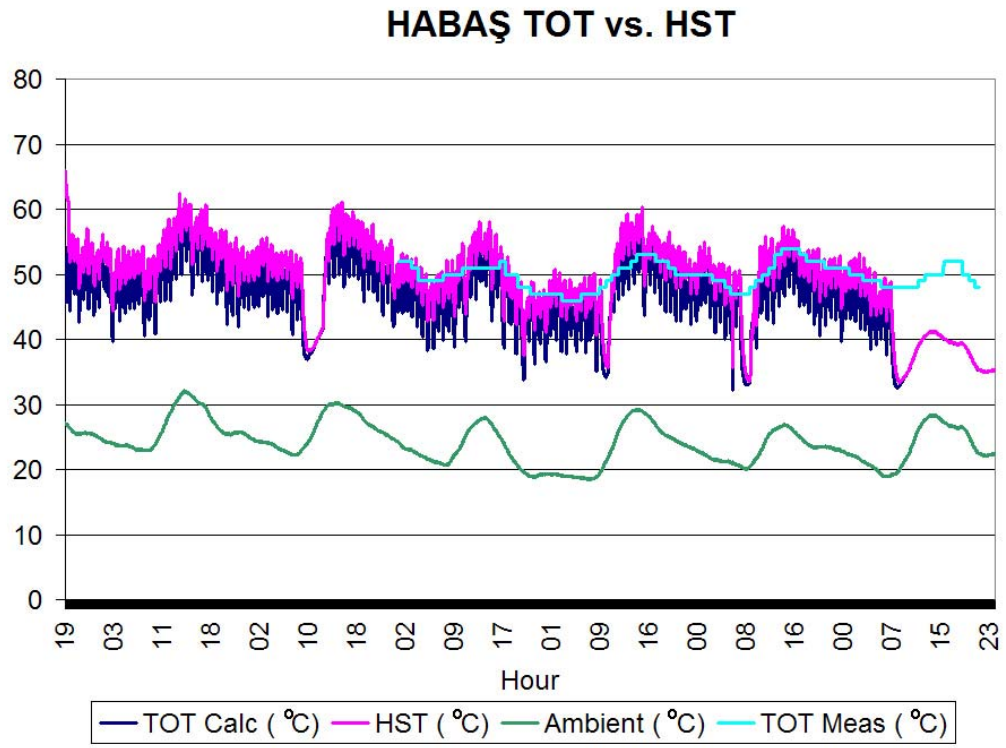

Figure 137 Habaş-C, Calculated vs. Measured TOT excluding Loading (Averaged in each 20 seconds)

To analyze the deviations between the measured and the calculated temperature values more efficiently, the following Figures of 138 and 139 have been prepared showing the deviation between the calculated and measured data with respect to the pu loading and the ambient temperature respectively.

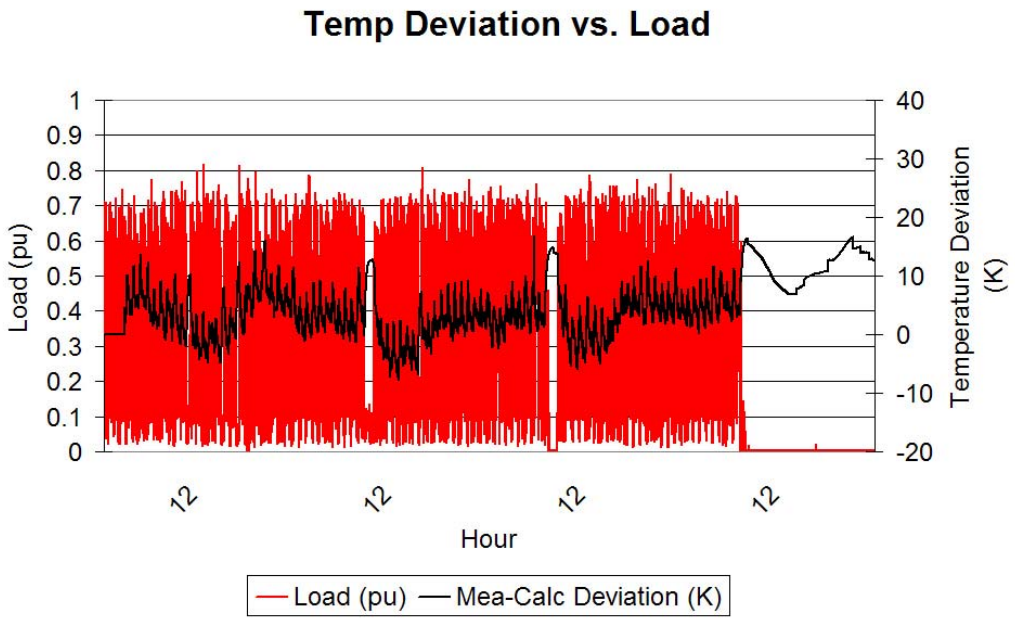

Figure 138 Habaş-C, TOT deviations between Calculated and Measured Temperatures with respect to Loading

It shall be noted that when there is loading, the deviations are generally in ±5 ^{o}C tolerance band. However when the transformer enters the shut-down operation, the deviations increase as described in section 4.1.2.2.

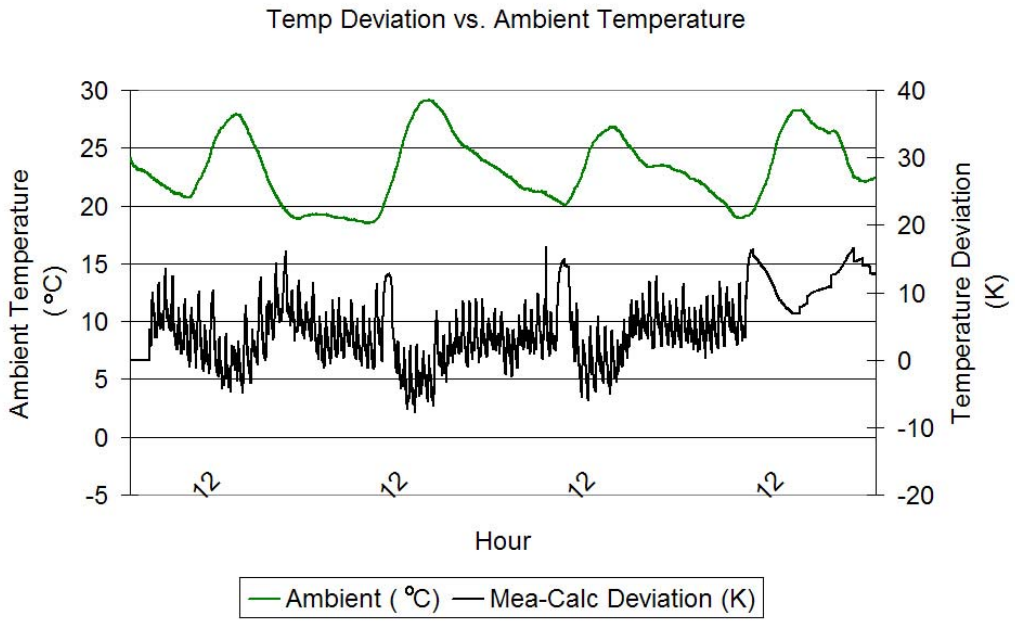

Figure 139 Habaş-C, TOT deviations between Calculated and Measured Temperatures with respect to Ambient Temperature

Also the same measurement on the Top-Oil and Hot-Spot temperature calculation on all 3 phases has been performed. The results are shown in Figures 140 and 141.

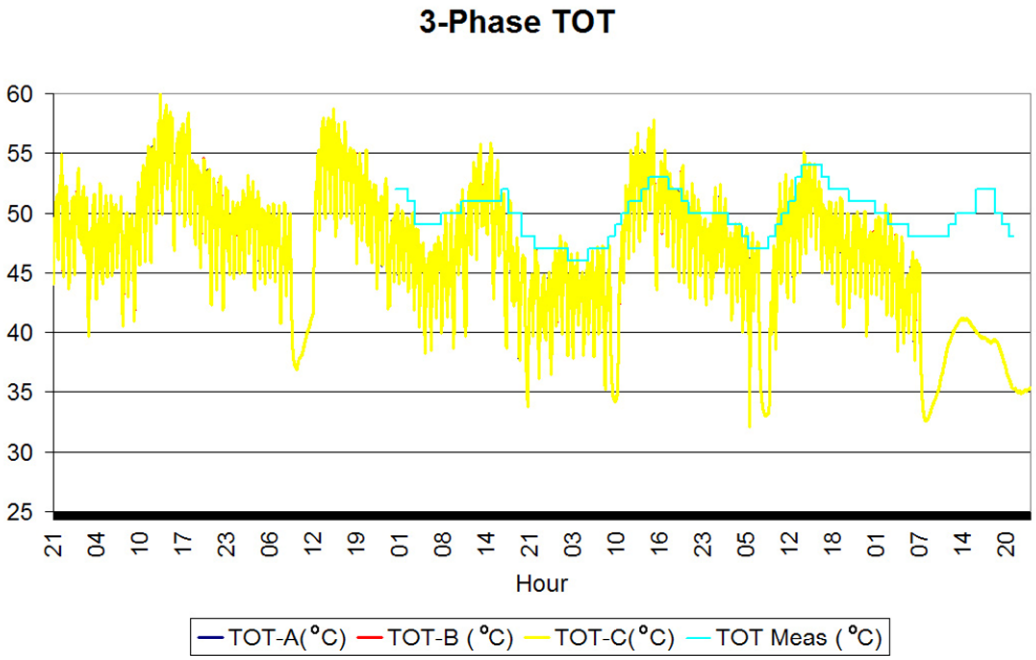

Figure 140 Habaş-C, TOT calculated from the currents of Phases A, B and C

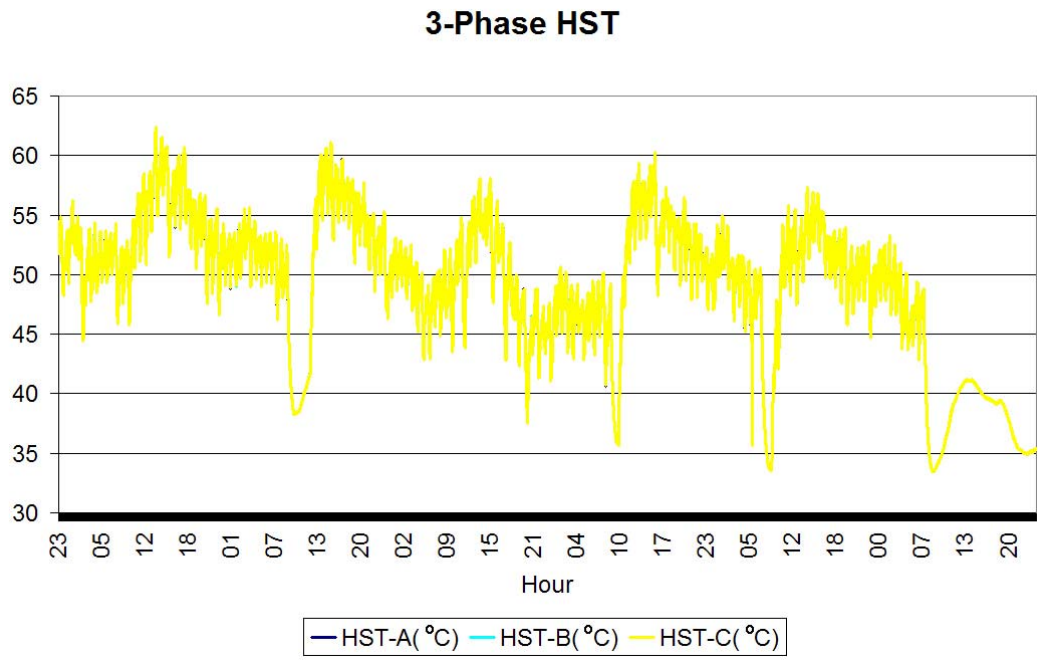

Figure 141 Habaş-C, HST calculated from the currents of Phases A, B and C

The differences between phases have been calculated. Figures 142 through 145 show the deviations of Top Oil and Hot Spot temperatures between phases C and B with respect to phase A.

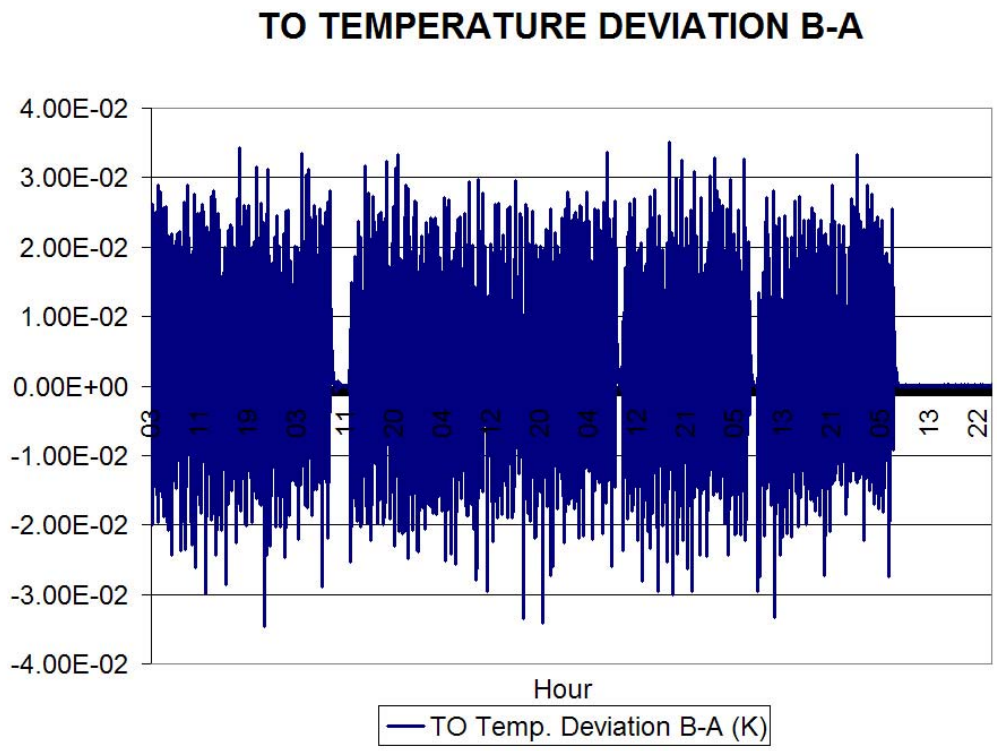

Figure 142 Habaş-C, TOT Deviation between the Phases B and A

Figure 142 shows;

- The maximum deviation for the Top Oil temperatures between Phase B and Phase A is 0.035 ^{o}C.
- The average deviation for the Top Oil temperatures between Phase B and Phase A is -0.00012 ^{o}C.

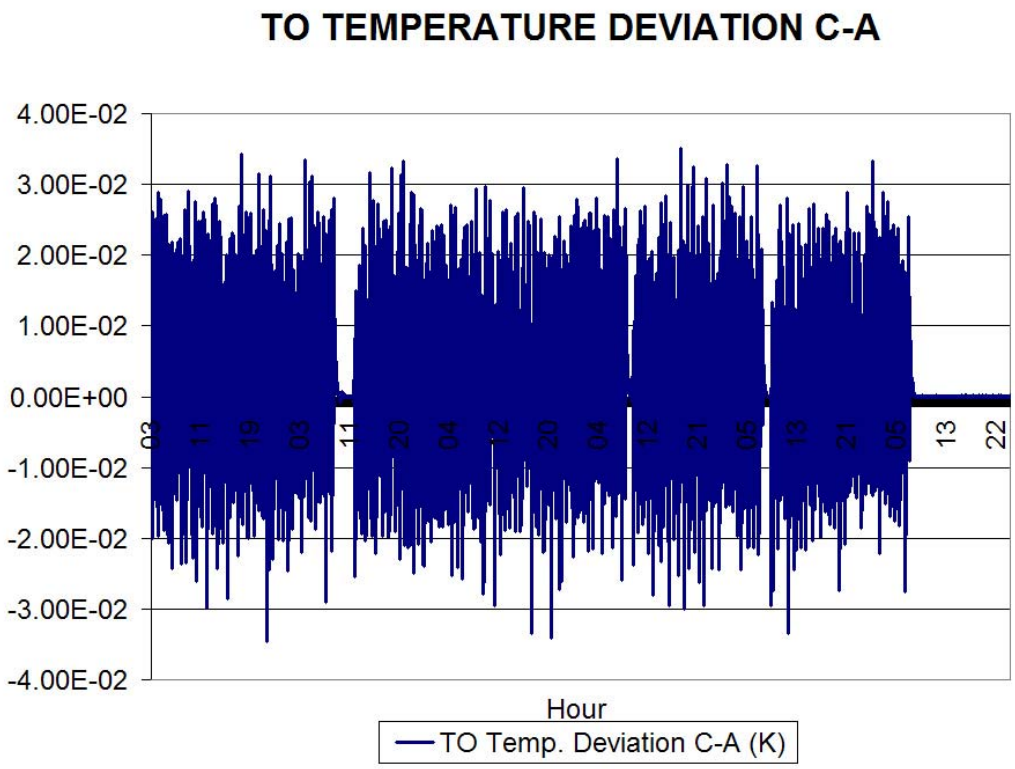

Figure 143 Habaş-C, TOT Deviation between the Phases C and A

Figure 143 shows;

- The maximum deviation for the Top Oil temperatures between Phase C and Phase A is 0.03 ^{o}C.
- The average deviation for the Top Oil temperatures between Phase C and Phase A is -0.00007 ^{o}C.

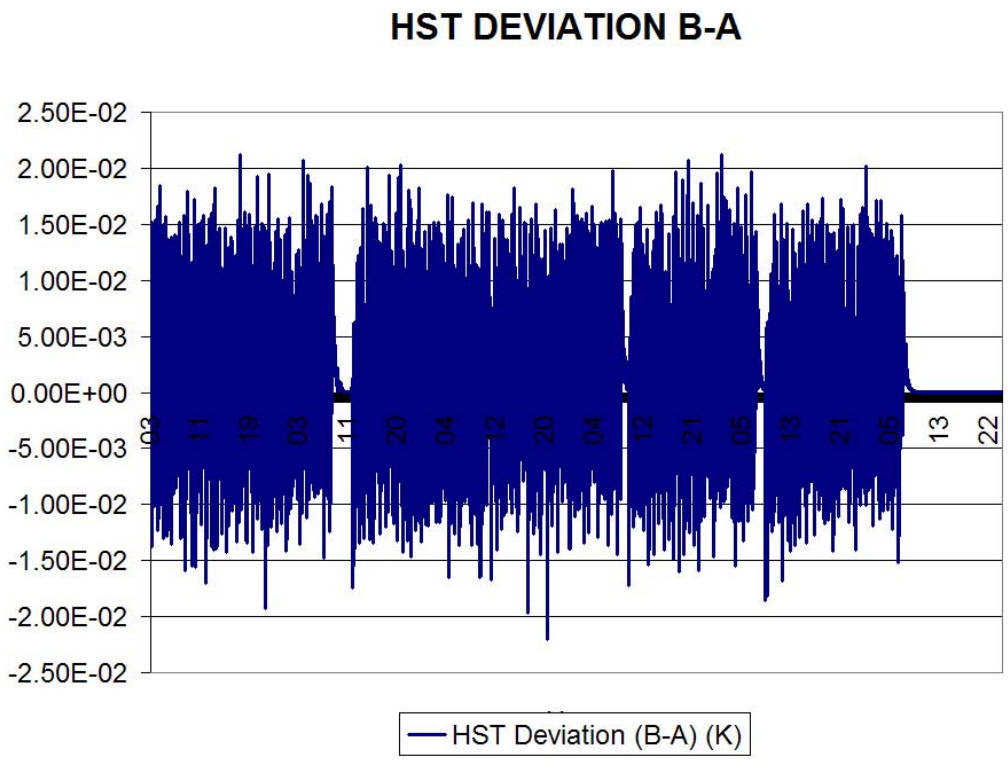

Figure 144 Habaş-C, HST Deviation between the Phases B and A

Figure 144 shows;

- The maximum deviation for the Hot Spot temperatures between Phase B and Phase A is 0.02 ^{o}C.
- The average deviation for the Hot Spot temperatures between Phase B and Phase A is 0.0004 ^{o}C.

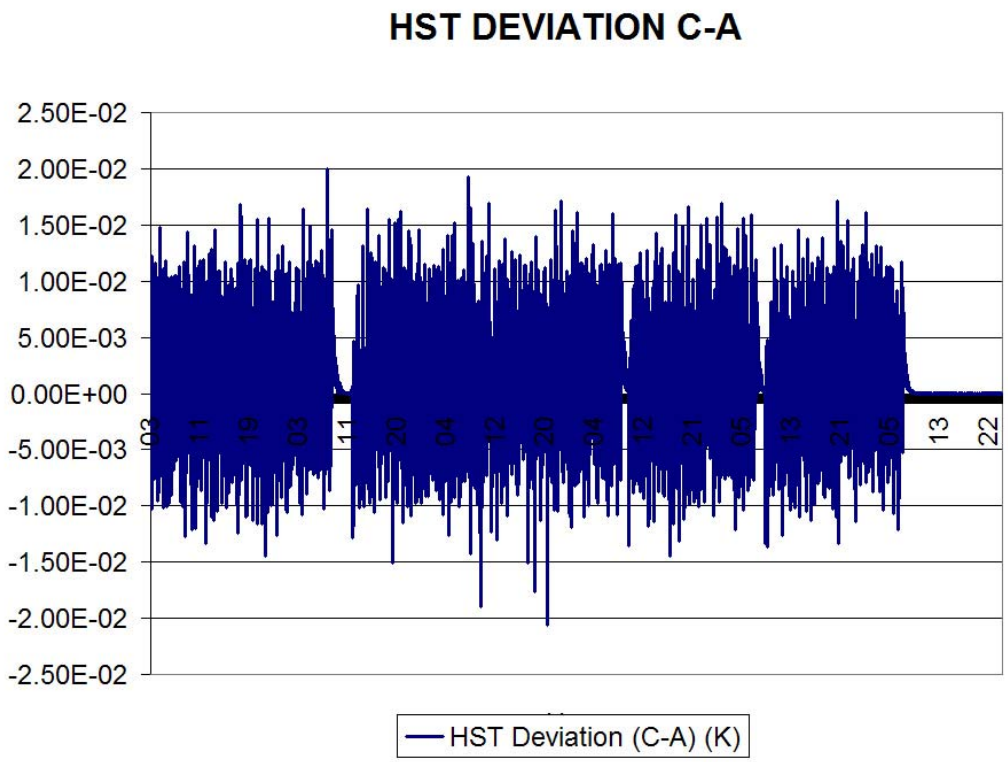

Figure 145 Habaş-C, HST Deviation between the Phases C and A

Figure 145 shows;

- The maximum deviation for the Hot Spot temperatures between Phase C and Phase A is 0.02 ^{o}C.
- The average deviation for the Hot Spot temperatures between Phase C and Phase A is 0.00009 ^{o}C.

The maximum deviation during the measurement duration is 0.03 ^{o}C. The average deviation is less than 0.004 ^{o}C. These data shows that the phase balance of the transformer loading is in acceptable values.

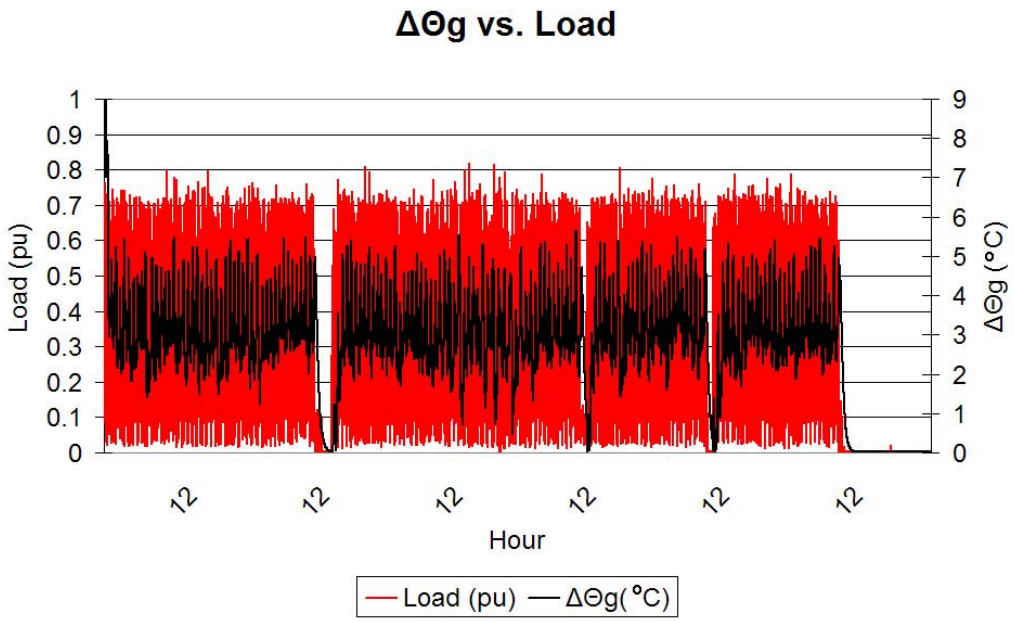

Figure 146 Habaş-C, Hot Spot Conductor rise over Top Oil Temperature (Averaged in each 20 seconds)

The Hot-Spot conductor rise over Top-Oil temperature has been shown in Figure 146. A comparison of Figure 146 to Figures 134 and 135 shows that harmonics can be more effective with higher loading.

A.3.3 80/100 MVA ONAN/ONAF Conventional Load

In the previous measurements, the results of the TEMPEST have been investigated for the intermittent loads. The priority has been given to the intermittent loading, considering the assumption that for steadier loading more accurate results will be achieved. To visualize the effectiveness of TEMPEST for the steady loading, the system has been applied to transformers with relatively constant loadings. The transformer is transformer-A of Ümitköy transformer center.

Figure 147 Transformer Ümitköy-A

Table 11 TEMPEST Input data for Ümitköy-A

ÜMİTKÖY-A TRANSFORMER	
Rated Capacity	100 MVA
HV	154000 V
LV	34500 V
No-Load Losses	32350 W
Load Losses	165000 W
HV Connection	Wye
LV Connection	Wye
Base Current	1718.3 A
Top Oil Time Constant	3.5 hours
Winding Time Constant	7 minutes

Table 11 shows the TEMPEST input data for transformer Ümitköy-A (Figure 147). These values have been acquired from manufacturer's certified test report.

A.3.3.1 Loading and Harmonic Content

This transformer's harmonic content is much lower than the previous measurements. Since the loading is steadier, the percentage of the harmonic content has been taken as constant. The harmonic spectrum of the load is as seen in Figure 148. The Figure shows that the load demand is sinusoidal (except a slight 5.Harmonic). The harmonic content will not be further discussed for Ümitköy-A transformer. Also, for the steady loading, the phase balance can be achieved with ease. Therefore the unbalanced phase calculations have been omitted.

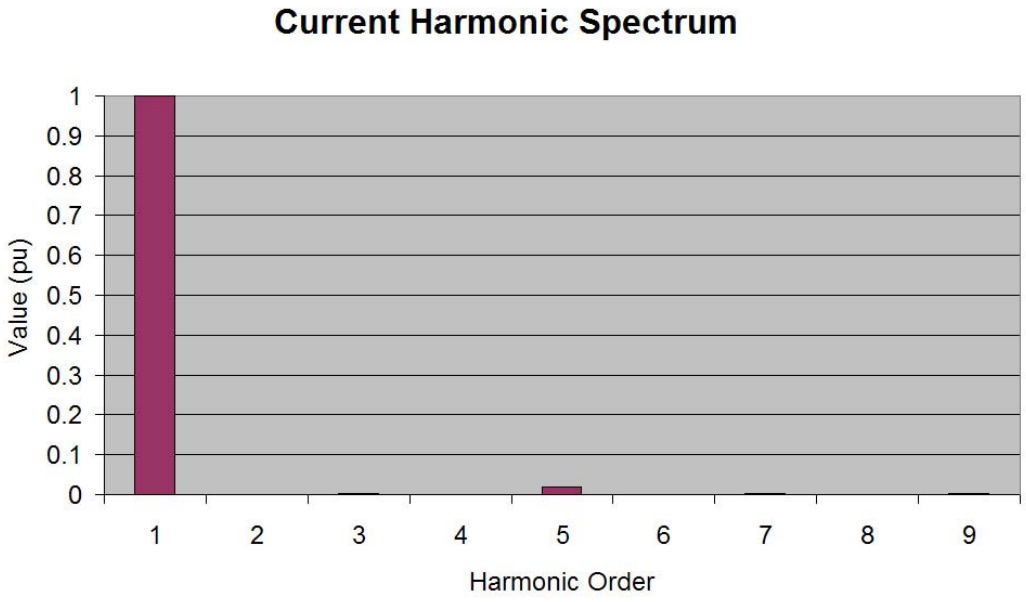

Figure 148 Ümitköy-A Harmonic Spectrum

A.3.3.2 Temperature Prediction

Figure 149 shows the Top-Oil temperature and Hot-Spot temperatures versus time. The Figure also shows the relatively steady power demanded by the load. Since this transformer is located in the urban area, the power demanded by the load side does not vary instantaneously. The response of TEMPEST is superior compared to the intermittent loading. This kind of loading is the preferred choose among tests of temperature prediction methods. There are even test setups which benefited from totally steady loading throughout the day (such as 0.5 (pu) for 10 hours duration).

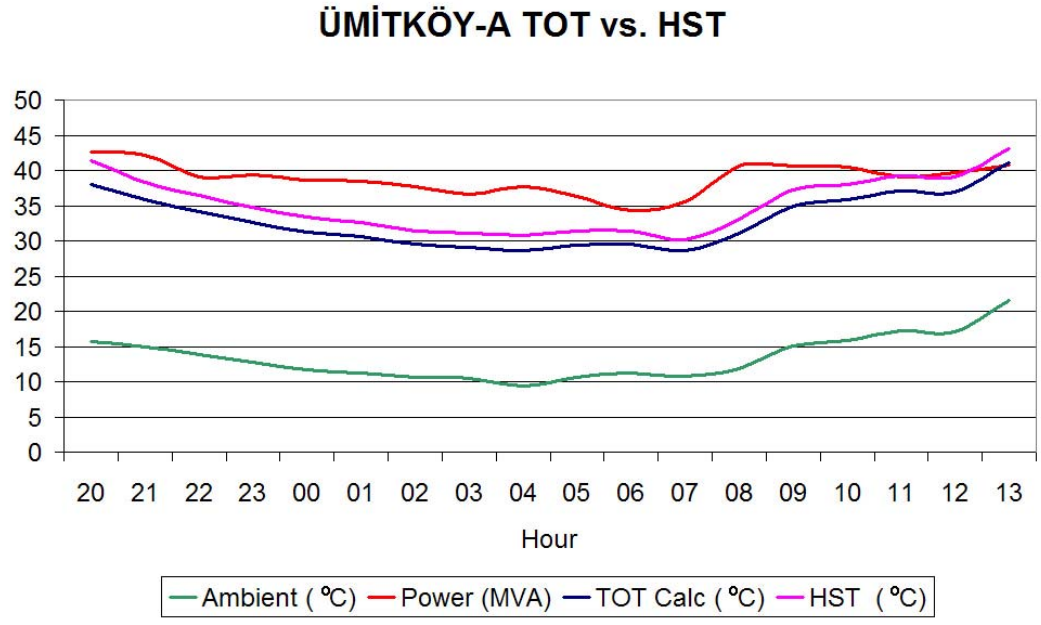

Figure 149 Ümitköy-A TOT vs. HST

A.3.4 100 MVA OFAF Conventional Load

Another measurement has been performed on transformer-B of Ümitköy transformer center, to visualize the effectiveness of TEMPEST for the steady loading.

Figure 150 Ümitköy-B Transformer

Table 12 TEMPEST Input data for Ümitköy-B

ÜMİTKÖY-B TRANSFORMER	
Rated Capacity	100 MVA
HV	154000 V
LV	34500 V
No-Load Losses	32350 W
Load Losses	165000 W
HV Connection	Wye
LV Connection	Wye
Base Current	1718.3 A
Top Oil Time Constant	5.4 hours
Winding Time Constant	7 minutes

Table 12 shows the TEMPEST input data for transformer Ümitköy-B (Figure 150). These values have been acquired from manufacturer's certified test report.

A.3.4.1 Loading and Harmonic Content

This transformer's harmonic content is much lower than the previous measurements even if it is higher than the Ümitköy-A to some degree. Since the loading is steadier, the percentage of the harmonic content has been taken as constant. The harmonic spectrum of the load is as seen in Figure 151. The Figure shows that the load demand is sinusoidal (except a slight 5.Harmonic). The harmonic content will not be further discussed for Ümitköy-B transformer. Also, for the steady loading, the phase balance can be achieved with ease. Therefore the unbalanced phase calculations have been omitted.

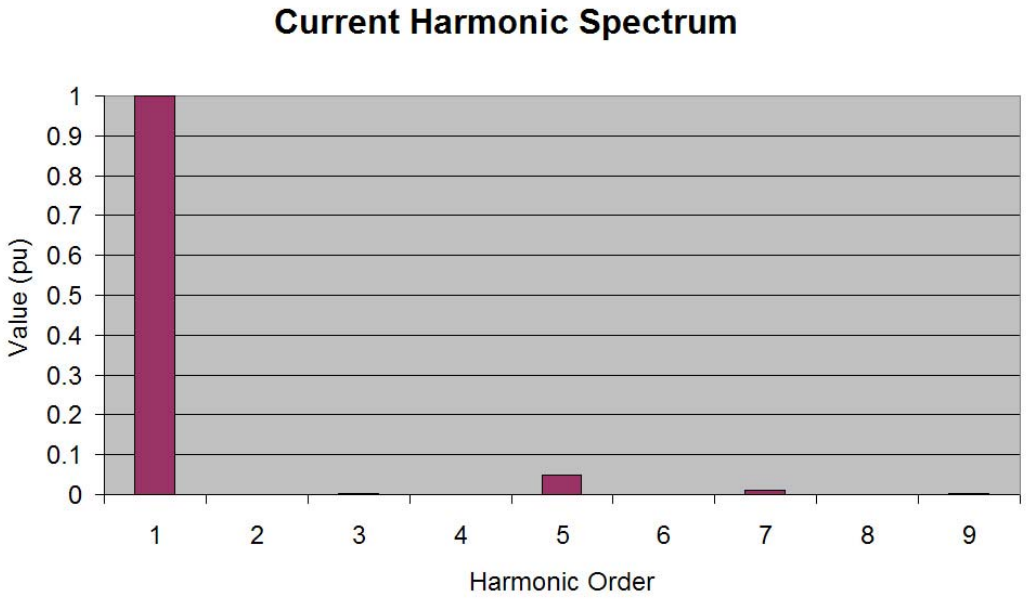

Figure 151 Ümitköy-B Harmonic Spectrum

A.3.4.2 Temperature Prediction

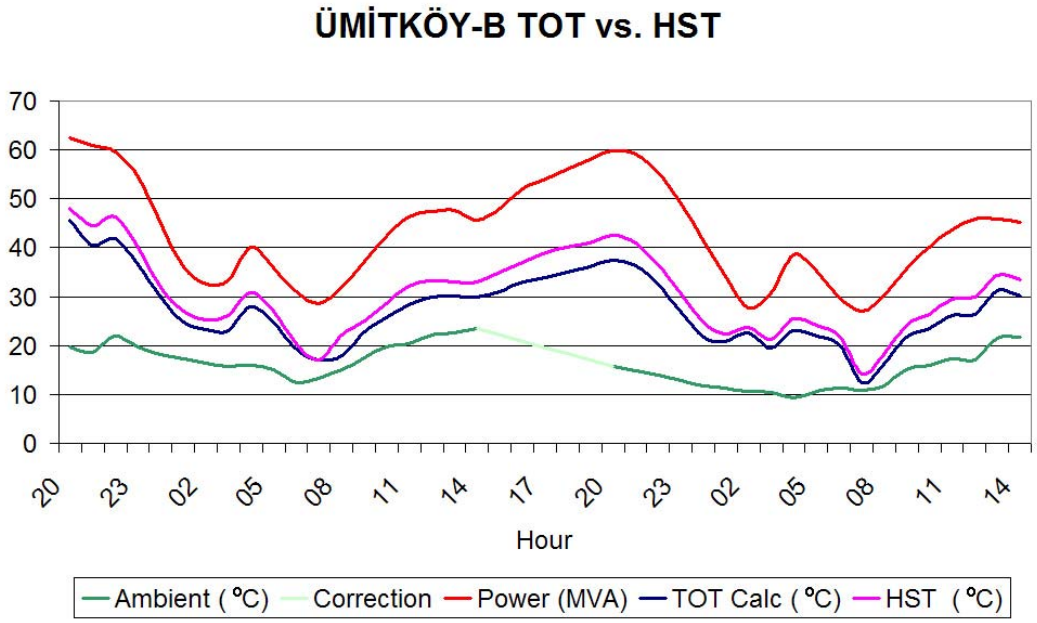

Figure 152 Ümitköy-B TOT vs. HST

Figure 152 shows the Top-Oil temperature and Hot-Spot temperatures versus time. The Figure also shows the relatively steady power demanded by the load. It can be seen that the power demanded on Ümitköy-B sometimes reach as high as 60 MVA where the power demanded from Ümitköy-A did not even reached 45 MVA. But the differences between the temperatures are not very significant. This is the result of the OFAF type of cooling of Ümitköy-B transformer.

Not only do the OFAF type transformers have longer oil time constants, they also can cool the oil more efficiently than the ONAN or ONAF type transformers. With the combination of these two properties, OFAF type transformers can withstand more power demand from the load side. One disadvantage of using them is the lowered efficiency due to the constant power loss on the air fans and oil pumps. These losses and increased maintenance costs result in the scarceness of OFAF type transformers and the general acceptance of ONAN/ONAF type transformers.

In the second day of the measurement, there is a malfunction of the ambient thermometer. The problem was fixed and the Figure shows a linear correction applied to keep the continuity of the measurement. The other functions of the measurement system functioned properly so the data had not been totally discarded.

APPENDIX B

INSTALLATION OF RESISTIVE THERMOMETER

Prior to the start of installation, necessary precautions such as gloves, helmets and grounding activities had been checked. This preventive equipment has been supplied to all personnel who took part in the installation process to avoid fatal injury.

Figure 153 Safety Precaution-Glove

Figure 154 Safety Precaution-Helmet

Figure 155 Safety Precaution-Grounding

Figure 156 Removal of oil tap

Figure 157 Oil tap Removed

Figure 158 Oil Thermometer adaptor installation

Figure 159 Oil Thermometer installed